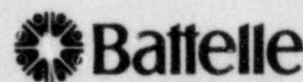

Design Basis Neutronics Calculations for NRU-LOCA Experiments

**S. W. Heaberlin R. T. Perry
U. P. Jenquin T. J. Trapp
G. W. McNair M. G. Zimmerman**

August 1979

**Prepared for
the U.S. Nuclear Regulatory Commission**

**Pacific Northwest Laboratory
Operated for the U.S. Department of Energy
by Battelle Memorial Institute**



PNL-3113

**THIS DOCUMENT CONTAINS
POOR QUALITY PAGES**

8007230694

NOTICE

This report was prepared as an account of work sponsored by the United States Government. Neither the United States nor the United States Nuclear Regulatory Commission, nor any of their employees, nor any of their contractors, subcontractors, or their employees, makes any warranty, express or implied, or assumes any legal liability or responsibility for the accuracy, completeness or usefulness of any information, apparatus, product or process disclosed, or represents that its use would not infringe privately owned rights.

PACIFIC NORTHWEST LABORATORY
operated by
BATTELLE
for the
UNITED STATES DEPARTMENT OF ENERGY
Under Contract EY-76-C-06-1830

Printed in the United States of America
Available from

National Technical Information Service
United States Department of Commerce
5285 Port Royal Road
Springfield, Virginia 22151

Price: Printed Copy \$ ____ *; Microfiche \$3.00

*Pages	NTIS Selling Price
001-025	\$4.00
026-050	\$4.50
051-075	\$5.25
076-100	\$6.00
101-125	\$6.50
126-150	\$7.25
151-175	\$8.00
176-200	\$9.00
201-225	\$9.25
226-250	\$9.50
251-275	\$10.75
276-300	\$11.00

DESIGN BASIS NEUTRONICS CALCULATIONS
FOR NRU-LOCA EXPERIMENTS

by
S. W. Heaberlin
U. P. Jenquin
G. W. McNair
R. T. Perry
T. J. Trapp
M. G. Zimmerman

Prepared for NRC under related services
contract with DOE
Contract No. EY-76-C-06-1830

August 1979

Pacific Northwest Laboratory
Richland, Washington 99352

ACKNOWLEDGMENTS

The authors would like to acknowledge the assistance and support provided by the NRU-LOCA project manager C. R. Hann and that of the project task leaders. We would like to remember here Theron G. Odekirk who was our colleague and our friend.

CONTENTS

ACKNOWLEDGMENTS	ii
1.0 INTRODUCTION	1-1
2.0 SUMMARY	2-1
3.0 REACTOR AND TEST DESCRIPTION	3-1
3.1 REACTOR DESCRIPTION	3-1
3.2 TEST ASSEMBLIES	3-1
3.3 TEST OPERATION	3-9
4.0 REACTOR VALIDATION	4-1
4.1 AECL DATA	4-1
4.2 NEUTRONICS MODELS AND RESULTS	4-2
4.3 VALIDATION CONCLUSIONS	4-6
5.0 POWER	5-1
5.1 CROSS SECTION PREPARATIONS	5-1
5.2 EXPOSURE MODELING	5-9
5.3 FULL CORE MODELING	5-12
5.4 RESULTS	5-19
6.0 POWER PROFILES	6-1
6.1 FULL CORE RADIAL FLUX PROFILES	6-1
6.2 QUARTER CORE MODEL AND RESULTS	6-1
6.3 AXIAL MODEL AND RESULTS	6-19
7.0 SHIELDING	7-1
8.0 TRANSIENTS	8-1
8.1 WATER LOSS FROM THE TEST LOOP	8-1
8.2 REACTOR POWER AFTER SCRAM	8-3
8.3 DECAY POWER FROM TEST ASSEMBLY	8-6
9.0 NEUTRON AND GAMMA HEATING	9-1
9.1 HEATING RATES IN TEST FUEL COOLANT	9-1
9.2 GAMMA HEATING IN STRUCTURAL MATERIAL	9-5
APPENDIX A - NEUTRONICS CODE DESCRIPTION	A-1
APPENDIX B - ORIGEN DATA	B-1
APPENDIX C - SUMMARY OF PRELIMINARY STUDIES	C-1

FIGURES

3.1	NRU Core Loading on December 31, 1978	3-2
3.2	NRU Reactor Driver Fuel Rod	3-3
3.3	Reactor Test Bundle (Nominal Shroud)	3-7
3.4	Reactor Test Bundle (Thickened Shroud)	3-8
4.1	Percent Deviation Between Calculated Powers and AECL Powers	4-3
4.2	Comparison of Calculated Powers and AECL Powers	4-4
4.3	Quarter Core Benchmark Results	4-5
5.1	NRU Reactor Driver Fuel Rod	5-3
5.2	Thorium and Fast Neutron Rod Model	5-4
5.3	Reactor Test Bundle	5-5
5.4	Formation of Smear X-Sections	5-7
5.5	Formation of Discrete X-Sections	5-8
5.6	Fission Product Cross Section as a Function of Exposure for NRU Driver Fuel (Group 4-thermal, Group 3-lowest epi-thermal)	5-10
5.7	K-Infinity Values as a Function of Exposure for NRU Driver Fuel Rods	5-11
5.8	K-Infinity Values as a Function of Exposure for NRU Fast Neutron Rods	5-13
5.9	^{235}U Burnout Rate and ^{239}Pu Buildup Rate for NRU Fast Neutron Rods	5-14
5.10	2DBS Full Core Unit Cell Representation	5-16
5.11	Full Core Model	5-17
6.1	NRU Radial Flux Profile	6-2
6.2	Quarter Core Model	6-4
6.3	Detail of Nominal Shroud Test Assembly in Quarter Core Model	6-5
6.4	Detail of Thick Shroud Test Assembly in Quarter Core Model	6-6

FIGURES

6.5A Normalized Pin Power Map, Nominal and Thick Shrouds	6-7
6.5B Normalized Pin Power Map, Nominal and Thick Shrouds	6-8
6.5C Normalized Pin Power Map, Nominal and Thick Shrouds	6-9
6.5D Normalized Pin Power Map, Nominal and Thick Shrouds	6-10
6.5E Normalized Pin Power Map, Nominal and Thick Shrouds	6-11
6.5F Normalized Pin Power Map, Nominal and Thick Shrouds	6-12
6.6A Normalized Pin Power Map, Nominal and Hot Configurations	6-13
6.6B Normalized Pin Power Map, Nominal and Hot Configurations	6-14
6.6C Normalized Pin Power Map, Nominal and Hot Configurations	6-15
6.6D Normalized Pin Power Map, Nominal and Hot Configurations	6-16
6.6E Normalized Pin Power Map, Nominal and Hot Configurations	6-17
6.6F Normalized Pin Power Map, Nominal and Hot Configurations	6-18
6.7 Axial Model	6-20
6.8 Normalized Radial Power Distribution from Axial Model, Thick Shroud	6-22
6.9 Normalized Axial Power Distribution - Nominal Shroud Uniform Axial Driver Exposure	6-23
6.10 Normalized Axial Power Distribution - Thick Shroud, Uniform Axial Driver Exposure	6-24
6.11 Normalized Axial Power Distribution - Driver Fuel	6-25
6.12 Normalized Axial Power Distribution - Thick Shroud, Water Coolant	6-26
6.13 Normalized Axial Power Distribution - Thick Shroud, Steam Coolant .	6-27
6.14 Normalized Axial Power Distribution - Thick Shroud, Water Coolant, Distributed Driver Exposure	6-28
7.1 Dose Rate From NRU Test Assembly as a Function of Distance in Water Filled Pool, Thermal-Hydraulic Test, One Day Cooling . . .	7-3

FIGURES

8.1	Ramp Reactivity Insertion	8-4
8.2	Step Reactivity Insertion	8-5
8.3	Total Reactor Power After Scram	8-7
8.4	Test Assembly Decay Heat	8-8
9.1	Neutron and Gamma Deposition in the Water Coolant	9-6

TABLES

3.1	NRU Driver Fuel Description and Enrichment	3-4
3.2	Test Bundle Data	3-6
5.1	Range of Burnups Covered by Modeled Burnups	5-18
5.2	Calculated Powers for Various Test Bundle Configurations (Reactor at 127 MW)	5-20
5.3	Reactor Power Required to Obtain Specific Power in Test Bundle . .	5-21
7.1	Primary ORIGEN Input Assumptions	7-2
8.1	Nuclear Constants for Delayed Neutron Precursors	8-2
8.2	The Normalized Reactor Power After a Ramp Reactivity Insertion . .	8-3
9.1	Gamma Heating Rates (at Full Reactor Power - 135 MW)	9-7

1.0 INTRODUCTION

One of the primary concerns in commercial light water reactor (LWR) safety is the hydraulic and material behavior during a loss of coolant accident. As part of its response to that concern, the Fuel Behavior Research Branch of the USNRC Division of Reactor Safety Research is sponsoring a series of LOCA experiments. These experiments will be conducted in the Nation Research Universal (NRU) reactor at Deep River, Ontario. The experimental program will allow the unique opportunity to study full length multi-rod bundles.

In all six test assemblies will be irradiated. Each assembly will be a 6 x 6 segment of a 17 x 17 Pressurized Water Reactor (PWR) assembly. The tests will examine the heatup, reflood and quench phases of a hypothetical LOCA event. Low level fission heat within the test assembly driven by the NRU reactor, will be used to simulate the decay heat power and system stored energy which are the energy sources acting on the fuel during LOCA.

The Pacific Northwest Laboratory (PNL) has overall responsibility for experiment design, operation and evaluation. A neutronics task was established as part of this effort. The basic objectives of this task were to provide estimates of nuclear parameters, in support of the experiment design and evaluation. This entailed the development of reactor models which were used to calculate parameters such as the relation between reactor power and power produced in the test assembly, the spatial variations in power generation and gamma energy deposition rates. Other areas included the calculation of neutron energy deposition rates, fission product generation, shielding requirements for the irradiated test assemblies, and a limited amount of reactor kinetics.

The NRU reactor, while providing an excellent experimental tool for these tests, presents a series of challenges to neutronics analysis. The reaction is driven with low density, highly enriched metallic fuel moderated by heavy water. This is quite unlike the high density, low enriched ceramic light water moderated fuel of LWR's which is used in the test assembly. It is necessary to model both types of fuel simultaneously in a self-consistent manner. The reactor offers another difficulty common to many research reactors. The rods

making up the reactor are of many types. Their heterogeneous arrangement leaves no simplifying axis of symmetry. The test itself adds one other complication. The heatup phase of the test is steam cooled. This presents a region of very low moderator density among regions of high moderation and absorption, a difficult situation for neutronics analysis.

This report describes the approaches taken, models used and results generated to answer the neutronics questions posed. It includes a broad range of nuclear physics activities and as such provides a summary of the work performed under the NRU Neutronics Task.

2.0 SUMMARY

The report describes the neutronics analysis for the LOCA simulation experiments in the NRU reactor. The experimental program will provide greater understanding of nuclear fuel assembly behavior during the heatup, reflood and quench sequence of a hypothetical LOCA. The decay heat and stored heat, which are the energy source in a LOCA will be simulated by fission heat provided by the NRU reactor. The reactor, the test and test operation are described in Section 3.

A neutronics task was needed to predict a number of important parameters which effect the experiment design and operation. Since the analysis was conducted during and in support of the design a range of conditions were studied. These included fuel enrichments from 2.0 to 3.0 wt% ^{235}U , different shroud thicknesses, different NRU fuel configurations and different coolants within the test. A full core, quarter core and axial model of the NRU reactor were developed.

In support of the reactor models a reactor validation calculation was performed. In this the neutronics analysis results were compared to AECL best estimate values. The primary function was to sharpen those models and illuminate weak points in early versions of those models. The reactor validation is described in Section 4.

One of the most important parameters predicted by the neutronics analysis is the relationship between reactor power and power generated in the test. At a high reactor power (taken as 127 MW) the radial and axial averaged power in the test ranged from 22 kW/m to 13 kW/m depending on the conditions of coolant, test fuel enrichment, shroud type and reactor fuel loading. The 2.5 wt% ^{235}U enriched, thick shroud, hot fuel loading cases, which represent perhaps the most likely set of conditions for the test, have predicted powers of 16 kW/m and 17 kW/m for the steam and water cooled cases respectively. Section 5 discusses the models used in the prediction of power and details the results.

Another important parameter is the shape of the power, the relation of power to position. Section 6 gives these power profiles. The full core model was used to give radial power shapes across the reactor. The quarter core model

gave two dimensional plan view power shapes within the test assembly, and the axial model gave power shapes as a function of height along the assembly.

In addition to the reactor models a series of other neutronics calculations were performed. One such additional calculation concerns the fission product source term in the test assembly and the post-test examination shielding requirement needed because of that source term. These are described in Section 7. Another set of calculations fall under the heading of transients. These include reactor transients caused by accidental voiding of the test loop, reactor power after a scram, and decay heat in the test assembly. These are considered in Section 8. Neutron and gamma heating rates within the coolant and structural materials of the test make up the last of the additional studies. These are discussed in Section 9.

Three appendices are included in the report. The first presents abstracts of the major neutronics computer codes used in the study. Appendix B gives a collection of fission product data which are estimated for three different cases associated with the test assembly. The last appendix summarizes the preliminary neutronics calculations which preceded this report, but were required for early design choices.

3.0 REACTOR AND TEST DESCRIPTION

The NRU-LOCA experiments will be conducted in the National Research Universal (NRU) reactor at the AECL research facility at Deep River, Ontario. In order to understand the neutronics calculations performed in support of the experimental program a brief background description of the NRU reactor, the test assemblies and the test operation is required.

3.1 REACTOR DESCRIPTION

The NRU reactor, located at the Chalk River Nuclear Laboratories, Ontario, Canada, is owned and operated by Atomic Energy of Canada Limited. The NRU is a thermal neutron, heterogeneous, heavy water moderated and cooled reactor. It was designed for operation with natural uranium metal fuel rods and converted to operation with enriched driver fuel rods in 1964. The reactor has a rated maximum power of 135 MW. In any given core loading the nominal reactor power is set to give the specified thermal neutron flux levels at loop experiments. The core loading as seen on December 31, 1978 is shown in Figure 3.1.

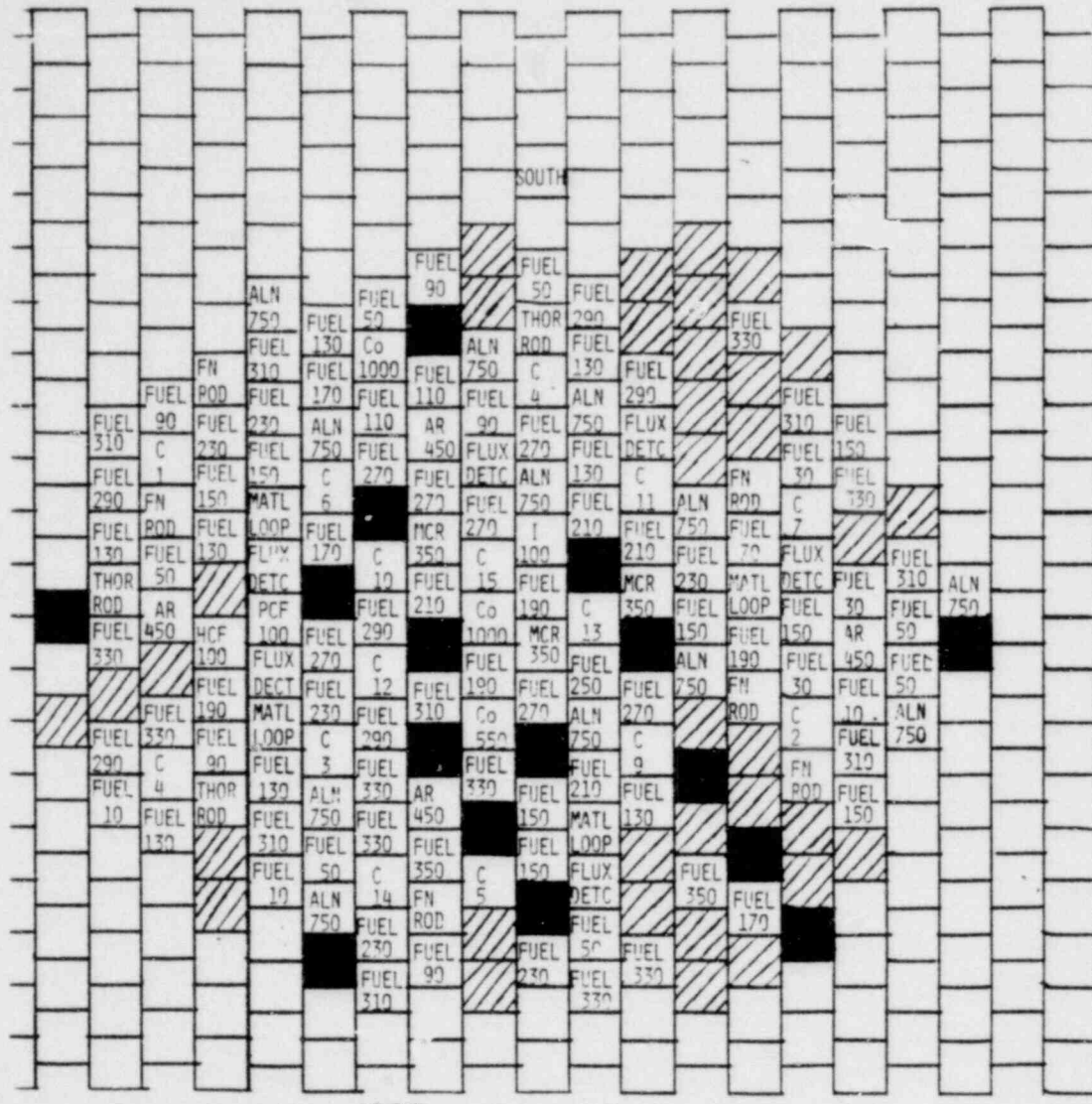
The NRU vessel is an aluminum cylinder with stainless steel headers at the top and bottom. The vessel is 3.51 m in diameter with an inside depth of 3.66 m. There are 227 lattice spaces located within the vessel with a lattice spacing of 197 mm.

The fuel sections of the rods are 610 mm shorter than the vessel and the lattice diameter is 406 mm less than that of the vessel. This space around the fueled core is filled with a heavy water moderator.

The NRU fuel is an enriched uranium (93 wt% ^{235}U) aluminum alloy. The uranium makes up 21 wt% of the alloy. Each rod has twelve UAl fuel pencils extrusion clad with aluminum with six fins per element (see Figure 3.2). Fuel rod data are given in Table 3.1.

3.2 TEST ASSEMBLIES

In all, six different test assemblies will be irradiated during the test program. The first to be tested will be the thermal-hydraulic assembly. The remaining six are material test assemblies. While there are significant dif-



LEGEND



DUMMY ROD



VACANT POSITION



FUEL
XXX
NRU DRIVER FUEL
WITH BURNUP GIVEN IN MWd/ROD



THOR ROD



FN
ROD
FAST NEUTRON POD



ALN
XXX
COBALT OR ISOTOPE RODS
(OTHER INCLUDE AR, HCF,
PCF, CO, MCR, AND I)



C
XX
CONTROL RODS IN FULL
OUT POSITION

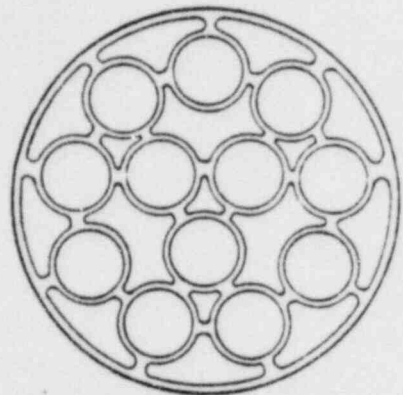


FLUX
DETC
FLUX DETECTOR



MATL
LOOP
MATERIAL TEST
LOOP

FIGURE 3.1. NRU Core Loading on December 31, 1978



FLOW SPACER

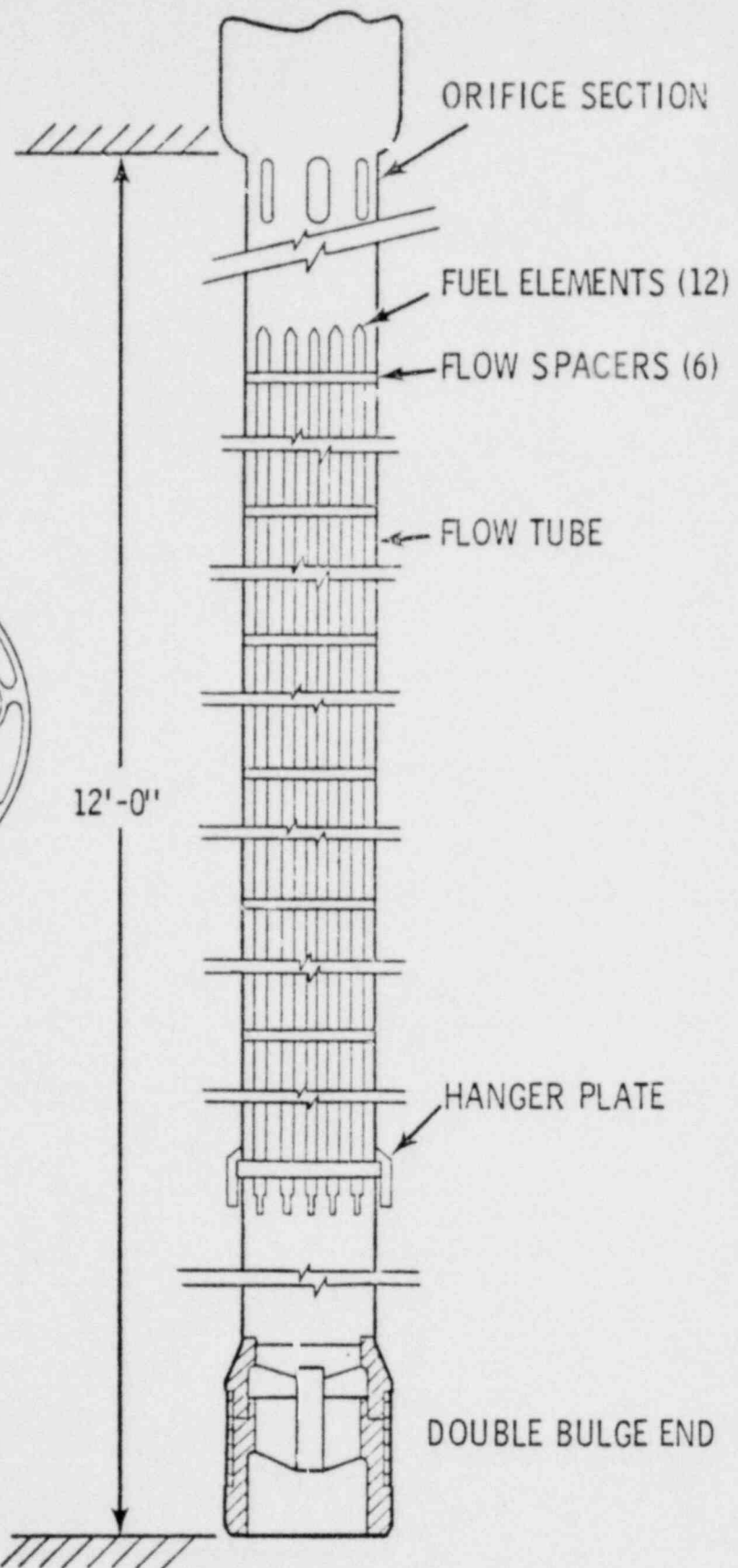


FIGURE 3.2 NRU Reactor Driver Fuel Rod

TABLE 3.1. NRU Driver Fuel Description and Enrichment

Fuel Rod Data	
Flow Tube ID	49.99 mm
Flow Tube Wall	1.27 mm
Flow Tube OD	52.53 mm
Diameter of Bundle	43.99 mm
Radius of Centers of Three Inner Elements	11.25 mm
Radius of Centers of Nine Outer Elements	17.22 mm
Element Spacing	4.27 mm
Element Diameter	7.01 mm
Sheath Thickness	0.76 mm
Fuel Diameter	5.49 mm
Fuel Length	2.74 m
Fuel Cross Section per Bundle	283 mm ²
Sheath Cross Section (including fins)	249 mm ²
Flow Cross Section	1431 mm ²
Material Cross Section (including tube)	726 mm ²
Hydraulic Diameter	2889 mm ²
Weight of U-235 per Rod	500 g

Materials

Fuel	Uranium-aluminum alloy	21 wt% uranium (93 wt% u-235) and 79 wt% aluminum super-pure
------	------------------------	--

Cladding Fuel is extrusion clad with
 #6102 (Spec. 1S) aluminum

ferences between the thermal-hydraulic assembly and the materials test assemblies (instrumentation, internal rod pressure, etc.) these differences have little impact on the nuclear physics behavior of the fuel. The basic design of the assemblies is uniform.

The test bundle fuel element is a full length 31 pin design modeled after a typical Babcock and Wilcox 17 x 17 light water reactor element. The pertinent data are given in Table 3.2 and the test bundle is shown in Figures 3.3 and 3.4.

The 31 fuel pins are placed inside of a stainless steel shroud. The shroud designs analyzed in the neutronics calculations are shown in Figures 3.3 and 3.4. The final shroud design had not been decided upon by the completion of the neutronics analysis. The various clips and spacers which will appear on the outside surfaces of the shroud are taken into account by a smearing process within the analysis for the nominal shroud case. The total weight of the shroud and associated structural materials which appears in the core, is transformed into an equivalent uniform cylinder of equal weight. The smearing process is not used in the thickened shroud case due to the small percentage of extra area that the clips and spacers add to the thickened shroud.

Outside of the stainless steel shroud tube there is a double wall pressure tube. The inner wall is constructed with zircaloy-4 while the outer wall is a mixture of zircaloy-4 and niobium.

The enrichment for the test fuel pins was varied between 2 and 3 percent throughout the neutronics analysis as the final fuel pellet specs had not been decided upon by the completion of the analysis.

The two coolants used for these experiments were steam and hot water. The steam was at a gage pressure of 520 kPa and 800° K with a density of 0.0017 g/cc. The hot water was saturated at 12.1 MPa and 600° K with a density of 0.6457 g/cc.

TABLE 3.2. Test Bundle Data

Fuel Element O.D.	9.6	mm
Fuel Element Pitch	12.7	mm
Pitch/Diameter	1.32	
Clad Thickness	0.597	mm
Fuel Pellet Diameter	8.23	mm
Pellet - Clad Gap	0.10	mm
Water Thimble O.D.	11.81	mm
Water Thimble I.D.	10.92	mm
Pressure Tube I.D.	103.38	mm
Pressure Tube O.D.	119.4	mm
Active Fuel Length	3.55	m
Mass Nominal Shroud*	33	kg
Mass Thick Shroud*	60	kg

*Over 3.66 m of active fuel length

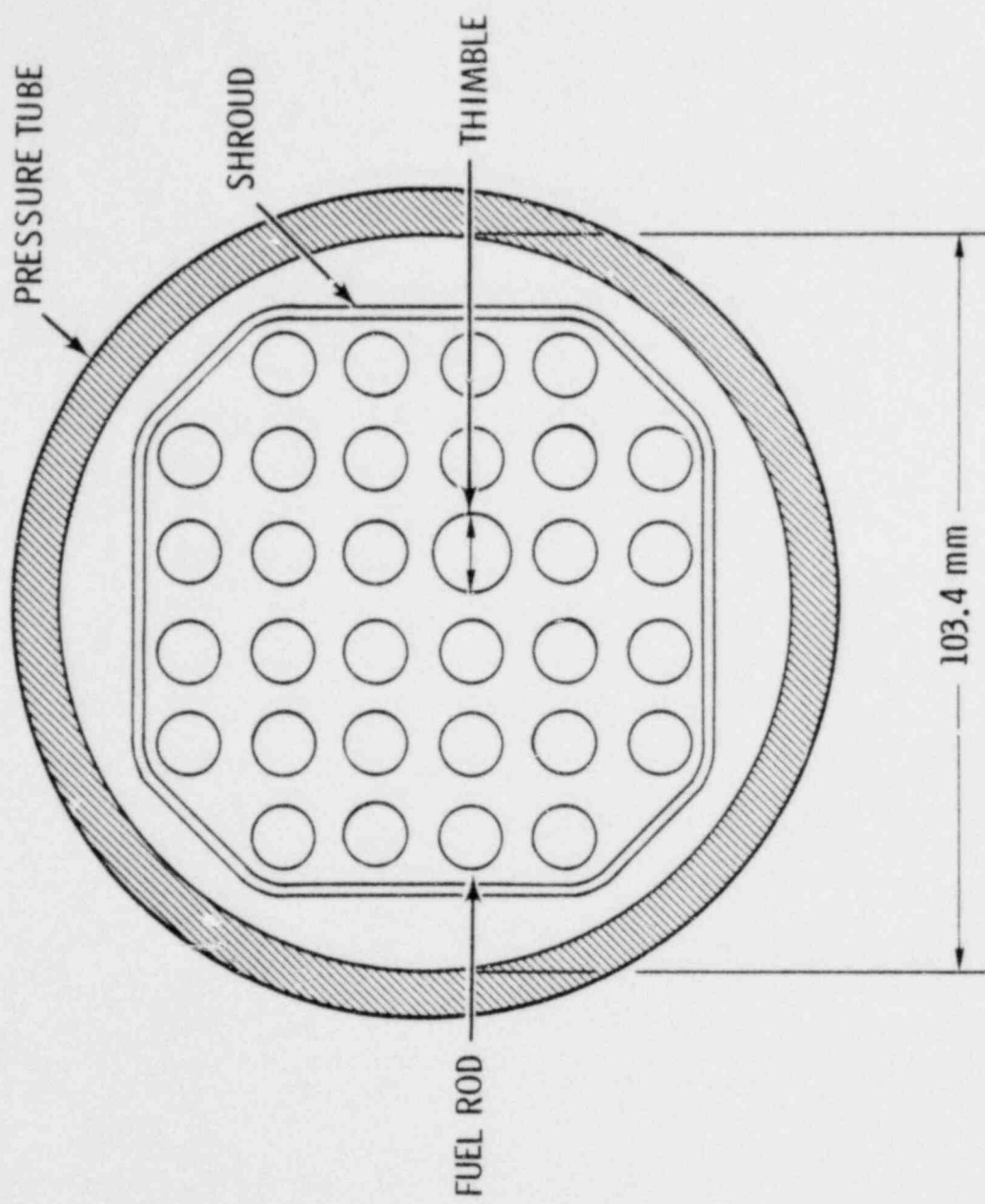


FIGURE 3.3 Reactor Test Bundle (Nominal Shroud)

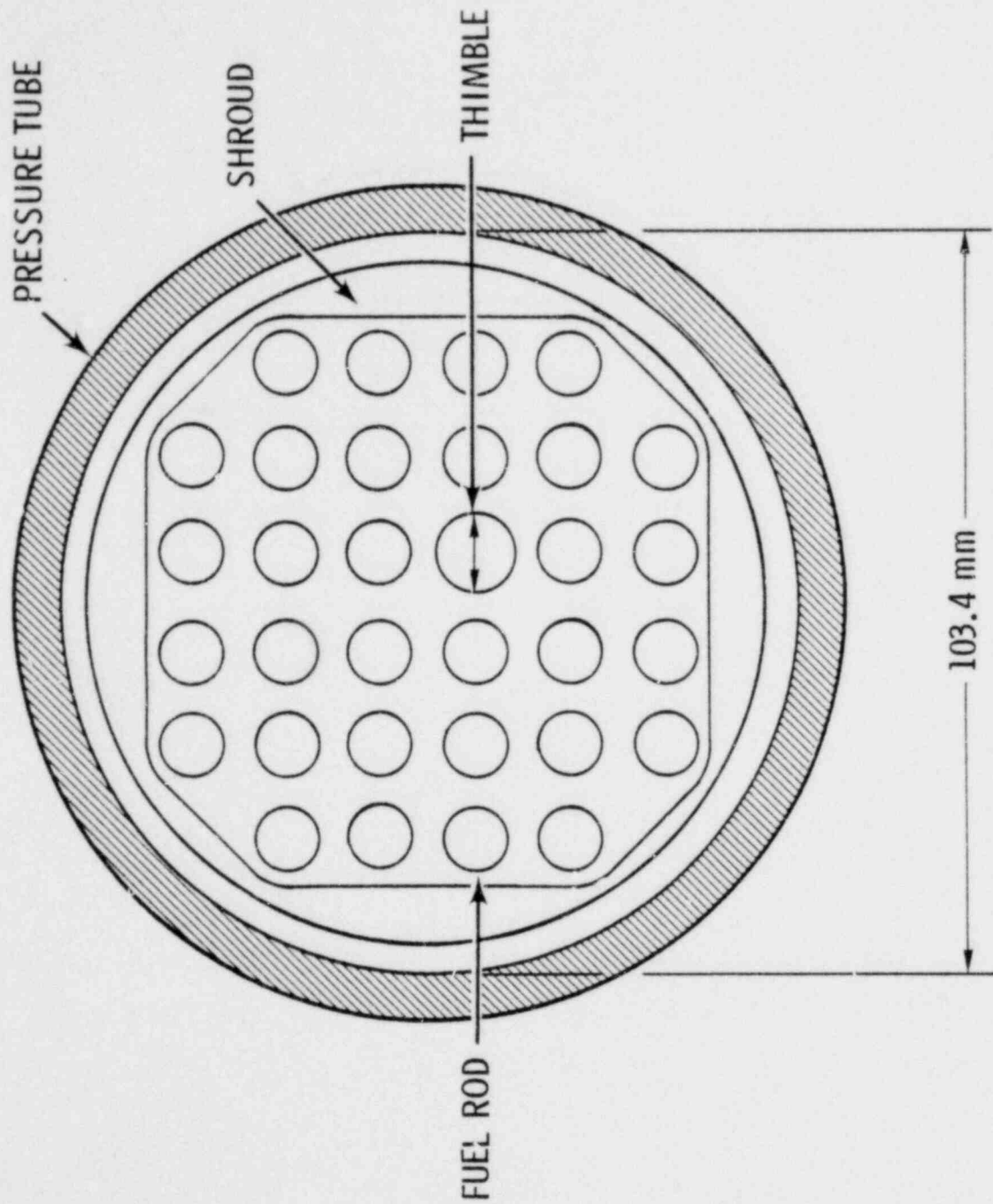


FIGURE 3.4 Reactor Test Bundle (Thickened Shroud)

3.3 TEST OPERATION

As described earlier the test program has two distinct types of test assemblies. These being the one thermal-hydraulic assembly and the five materials test assemblies. The different assembly types correspond to a different set of experimental conditions. However, as in the assemblies themselves, the experimental conditions appear nearly the same in regard to neutronics conditions. The basic test operation is described below, the relevant differences between the two experiment types are noted.

After the test is installed into the reactor, the test loop is charged with light water. The reactor is brought by steps to a high power, pausing to conduct instrument calibrations. This phase of the test is called preconditioning since its main purpose is to crack the fuel pellets to simulate some reactor residence time. The total time of the irradiation is short (approximately one hour).

After preconditioning the loop is drained and replumbed for the next phases of the test. The time before the next irradiation may be a day. To begin the next phase steam flow is initiated through the loop. Reactor power is brought, stopping for calibrations, to a low power level. This establishes the pretransient conditions. Steam flow is then cut off causing a temperature transient in the fuel. At a predetermined time and predetermined rate, reflood water is introduced from the bottom of the loop.

The complete sequence simulates the heatup, reflood and quench portions of a LWR-LOCA. The thermal-hydraulic test will undergo not one but a series of heatup-reflood cycles. The total irradiation time, excluding preconditioning, could be as long as twenty hours. The materials tests, in contrast, will undergo only one heatup-reflood cycle each, the irradiation period of the cycle probably less than one hour.

After a test sequence the test assembly will be removed from the reactor and transported to the NRU fuel storage basin for inspection. The inner test rods will be removed and the next set of inner test rods mounted into the guard heater rods/shroud assembly. If the guard heater rods are damaged, they too will be replaced. The reassembled test is returned to the reactor for

the next test sequence. The time period between tests will be approximately two months.

From the neutronics standpoint we have two test configurations of interest. The distinguishing attribute is the density of the moderating water within the test loop. The two cases are the water cooled case of preconditioning and reflood, and the steam cooled case of the heatup phase. In actuality the conditions of the water during the reflood are likely to be widely variable but for simplicity they were assumed to be that of the constant high pressure, high temperature preconditioning.

There are also two types of irradiation. The thermal-hydraulic test with its multiple cycles represents one. The materials tests with a single cycle represent the other variety.

4.0 REACTOR VALIDATION

In any scientific or engineering analysis effort in which mathematical models are used to simulate physical processes, it is necessary to compare the results of those models to empirical measurements. Such comparisons can be used to improve and sharpen the calculational model. In the neutronics calculation we were fortunate to obtain a set of data from AECL for the NRU reactor itself. This data took the form of a reactor description and the associated rod power values. This data and the results yielded by our final models are described below.

4.1 AECL DATA

The AECL benchmark data is evolved by their staff through a process which attempts to match the measured power distribution to the theoretical power distribution.

The measured power distribution is derived from driver rod flows and outlet temperatures which are assumed to be only accurate to $\pm 10\%$ for each measurement. The confidence level for this stated uncertainty is not available. Particular sites may be much worse, or not responding properly. These inaccuracies lead to a measured power at any location to be in error on the order of $\pm 20\%$.

The theoretical power distribution is derived from the AECL code LATREP which is empirically adjusted to give good results for CANDU fuel bundles. In a reactor of the complexity of NRU, this may give poor cell parameters, especially for fuel at high burn-up.

The measured and theoretical power distributions do not match very well. Therefore a compromise is produced by adjusting both measured and theoretical lattice parameters to produce a good match which will remain good under many different reactor configurations and flux distributions.

This AECL "best match" or "best estimate" power distribution data is used as our benchmark data.

4.2 NEUTRONICS MODELS AND RESULTS

Full Core Validation Results

The full core was modeled in a two dimensional hexagonal geometry by the 2DBS computer code. Each individual lattice was modeled by a set of homogenized cross sections which represented the material within the lattice. The NRU driver fuel was modeled as fuel having one of four distinct burnups. Due to insufficient modeling data the cross sections representing the four material test loops have been adjusted to generate the approximate power shown by the AECL data. A detailed description of the full core model is given in Section 5. A comparison between the lattice powers predicted by the 2DBS computer code for the full core model and the "best estimate" AECL data is shown in Figures 4.1 and 4.2. The average deviation between the predicted powers and the AECL data is approximately $\pm 17\%$ across the core.

Quarter Core Validation Results

A quarter core model of the reactor in the benchmark configuration was also constructed. The quarter core model allows more detail and was used in modeling pin to pin interactions within the test assembly. Section 6.3 describes this in much more detail.

The quarter core examines only the southwest fourth of the reactor. Reflecting boundaries are put along the centerline interfaces. In the non-symmetric NRU this assumption causes some difficulty.

The results of the benchmark calculation are shown in Figure 4.3. The average deviation from the AECL data is slightly more than $\pm 20\%$. If the deviations are weighed against rod powers the average is just under $\pm 19\%$.

While within the bounds of the AECL uncertainties, the quarter core deviations are clearly larger than those of the full core model. The reflecting boundaries are the prime suspect for this offense. The area around the U2D materials loop shows this. The parameters for the loop itself are adjusted to match the AECL power prediction. However, the materials loop and several of the neighboring rods in the region are

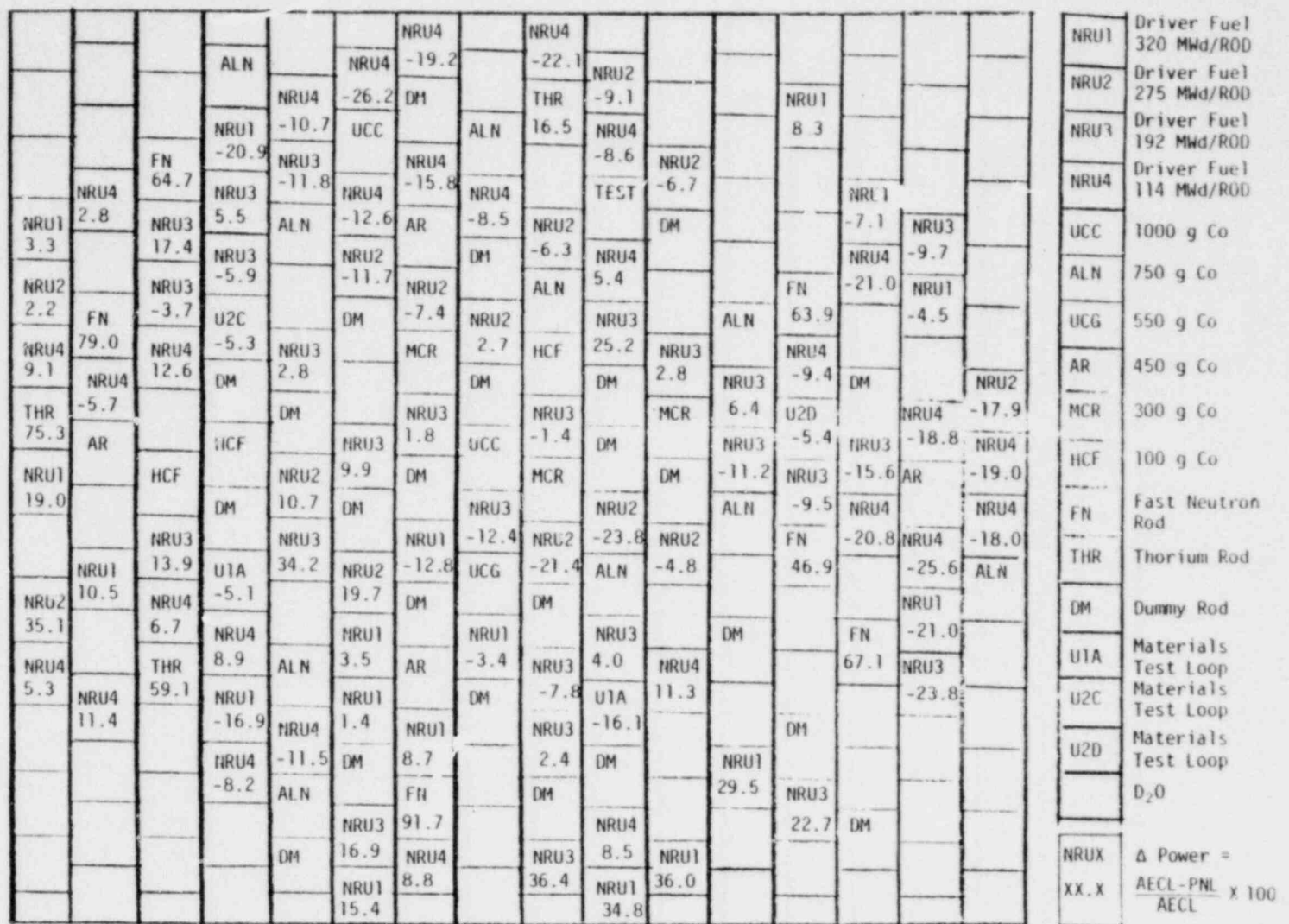


FIGURE 4.1. Percent Deviation Between Calculated Powers and AECL Powers

XXX	Calculated Power, MW
XXX	AECL Power, MW
UCC	1000 g Co
ALN	750 g Co
UCG	550 g Co
AR	450 g Co
MCR	300 g Co
HCF	100 g Co
FN	Fast Neutron Rod
THR	Thorium Rod
DM	Dummy Rod
U1A	Materials Test Loop
U2C	Materials Test Loop
U2D	Materials Test Loop
	D ₂ O

FIGURE 4.2. Comparison of Calculated Powers and AECL Powers

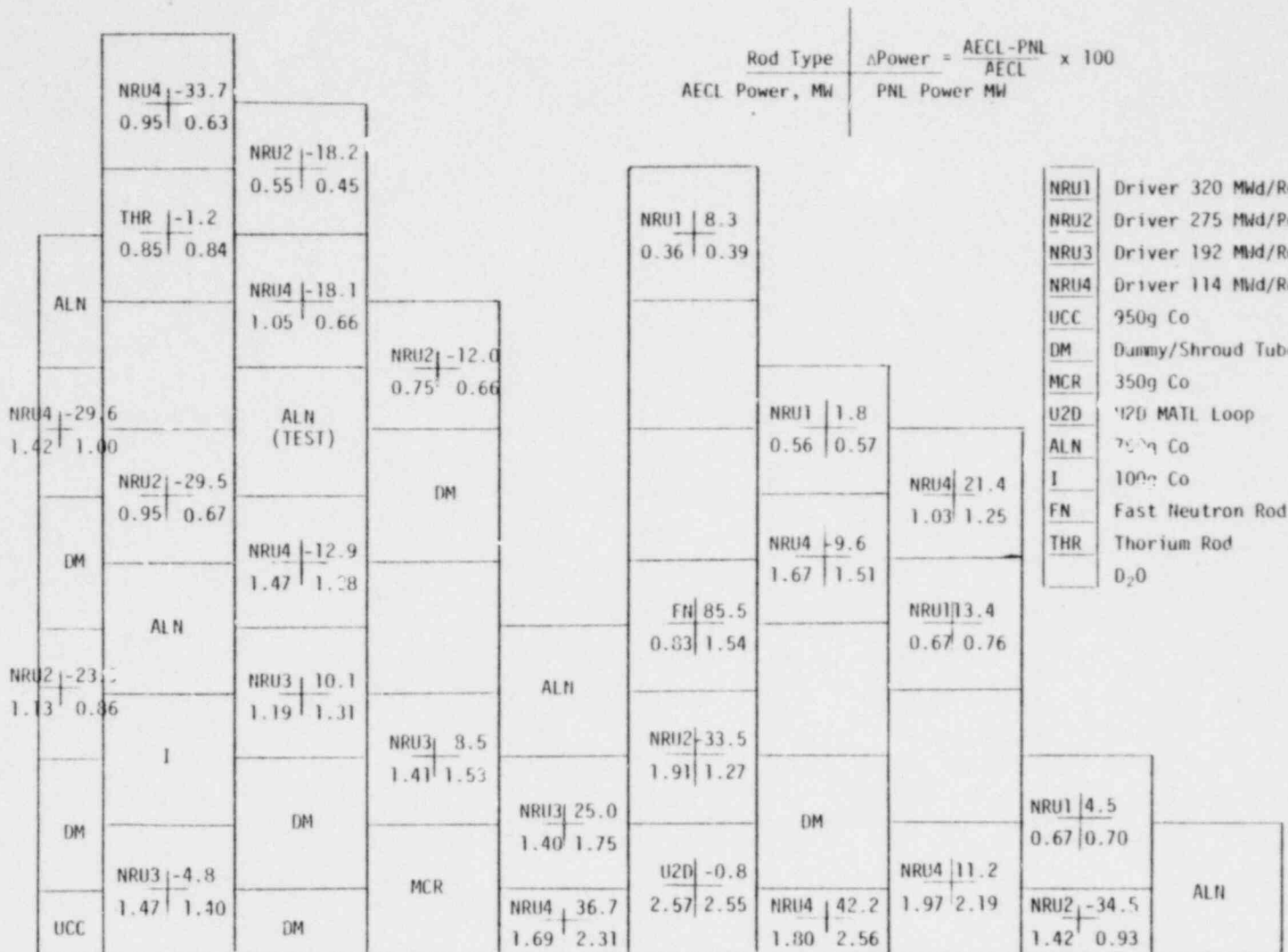


FIGURE 4.3. Quarter Core Benchmark Results

relatively high in power. The mirror boundary places equivalent high power rods on the other side of the boundary. This causes an artificial flux amplification in the region. This complication necessitates a depletion in other portions of the quarter core. The result is an imbalance which increases the deviations in calculated rod powers.

4.3 VALIDATION CONCLUSIONS

As stated earlier the primary usefulness of the validation effort was to enhance the neutronics models by providing a standard to compare against. In this regard the validation was a great success. A significant improvement was obtained between early and final models. The deviations from the AECL power data were reduced and flux imbalances smoothed.

It would have been desirable to also obtain an absolute assessment of the uncertainty in the power results predicted by the models. The data used in the validation does not, however, permit such an assessment. In the first place the data lacks a clear statement of experimental uncertainty. It is partly empirical (temperature and flow measurements) and partly theoretical (calculated correction factors). The temperature and flow measurements have a stated uncertainty of $\pm 10\%$ each, but no confidence level could be assigned to that uncertainty. The theoretically derived correction factors applied to the rod powers are an improvement over measurements, but from a propagation of errors viewpoint must increase uncertainty. We have no estimate of what that additional uncertainty might be. The total uncertainty in the AECL best estimates for rod powers is then not precisely known, but on the order of $\pm 20\%$.

In addition, to be able to assess uncertainties in the predictions of power within the test, experimental data for similar tests within the NRU reactor would be needed. An attempt was made to secure such data. For a variety of reasons including proprietary considerations this data could not be obtained. Therefore an absolute determination of uncertainties associated with the neutronics predictions of power is not possible.

5.0 POWER

Perhaps the single most important parameter predicted by the neutronics analysis is the relation between reactor power and power produced in the test assembly. The power produced in the test must fall within certain bounds. During preconditioning the power must be as high as possible to cause pellet cracking. This requires a high test/reactor power ratio. During the heatup and transient the power in the test is to be set at a low level. Since the reactor is unstable at very low power levels the test/reactor power ratio should be low for this case. Obviously a balance must be struck.

The power production for the test assembly was calculated for a variety of conditions. A full core reactor model was used to yield the power relations. That model is described below. The description includes discussion of neutron cross section preparation, exposure analysis and the reactor model itself. This is followed by the presentation of the estimated power results.

5.1 CROSS SECTION PREPARATIONS

The preparation of the cross sections to describe the various lattices is dictated by their relative importance neutronically and the amount of information available concerning their composition. The various methods are described in the following paragraphs.

Single Pass - Single Run

The single pass-single run method involves the use of the EGGNIT II computer code to generate an "infinite sea" cross section for a particular material. The EGGNIT II code with an imposed D₂O flux and current spectrum generates a 4 group (3 fast, 1 thermal) cross section from the ENDF/B-IV library. The majority of the cross sections for the materials in the non-fueled lattices, such as the various isotope and cobalt rods, are generated in this manner.

Single Pass - Double Run

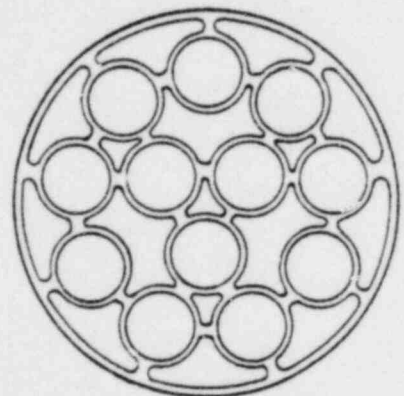
The single pass-double run method involves the same steps as the single run method with the addition of the BRT code to generate the thermal group cross sections. The thermal calculation performed by BRT is a more sophisticated treatment than that used by EGGNIT II.

The materials which have a higher importance neutronically are modeled in this manner. The materials included in this section include heavy water, light water, and stainless steel.

Double Pass - Double Run

The double pass-double run methods are used to prepare cross sections for the NRU fuel bundles, thorium rods, fast neutron rods, and the test bundle. The design of these elements (see Figures 5.1, 5.2 and 5.3) requires the inclusion of detailed analysis to describe the proper pin to pin interaction within a bundle and also the proper bundle to bundle interaction between neighboring lattice cells. There are presently two types of cross sections which are developed by this method.

The first type is called the SMEAR cross sections (see Figure 5.4, which gives an example for the test bundle). In this development the individual pin cell within a bundle is modeled in both EGGNIT II and BRT. EGNNIT II produces a single 20 group set of cross sections (19 fast groups, 1 thermal group) which characterize the homogenized fuel pin, BRT produces a single 30 group set of thermal cross sections which also characterize the homogenized fuel pin cell. The homogenized fuel pin cell cross sections produced by these two codes are now input into a discretely modeled rod bundle lattice cell as calculated by ANISN and BRT. The ANISN calculation utilizes the homogenized fuel pin cell cross sections produced by EGNNIT II, along with single pass-single run cross sections produced for the remaining regions of the lattice cell, and generates a single 4 group (3 fast, 1 thermal) set of cross sections which describe the fuel bundle lattice cell. The BRT code uses the homogenized fuel pin cell cross sections previously generated by BRT, along with internally produced cross sections for the remaining regions, to calculate a single set of thermal cross sections which describes the fuel bundle lattice cell. The 3 fast group



FLOW SPACER

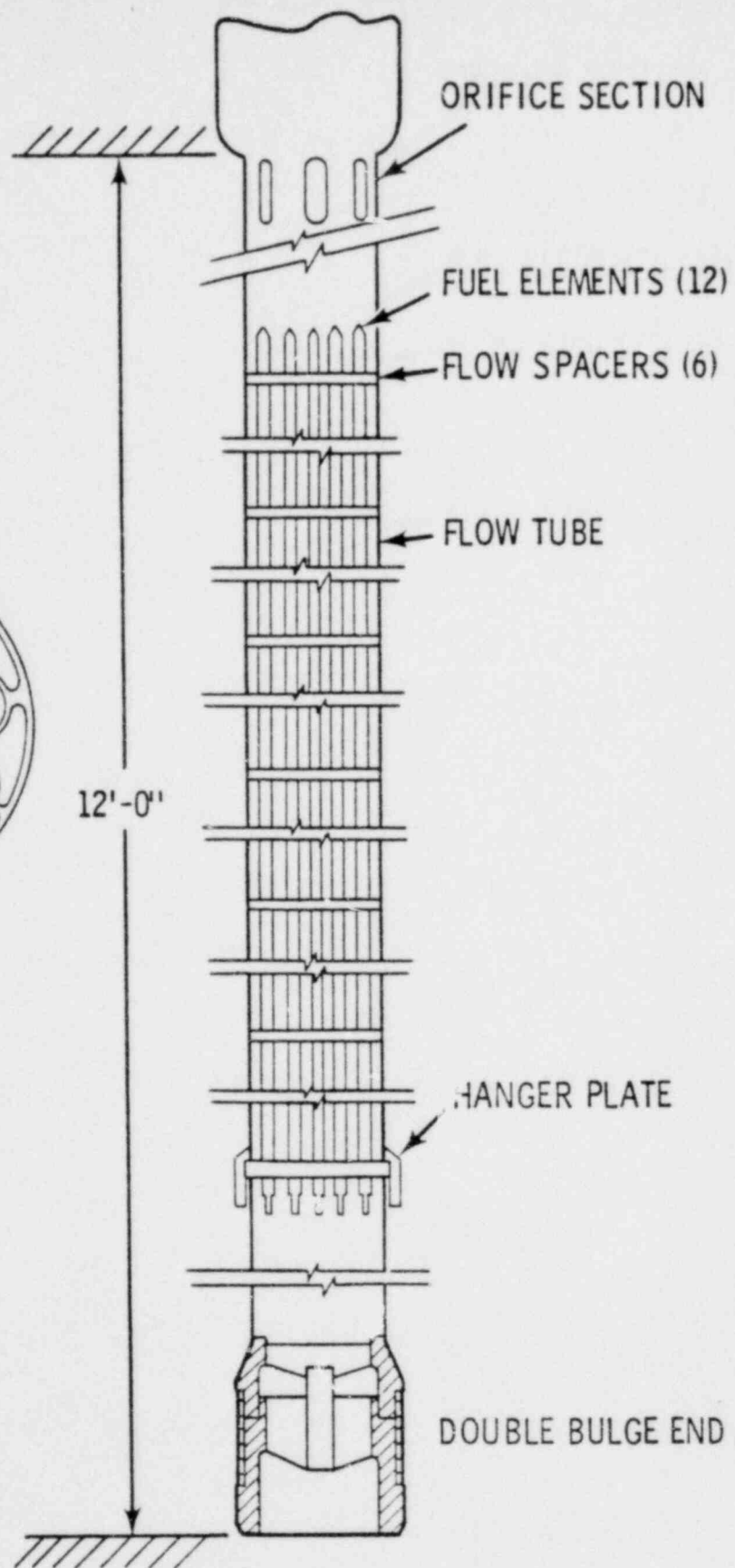


FIGURE 5.1 NRU Reactor Driver Fuel Rod

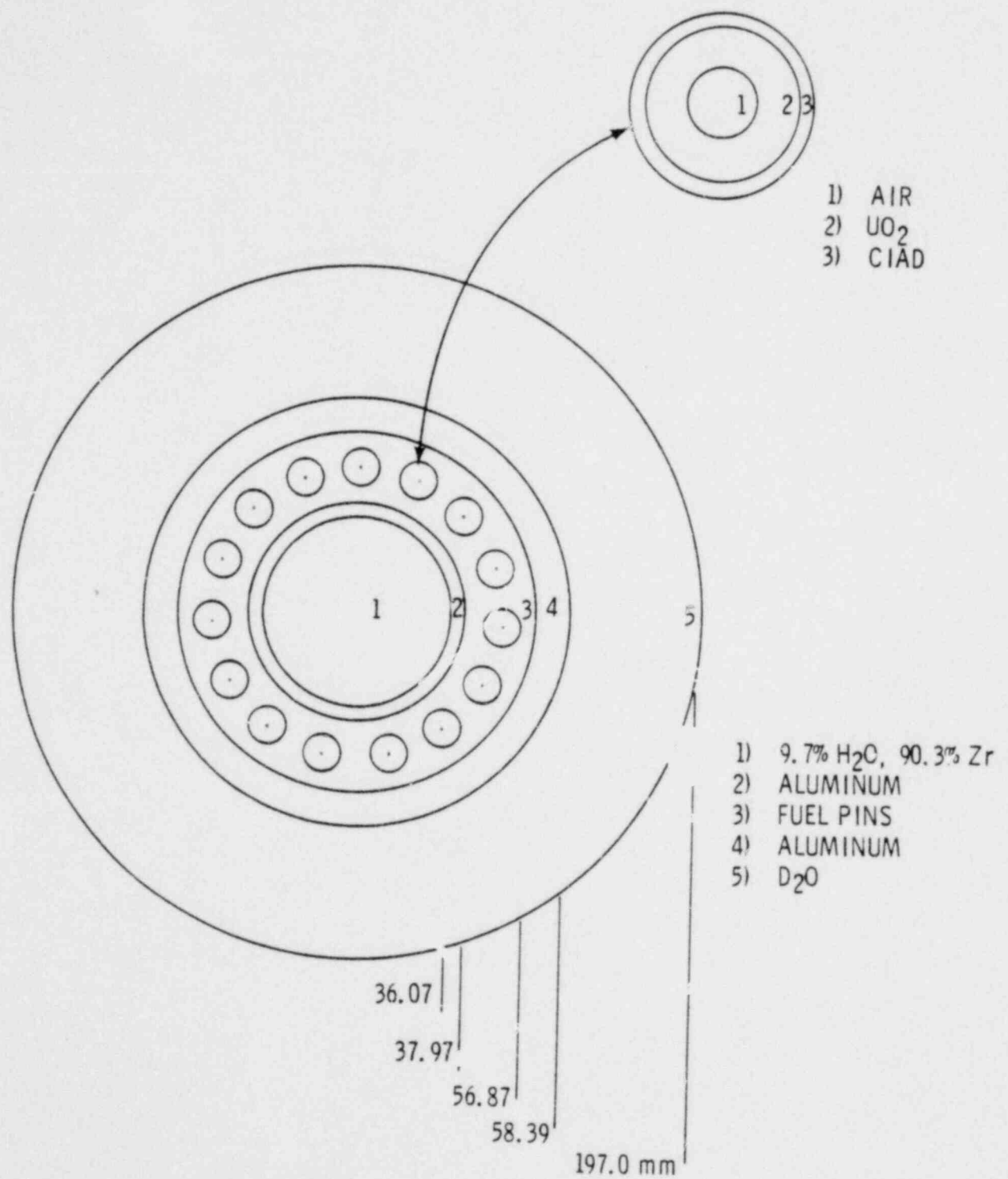


FIGURE 5.2 Thorium and Fast Neutron Rod Model

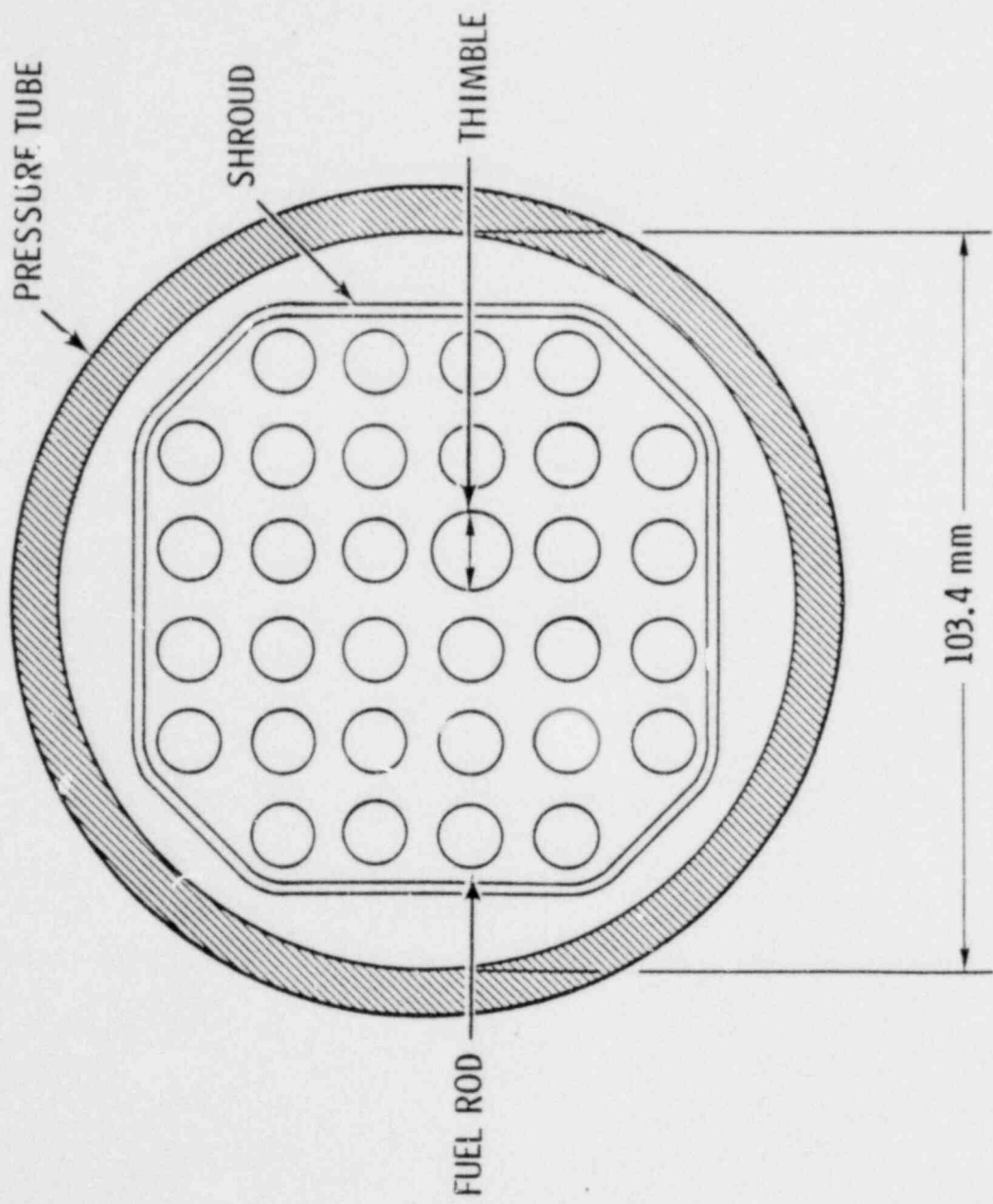


FIGURE 5.3 Reactor Test Bundle

cross sections from ANISN are combined with the thermal group cross sections from BRT to produce a single 4 group set of cross sections to describe the fuel bundle lattice cell. The SMEAR cross sections are used to model the NRU driver fuel, thorium rods, and fast neutron rods in all the reactor models. They are also used to model the test assembly in the 2D full core model.

The use of the SMEAR cross sections to model the test bundle lattice cell provides no discrete information concerning the flux profile across the fuel pins. The lack of discrete information is due to the smearing action present in the production of a single set of cross sections to model the entire lattice cell. To provide the discreteness necessary to generate flux profiles, a second type of cross section generation, for the test bundle, was developed.

The second type of cross section generation is called the DISCRETE model (see Figure 5.5). The DISCRETE model follows the same steps as the SMEAR model up to the point of producing a single set of cross sections for the entire lattice cell from both ANISN and BRT. The DISCRETE model takes the output from ANISN and extracts the cross sections calculated for only the fueled region of the lattice cell. The cross sections for each region of the lattice cell, at this point, have been both volume and flux weighted against the cell as a whole. The DISCRETE model corrects for the volume and flux weighting to produce a single set of cross sections (3 fast groups, 1 thermal) to describe the fuel region only. The output of BRT allows for the direct extraction of a single set of thermal cross sections which describes only the fuel region. 3 fast group cross sections from ANISN are then combined with the thermal group cross sections from BRT to produce a single set of cross sections which describe the fueled region of the test bundle lattice cell.

The DISCRETE model provides a method of discretely modeling the test bundle in the final 2D quarter core and axial models which allows for the extraction of flux profiles within the test fuel.

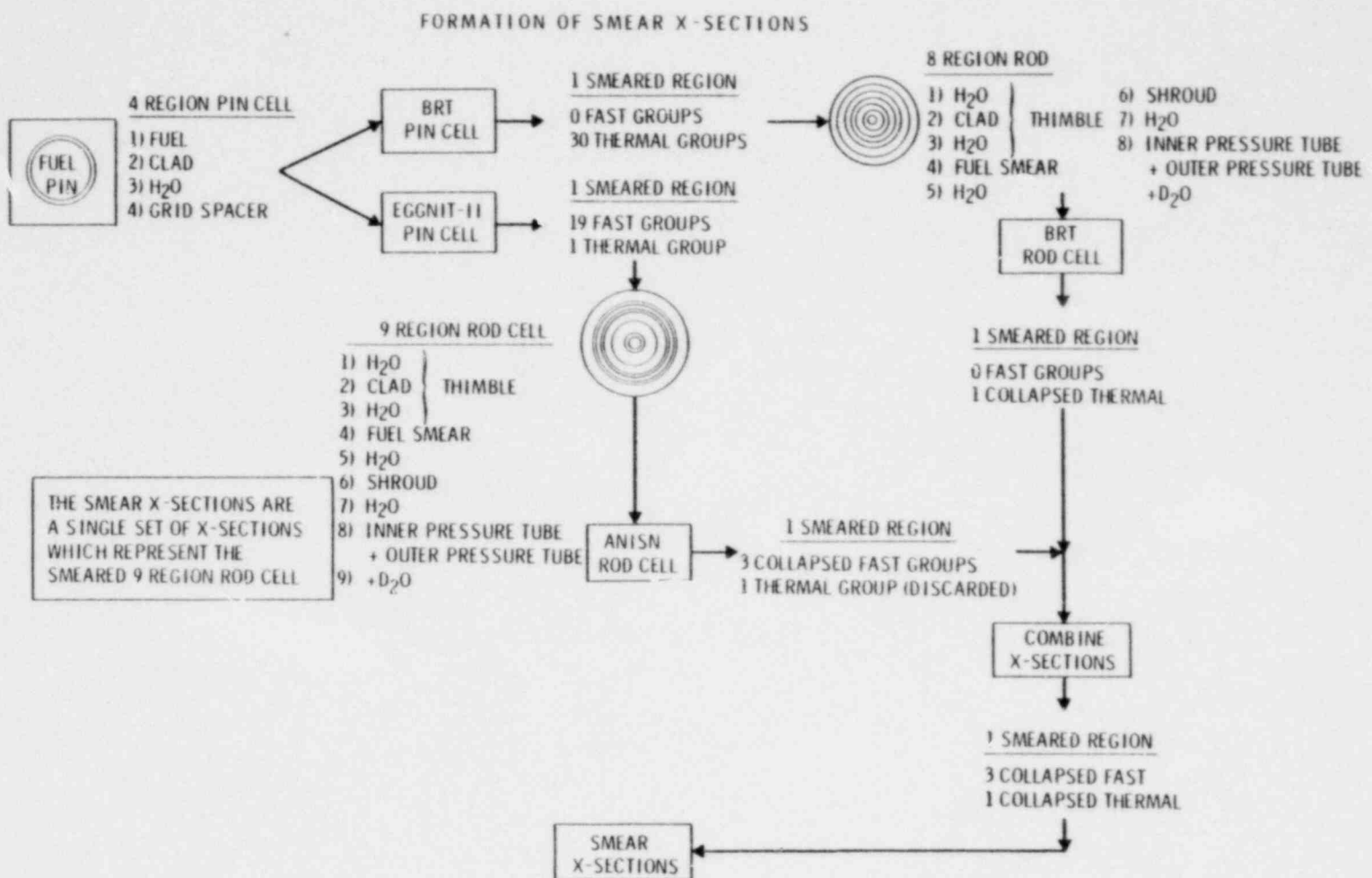


FIGURE 5.4 Formation of Smear X-Sections

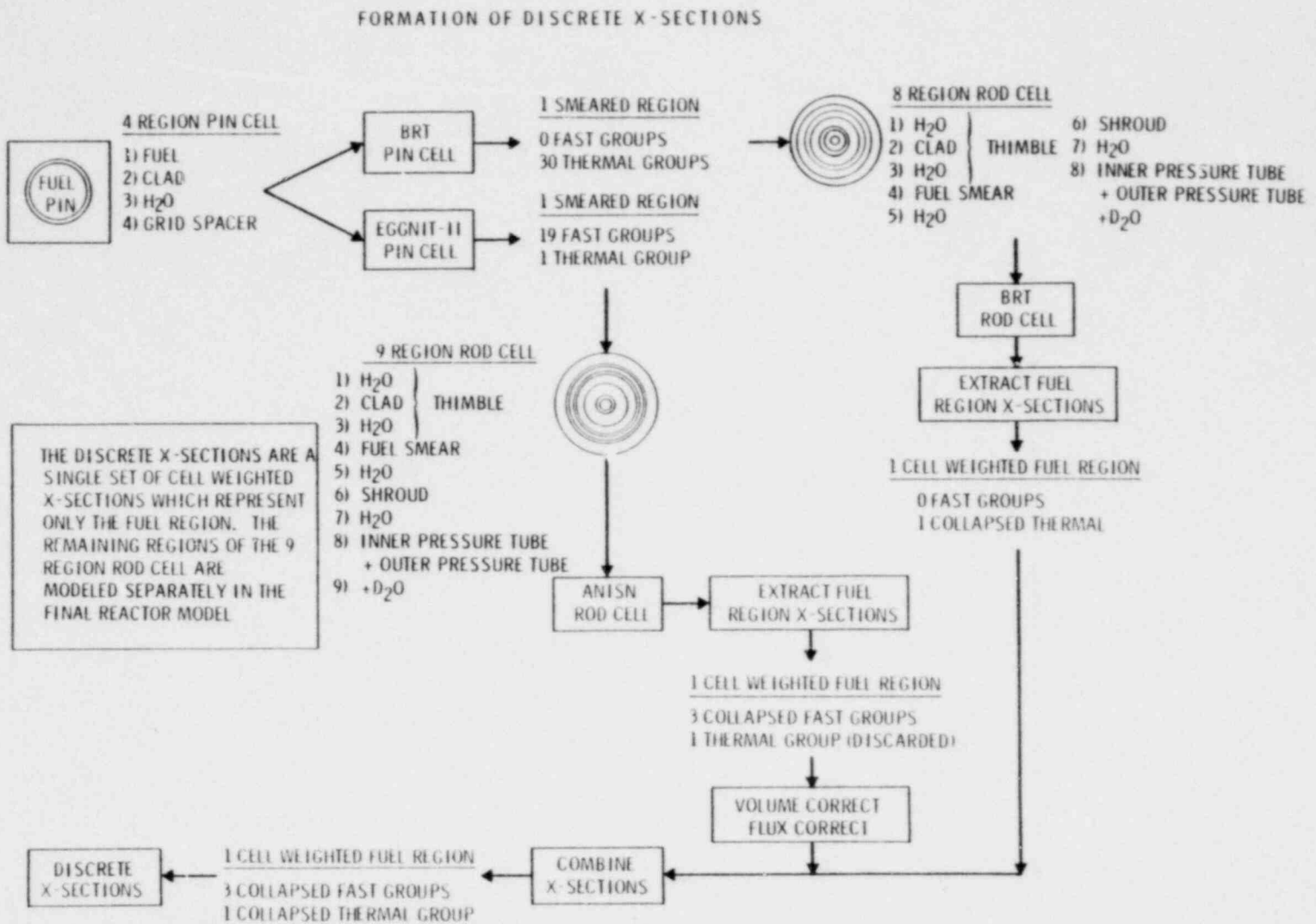


FIGURE 5.5 Formation of Discrete X-Sections

5.2 EXPOSURE MODELING

The fueled lattices present in the NRU reactor cover a wide range of burnups. The models which were used to account for the burnup in the different types of elements are presented below.

Driver Fuel Burnup

Burnup of the driver fuel was done with the LEOPARD code. Because of the limitations in LEOPARD, the parameters were adjusted such that the beginning-of-life reactivity matched that calculated with a simplified BRT/EGGNIT calculation.

The existing fission product model in the LEOPARD code was not adequate to track the burnup of the driver fuel, so considerable effort was expended in modifying it. Except for ^{135}Xe and ^{149}Sm , the fission products are combined and represented as a cross section per fission which varies with exposure in each group. The ^{135}Xe and ^{149}Sm are calculated and entered explicitly. We used the CINDER code to determine the value of the fission product cross section for the driver fuel. The data used in CINDER consist of ENDF/B-IV cross sections, actinide concentrations calculated by LEOPARD, and group fluxes calculated by LEOPARD. The resulting values are shown in Figure 5.6. For use in LEOPARD a table of values were input to the code.

The LEOPARD calculation was then repeated using the new fission product model. The calculated reactivity, k_{∞} , is compared to the AECL calculated curve in Figure 5.7. Our values show a 10% Δk early and late in life. At 400-500 GWd/MTM our values are 5% high. The discrepancy is not bad considering that the AECL values have been adjusted to match experimental results. It is important that the overall shape of our curve agrees with the AECL curve.

The isotopes from LEOPARD at several different exposures were used in double-pass EGNNIT/BRT/ANISN calculations. Pseudo fission products were used in BRT and EGNNIT such that the 2200 m/s value from LEOPARD and CINDER and the group 3 spectrum-averaged cross section from LEOPARD were preserved. The resulting k_{∞} values are also shown in Figure 5.7. At 357 GWd/MTM the reactivity effect due to fission products (except ^{135}Xe and ^{149}Sm) is -7.4% Δk for group 4 (thermal) and -0.9% Δk for group 3 (lowest epi-thermal). The effect of ^{135}Xe and ^{149}Sm is smaller than this and relatively constant through exposure.

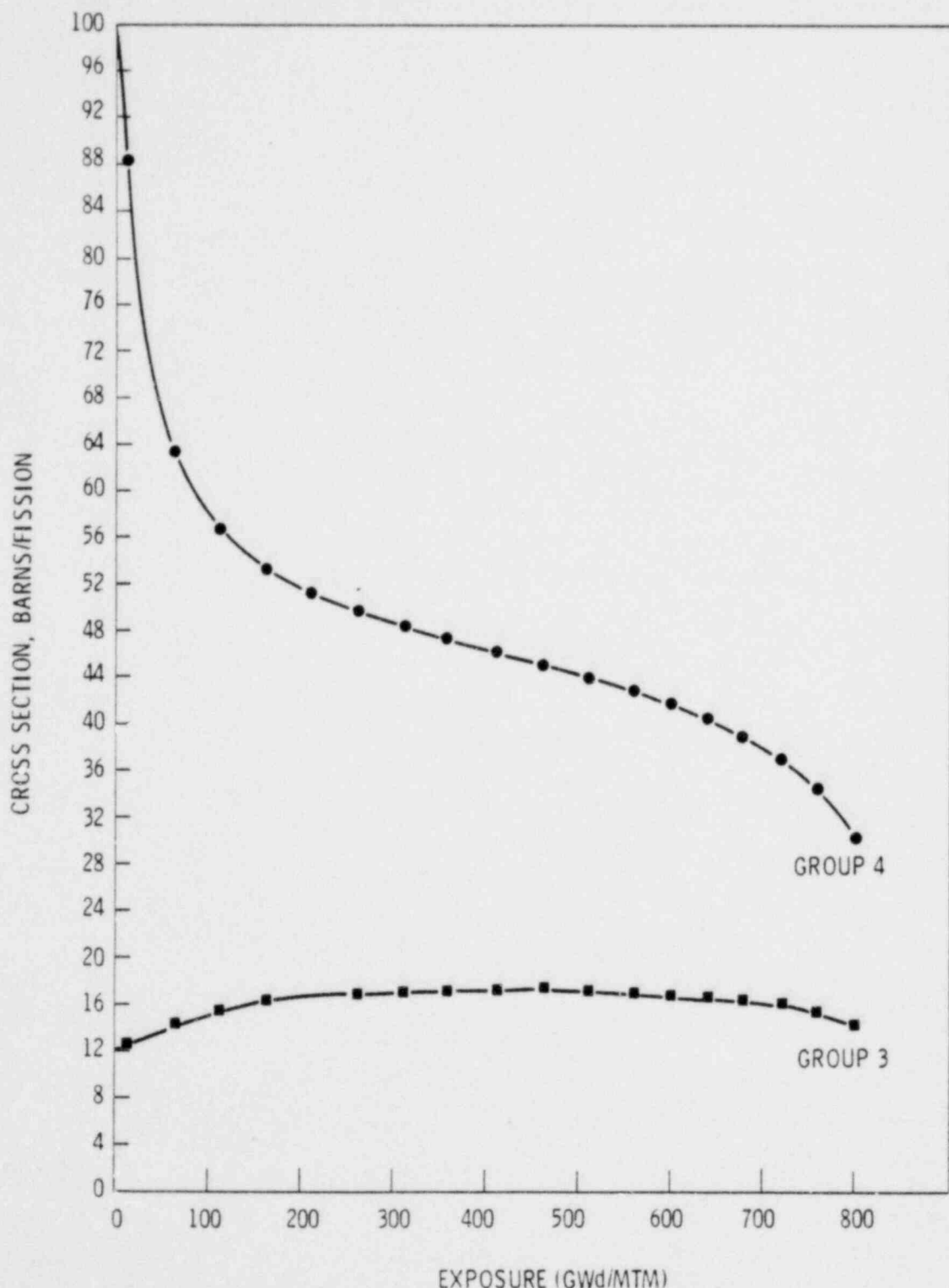


FIGURE 5.6 Fission Product Cross Section as a Function of Exposure
for NRU Driver Fuel (Group 4 - thermal, Group 3 - lowest
epi-thermal)

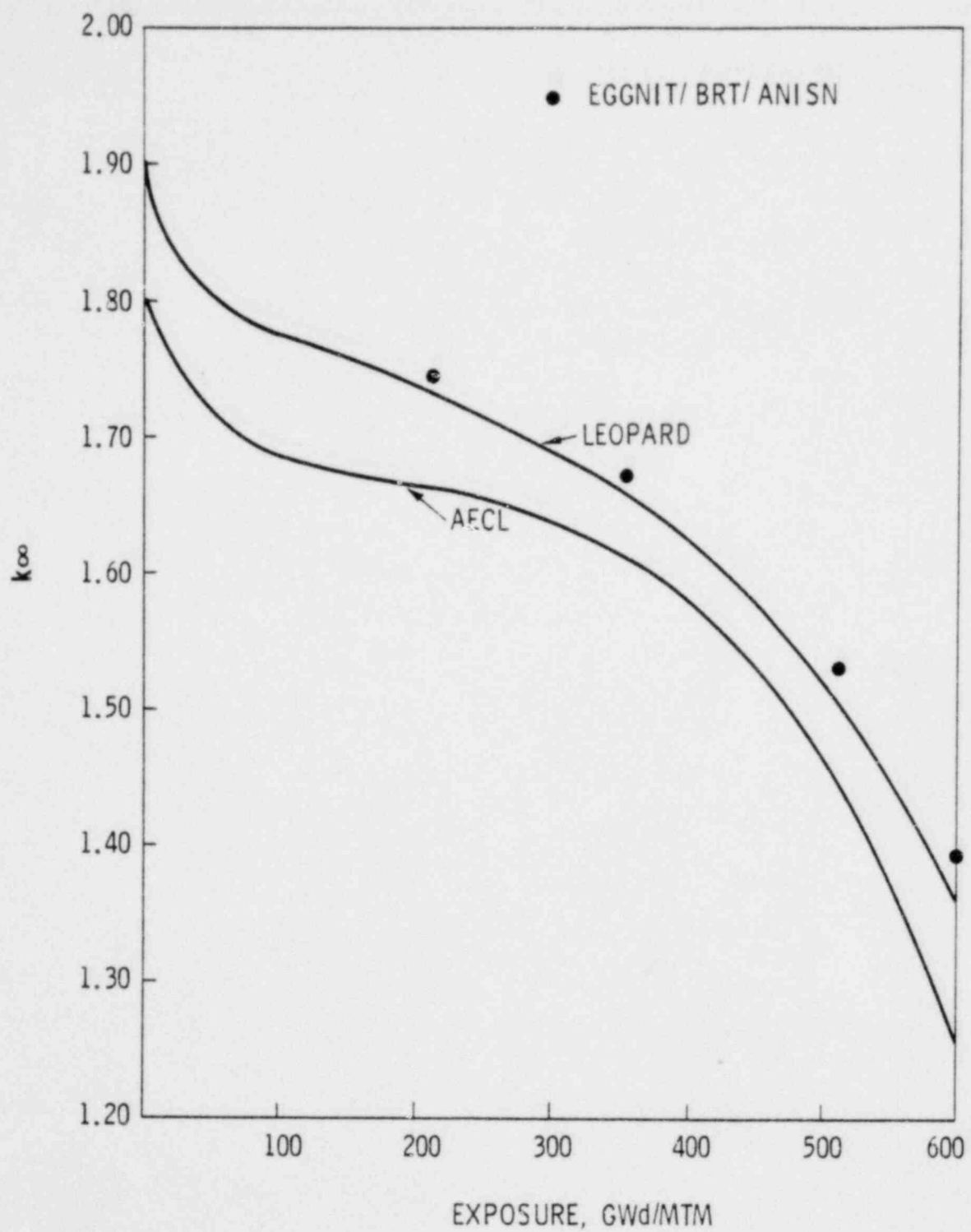


FIGURE 5.7 K-Infinity Values as a Function of Exposure for NRU Driver Fuel Rods

Fast Neutron Rod Burnup

Burnup calculations for the fast neutron rod were also performed with LEOPARD. The UO₂ fission product model already existing in PNL's version of LEOPARD was assumed to be adequate. This model is based on enriched UO₂ fuel, but since the exposure is not very high and the spectrum is very soft in the fast neutron rod, it was assumed that the model would predict the proper fission product absorption rate.

The fast neutron rod was modeled in LEOPARD such that the ²³⁸U resonance integral and the escape-to-thermal probability matched the results of double-pass BRT/EGGNIT/ANISN calculations. The resulting reactivity curve was much flatter than the curve generated by AECL. The most likely reason for our curve being too flat was the generation of too much ²³⁹Pu. The nonthermal-to-thermal flux ratio calculated with 2DB was much lower than the value calculated with LEOPARD or the value calculated with the double-pass model. Upon adjusting the LEOPARD parameters to match the 2DB nonthermal-to-thermal flux ratio, the reactivity curve became much steeper. It is compared to the AECL curve in Figure 5.8. In the softer neutron spectrum about 80% of the captures in ²³⁸U occur in the thermal neutron group. The ²³⁵U burnout rate and the ²³⁹Pu buildup rate are shown in Figure 5.9. Initially, ²³⁵U burns out very fast and ²³⁹Pu builds up very fast. At 6 GWd/MTM there is just as much ²³⁹Pu as ²³⁵U in the fast neutron rods.

At 12.9 GWd/MTM the fission products (except ¹³⁵Xe and ¹⁴⁹Sm) are worth -5.1% in Δk . 85% of this reactivity effect is in the thermal group. It is felt that a re-evaluation of the fission products with CINDER would not change their worth by more than 1.0% in Δk .

5.3 FULL CORE MODEL

The NRU core is modeled in two dimensions by the 2DBS computer code. Each hexagonal lattice cell is modeled by a set of six triangular mesh cells as shown in Figure 5.10. The material cross section sets used to describe each individual lattice cell are shown in Figure 5.11. In addition to the lattice cells which comprise the core of the NRU reactor, a representation is made of the

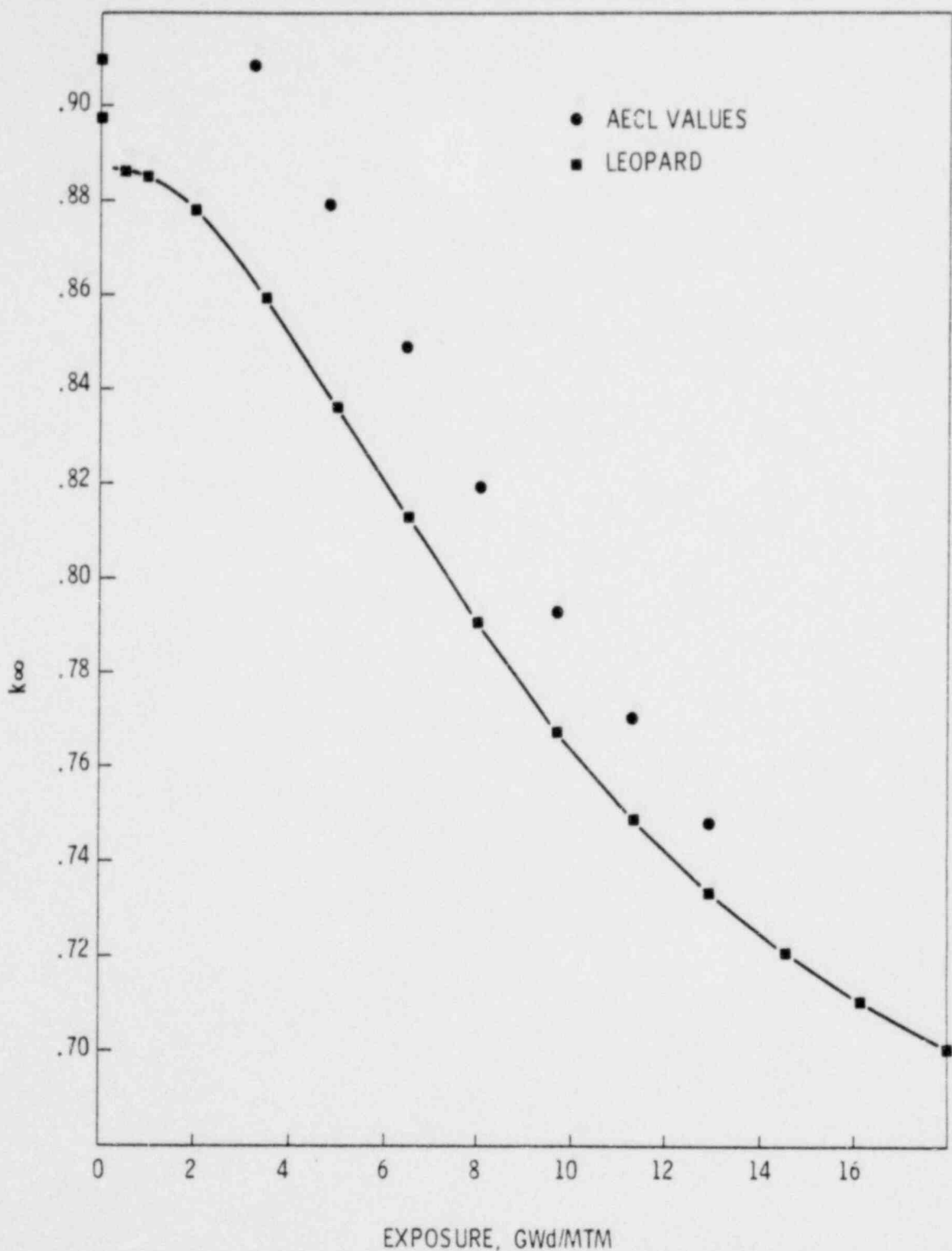


FIGURE 5.8 K-Infinity Values as a Function of Exposure for NRU Fast Neutron Rods

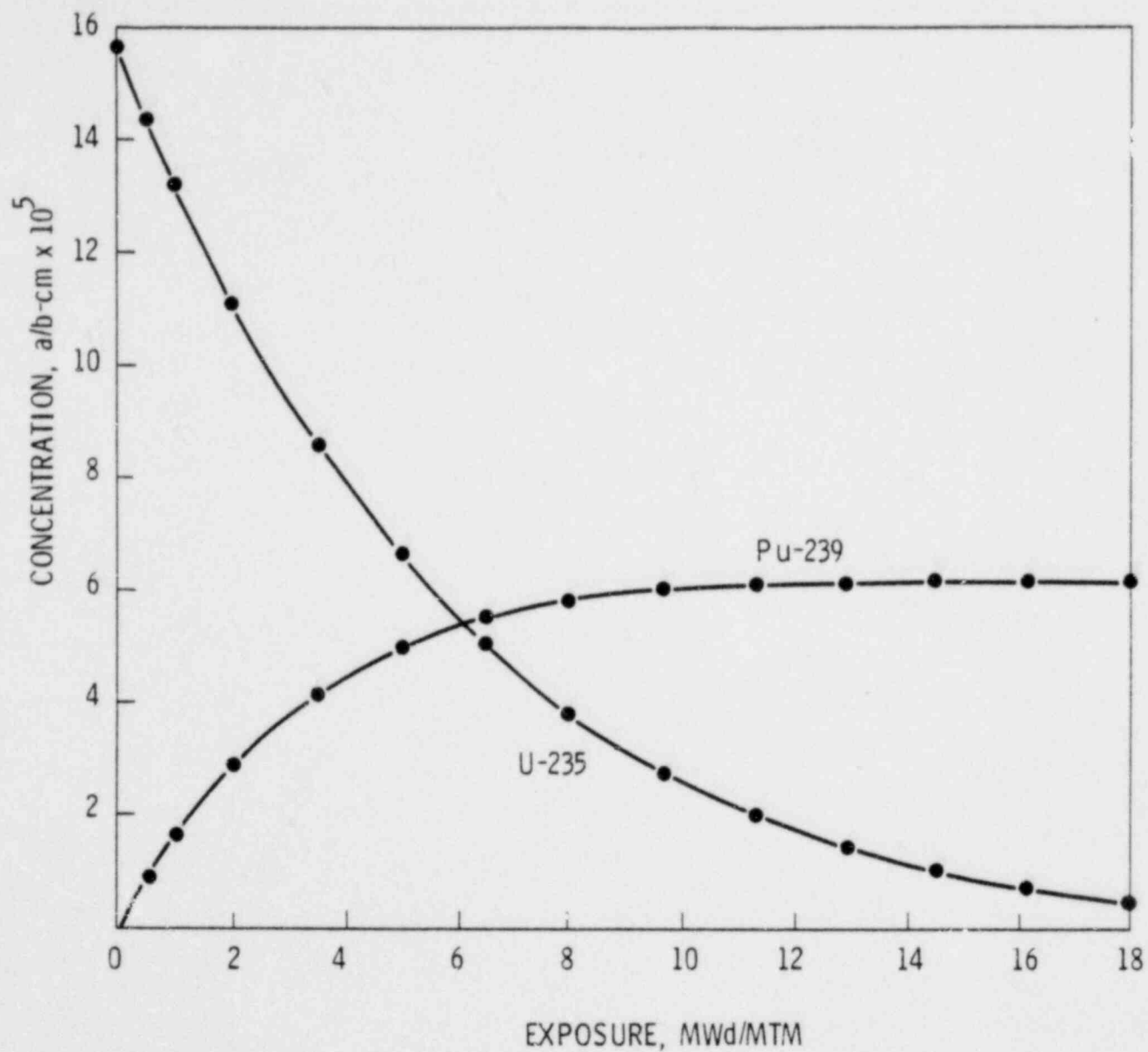


FIGURE 5.9 235U Burnout Rate and 239Pu Buildup Rate for NRU Fast Neutron Rods

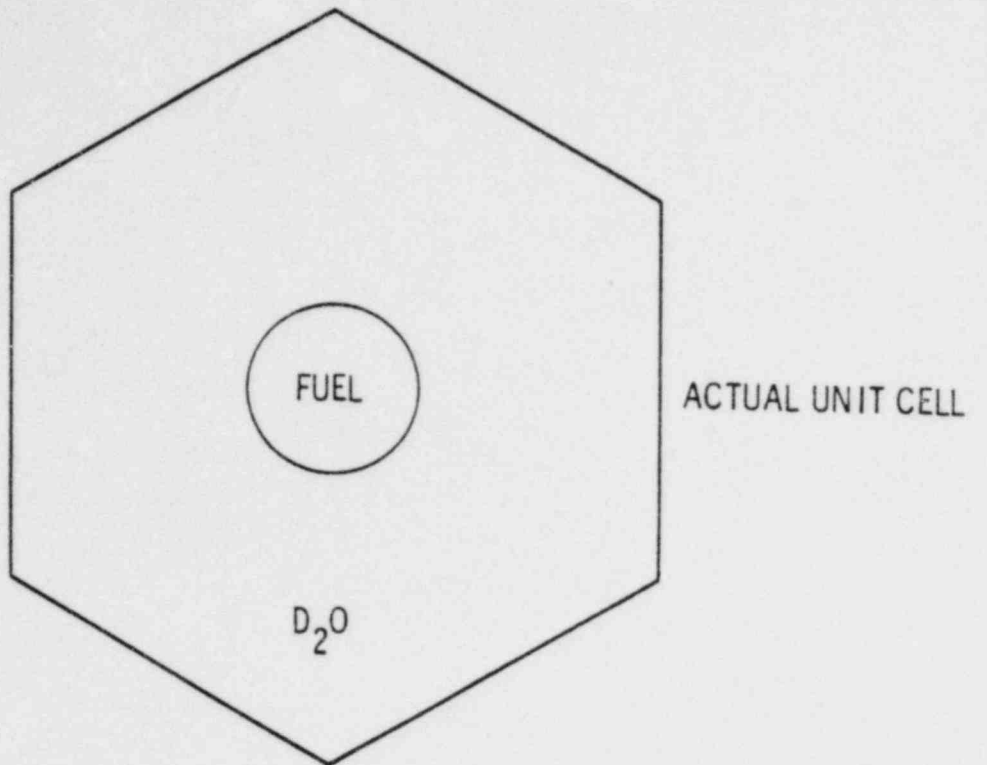
reactor's radial reflectors by placing approximately 200 mm of heavy water immediately adjacent to the core followed by 400 mm of light water and 150 mm of stainless steel structural material.

The NRU driver fuel is modeled by four distinct burnups. The range of actual burnups covered by each of the four modeled burnups is shown in Table 5.1. Cross sections have also been developed to describe thorium rods, fast neutron rods, and the four material test loops. The fission cross sections for the material test loops have been adjusted to give good agreement with the AECL power data. This adjustment is necessary due to the lack of proper modeling information caused by the complexity of the material within these rods.

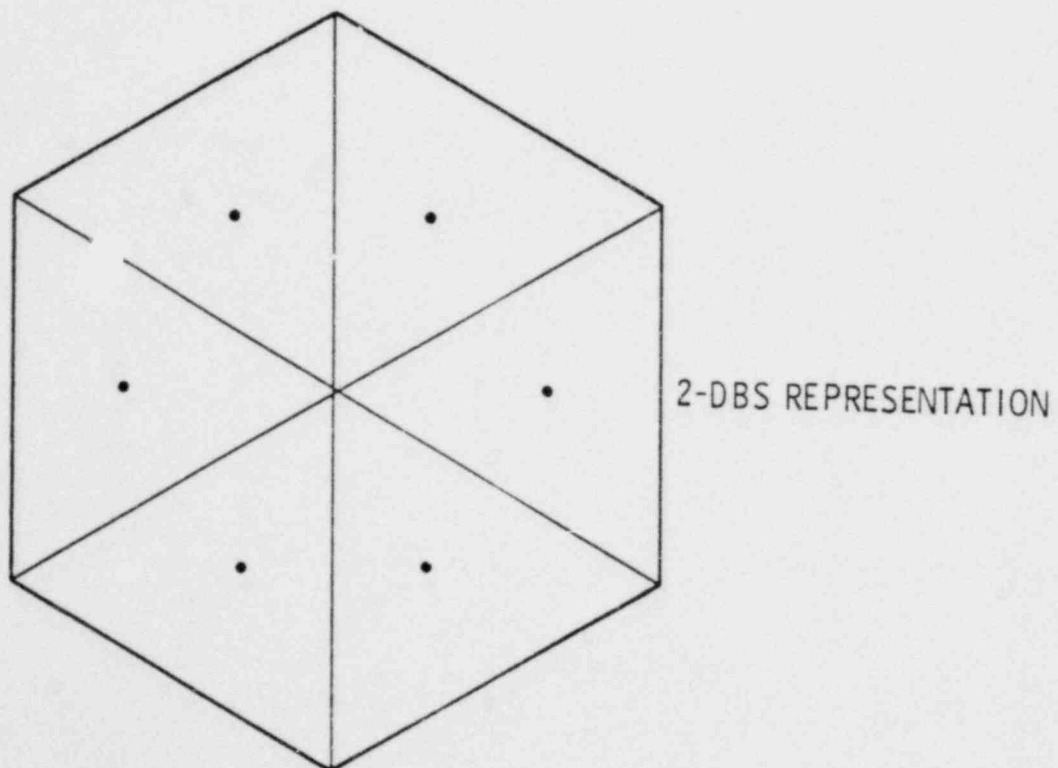
The NRU reactor contains 11 cadmium control rods and 7 cobalt control rods, but only a combination of the last three cobalt rods are normally used at power. Thus for simulation purposes the cadmium control rods have been modeled as D₂O cells while the removed cobalt rods, which have a shroud tube, are modeled as dummy rods. The dummy rod model is simply an aluminum tube 119 mm O.D. x .16 mm thick placed in a hexagonal cell of D₂O. The remaining cobalt rods are modeled by the effective amount of cobalt remaining in the core. An additional source of cobalt is obtained from the isotope and adjuster rods present in the core. The isotope and adjuster rods are also modeled according to the amount of effective cobalt presented in the core.

The remaining locations in the NRU core are taken by flux detectors or are vacant. The flux detectors are modeled by the dummy rod model mentioned above while the vacancies are modeled as a D₂O cell.

The test fuel bundle will be placed in the U-2 loop which is in the southwest portion of the reactor. This lattice position is normally occupied by an isotope rod containing 750 grams of cobalt. The test fuel bundle was modeled for three different enrichments ranging between 2 and 3 percent with two different shroud designs for both steam and hot water cooling. The various fuel enrichments and shroud designs were analyzed to support the selection of the fuel bundle design. The effect on the power generated by the test fuel bundle by increasing the surrounding flux was also investigated. The high flux or "hot configuration" replaces two higher exposure driver fuel rods adjacent to the test with two lower exposure rods. This surrounds the test.



ACTUAL UNIT CELL



2-DBS REPRESENTATION

FIGURE 5.10 2DBS Full Core Unit Cell Representation

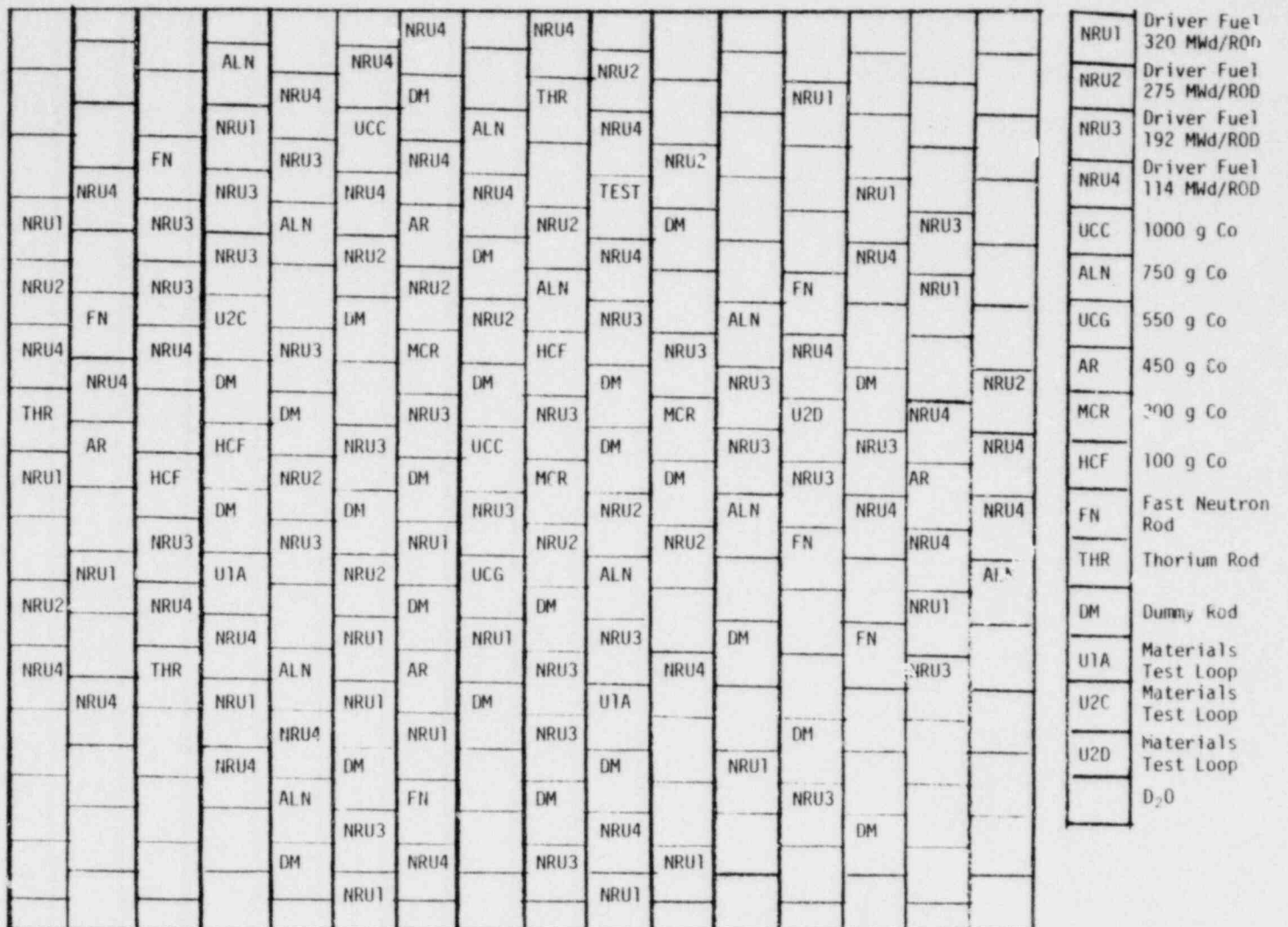


FIGURE 5.11. Full Core Model

TABLE 5.1. Range of Burnups Covered by
Modeled Burnups

<u>Driver Fuel Burnup</u>	<u>Modeled Burnup</u>
0 - 140 MWd/ROD	114 MWd/ROD
140 - 240 MWd/ROD	192 MWd/ROD
240 - 300 MWd/ROD	275 MWd/ROD
300 - 360 MWd/ROD	320 MWd/ROD

with four of the lowest exposure, hence hottest, driver fuel rods.

The powers generated by the test fuel bundle for the various enrichments, shroud designs and driver fuel configurations are given in the following section.

5.4 RESULTS

The powers predicted for test fuel bundle for various enrichments and shroud designs are given in Table 5.2. The powers predicted for the cases where the adjacent fueled locations are fueled with low burnup fuel (high flux cases, hot configuration) are also given.

The powers are taken from the 2DBS output for the full core model. The 2DBS computer code generates the total power produced within the test fuel bundle lattice cell. These powers are normalized to account for the test bundle's 3.66 m length when compared to the driver fuels 2.74 m length. The resulting power is divided by the number of pins in the test bundle and the total height of the pins. This procedure generates an axially and radially averaged linear power rate for the fuel pins.

Table 5.3 gives the reactor power required to give a specified linear power within the test assembly. Only the steam cooled cases are presented since it is the heatup and transient phases of the test operation which are concerned with relatively low reactor powers.

TABLE 5.2. Calculated Powers for Various Test Bundle Configurations
 (Reactor at 127 MW)

Enrichment	Coolant	Shroud Size	Flux Field	Power (kW/m)
2.0	Water	Nominal	Nominal	15.8
2.0	Water	Thick	Nominal	13.7
2.0	Water	Thick	Hot	14.5
2.5	Water	Nominal	Nominal	18.7
2.5	Water	Thick	Nominal	16.2
2.5	Water	Thick	Hot	17.1
3.0	Water	Nominal	Nominal	21.1
3.0	Water	Thick	Nominal	18.8
3.0	Water	Thick	Hot	19.7
2.0	Steam	Nominal	Nominal	16.9
2.0	Steam	Thick	Nominal	12.8
2.0	Steam	Thick	Hot	13.4
2.5	Steam	Nominal	Nominal	20.1
2.5	Steam	Thick	Nominal	15.0
2.5	Steam	Thick	Hot	15.7
3.0	Steam	Nominal	Nominal	22.2
3.0	Steam	Thick	Nominal	16.9
3.0	Steam	Thick	Hot	17.7

TABLE 5.3. Reactor Power Required to Obtain Specified Power in Test Bundle

<u>Enrichment</u>	<u>Coolant</u>	<u>Shroud</u>	<u>Flux</u>	Reactor Power Required (MW) to Obtain		
				.98 kW/m	1.31 kW/m	1.64 kW/m
2.0	Steam	Nominal	Nominal	7.35	9.83	12.30
2.0	Steam	Thick	Nominal	9.75	13.04	13.04
2.0	Steam	Thick	Hot	9.27	12.40	15.52
2.5	Steam	Nominal	Nominal	6.19	8.27	10.36
2.5	Steam	Thick	Nominal	8.32	11.12	13.92
2.5	Steam	Thick	Hot	7.92	10.58	13.25
3.0	Steam	Nominal	Nominal	5.60	7.49	9.38
3.0	Steam	Thick	Nominal	7.35	9.83	12.30
3.0	Steam	Thick	Hot	7.02	9.39	11.75

6.0 POWER PROFILES

After the magnitude of the power the next item of concern is the shape of that power in the reactor and in the test. This section describes the estimates obtained for those shapes. First, the profile of the neutron flux across the reactor as calculated by the full core model is shown. This shows the relation of the flux in the test to that in adjacent reactor regions. This model was described in the preceding section.

The reactor and test are also modeled in a quarter core and a R-Z axial geometry to provide more detail. The quarter core model provides pin to pin power shape information and the R-Z axial model shows the power as a function of height. The models and results of these two geometries are described below.

6.1 FULL CORE RADIAL FLUX PROFILES

A plot of total flux through the regions including the U-2 loop where the test bundle is located is shown in Figure 6.1. The flux depression near the center of the reactor is caused by a cobalt control rod. The test bundle is also shown to cause a depression in the total flux.

The flux profile was calculated with 2DBS using the model shown in Figure 5.11. The flux peak occurs near a NRU driver fuel rod at a radial distance of approximately 250 mm from the reactor center. This flux peak is shown as the flattened portion of the flux curve with a relative flux value of 1.0. The remaining flux values are normalized to this portion of the curve. The test bundle was modeled at a 2.5 percent enrichment with a thickened shroud and steam as a coolant. The flux profiles shown by the other various combinations of enrichment, shroud shapes, and coolants all exhibit the same characteristics as the case plotted.

6.2 QUARTER CORE MODEL AND RESULTS

Quarter Core Model

In order to get detail within the test bundle, a finer mesh 2D model was required, however, a fine mesh model of the full core generates an unmanageably large number of mesh spacings. Therefore, a quarter core model was developed. The hexagonal lattice cells were approximated by rectangular cells conserving cross sectional area. The resulting model

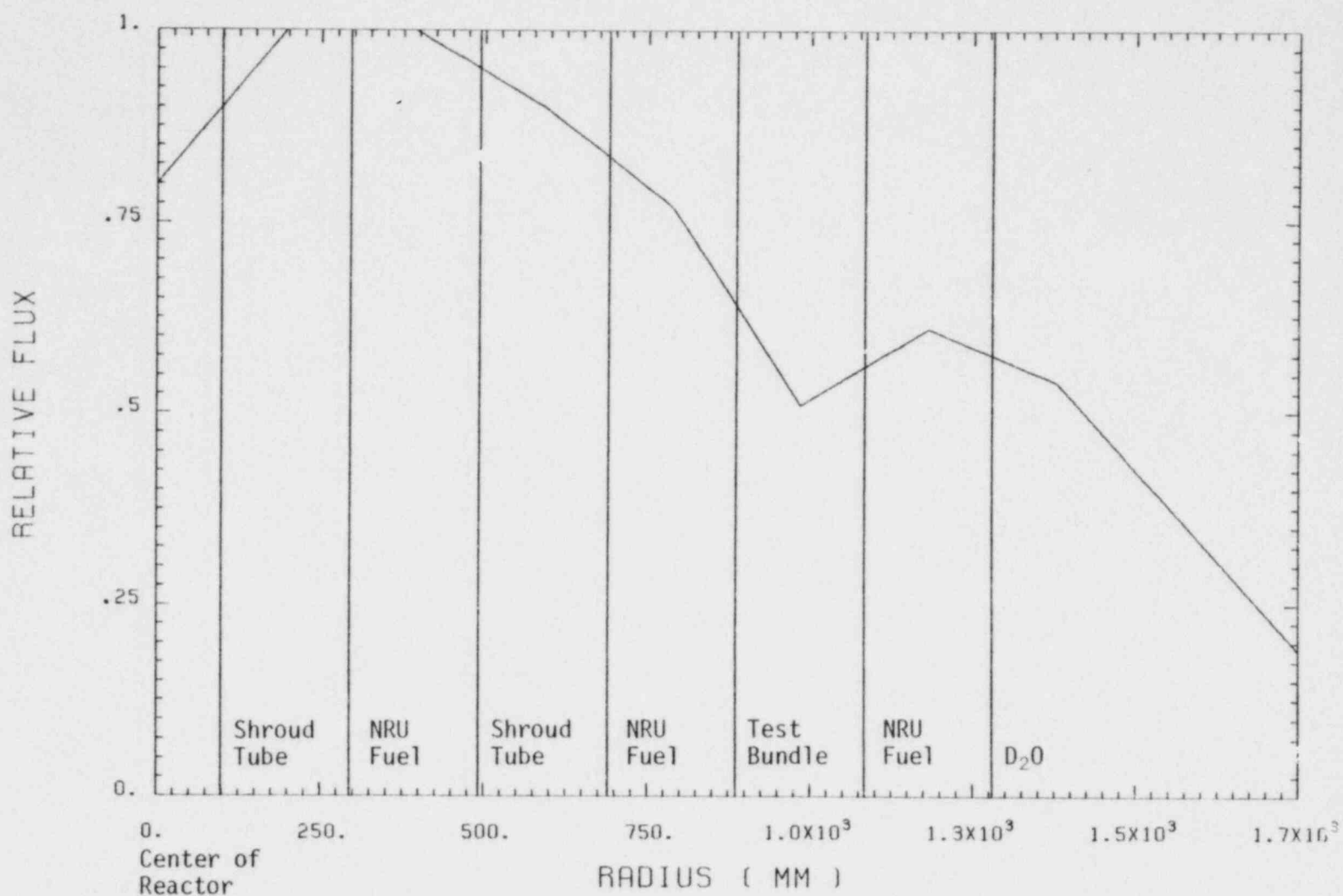


FIGURE 6.1 NRU Radial Flux Profile

is shown in Figure 6.2. The left hand, bottom corner of the figure is the reactor center. A reflecting boundary condition was applied on the left hand and bottom boundaries. This approximates the full reactor while requiring only a quarter core description. In a symmetric reactor the error in such an approximation is quite small. The NRU is, unfortunately, quite asymmetric and therefore, the absolute power values from this model are somewhat suspect and not used. The full core model is deferred to for absolute powers. However, the neutron flux is likely not to be highly asymmetric, despite the heterogeneous reactor composition. Relative powers, compared point to point, should be acceptable. Therefore, the error introduced in the power profiles from the quarter core approximation is felt to be small.

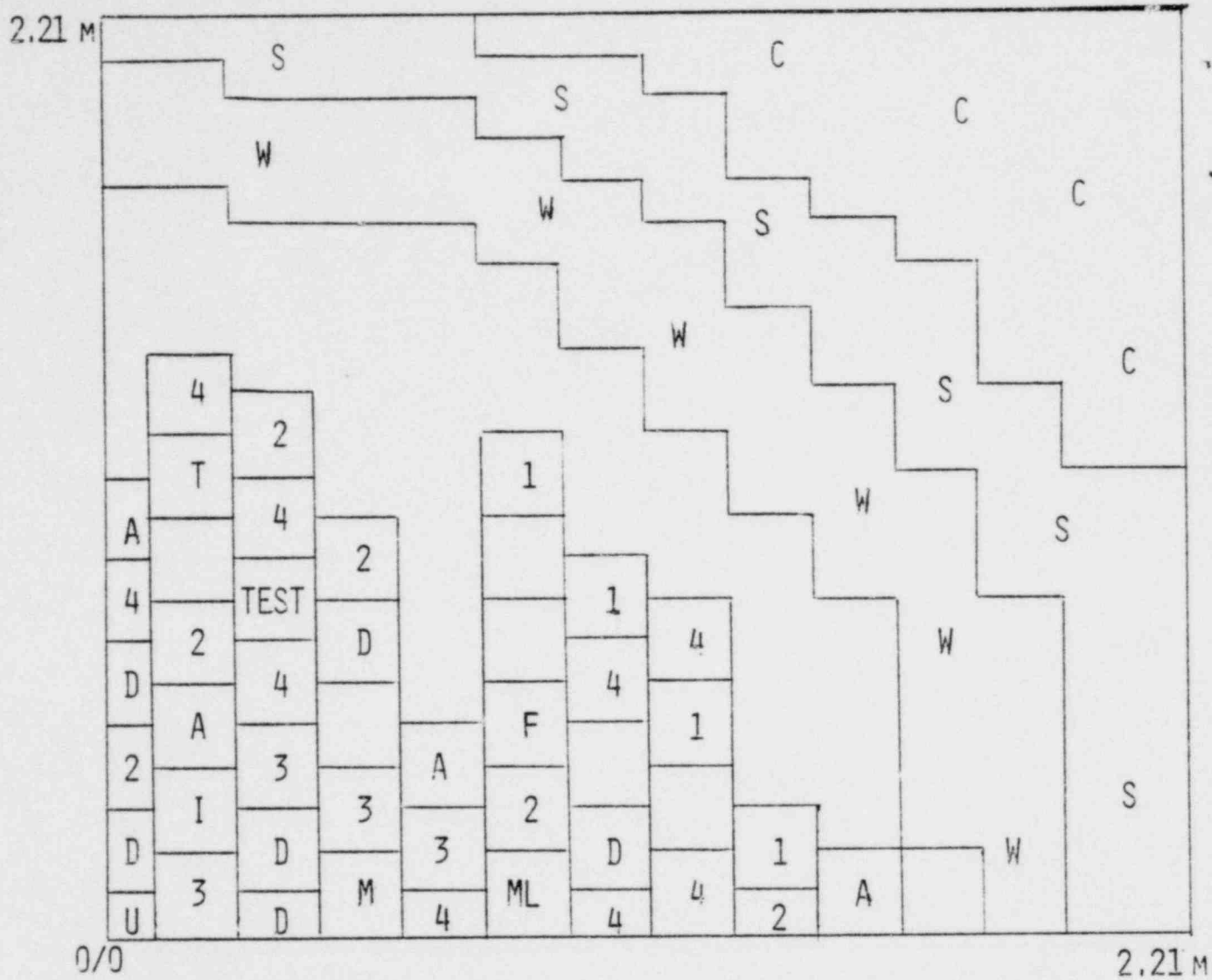
Figure 6.2 shows the location of the test within the quarter core model. Figure 6.3 and 6.4 describe the detail of the test for the nominal and thick shrouds respectively. Each fuel pin is modeled as a homogeneous region whose cross sections are prepared from the discrete model as described in Section 5.1. The fuel pin regions are shown as a blank square in the figures.

Quarter Core Results

The results from the quarter core model are shown in Figures 6.5A-F and 6.6A-F. These figures are pin power maps giving the normalized axially averaged power in the pins. The powers are normalized to the average power in the assembly.

Along with a description of the case being displayed, three other parameters are given in the legend associated with the maps. The first of these is the peaking. This is the ratio of the highest pin's power to the lowest pin's power. The tilt is the ratio of highest to lowest pin taken along a diagonal at the edge of the assembly. The maximum tilt tends to be along the southeast-northwest diagonal. The final parameter is the radially and axially averaged power for the assembly as predicted by the full core model. Thus the power in any rod can be found by multiplying the normalized value from the map by this average power.

Figures 6.5A-F compare the nominal and thick shrouds. The nominal shrouds are shown at the top of the figure, the thick shroud case at the



<u>1</u>	NRU Fuel #1 (320 MWd/Rod)	A	ALN 750g Co
<u>2</u>	NRU Fuel #2 (275 MWd/Rod)	I	Isotope 100g Co
<u>3</u>	NRU Fuel #3 (192 MWd/Rod)	F	Fast Neutron Rod
<u>4</u>	NRU Fuel #4 (114 MWd/Rod)	W	H ₂ O (20° C)
<u>U</u>	UCC 950g Co	S	Steel
<u>D</u>	Dummy/Shroud Tube	C	Concrete
<u>M</u>	MCR 350g Co	T	Thorium Rod
<u>ML</u>	U2O Materials Loop		D ₂ O

FIGURE 6.2 Quarter Core Model

TEST CELL IN NRU

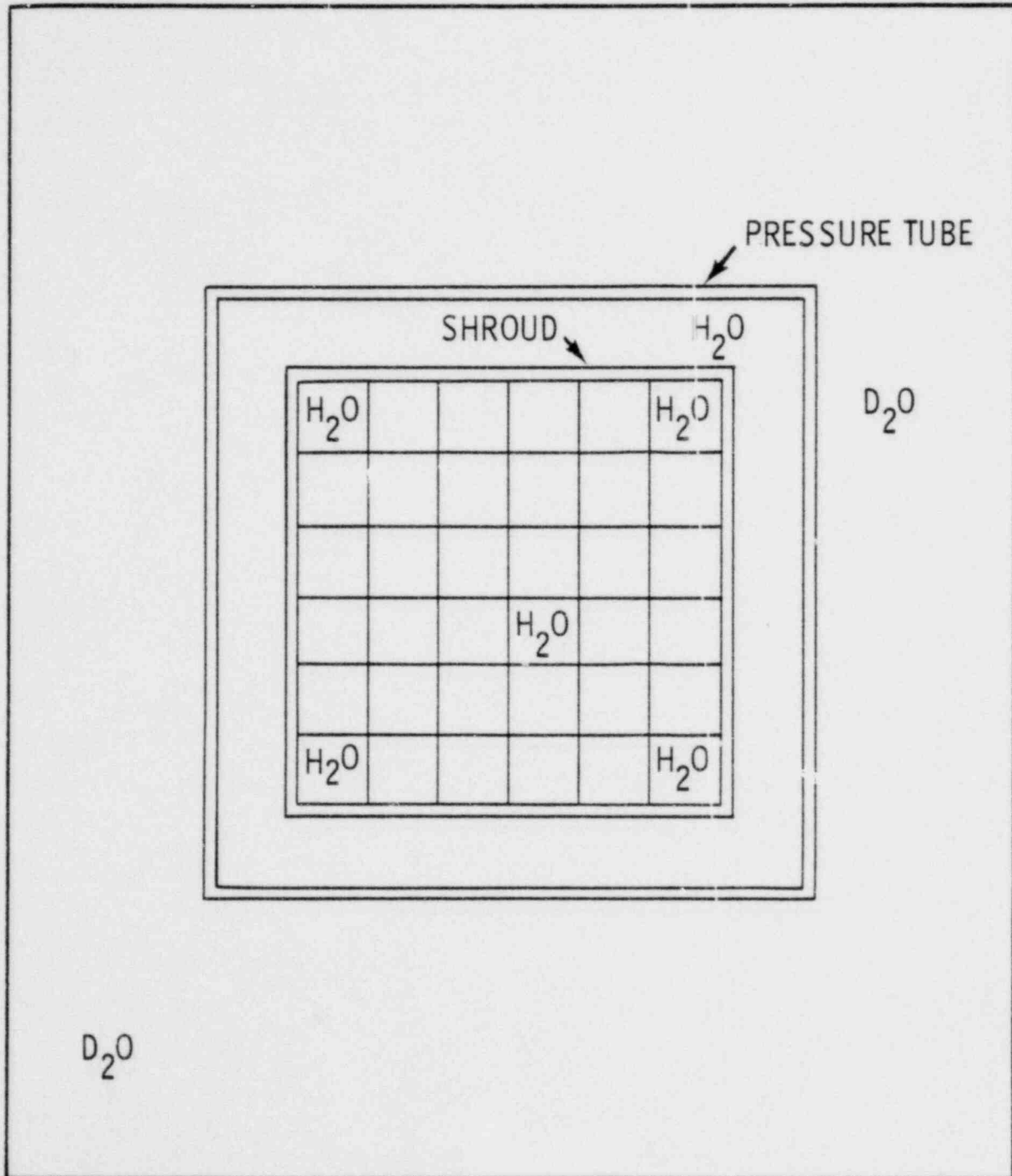


FIGURE 6.3 Detail of Nominal Shroud Test Assembly in Quarter Core Model

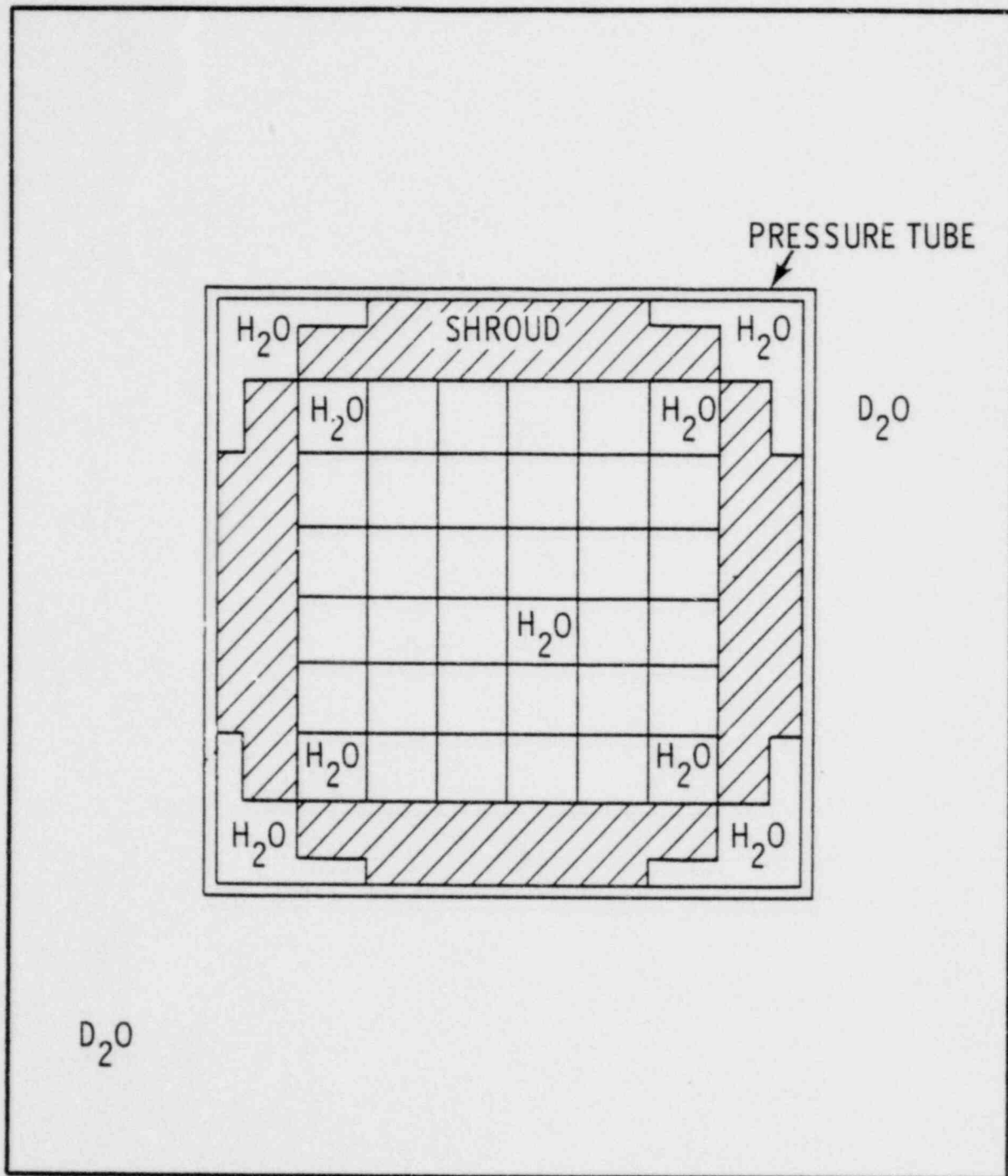
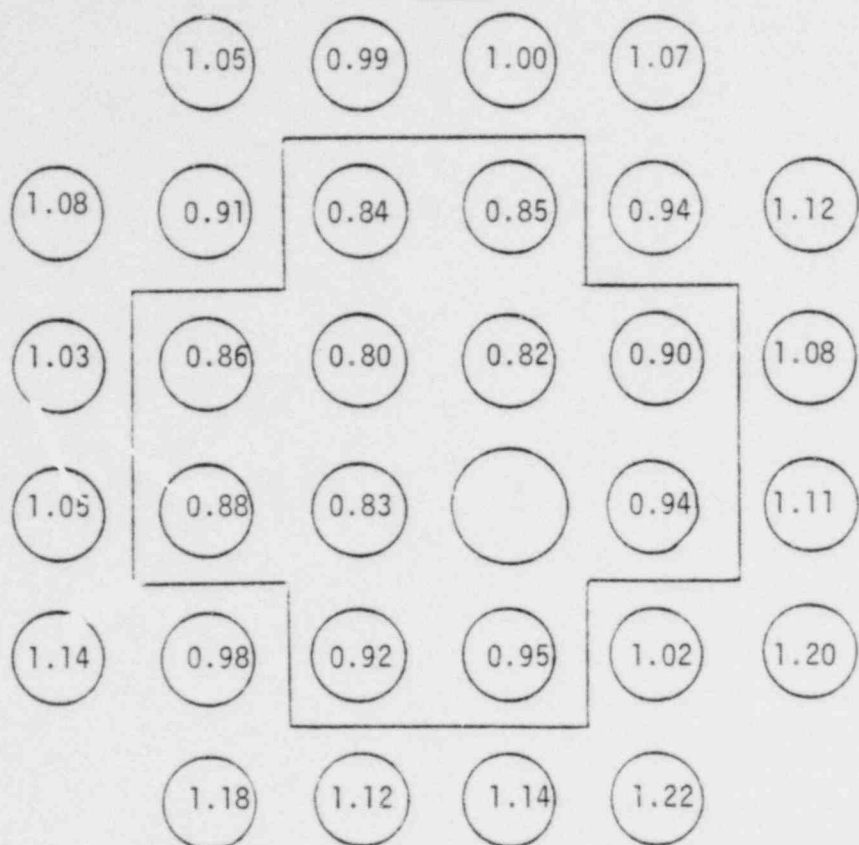


FIGURE 6.4 Detail of Thick Shroud Test Assembly in Quarter Core Model

FIGURE 6.5A. Normalized Pin Power Map, Nominal and Thick Shrouds

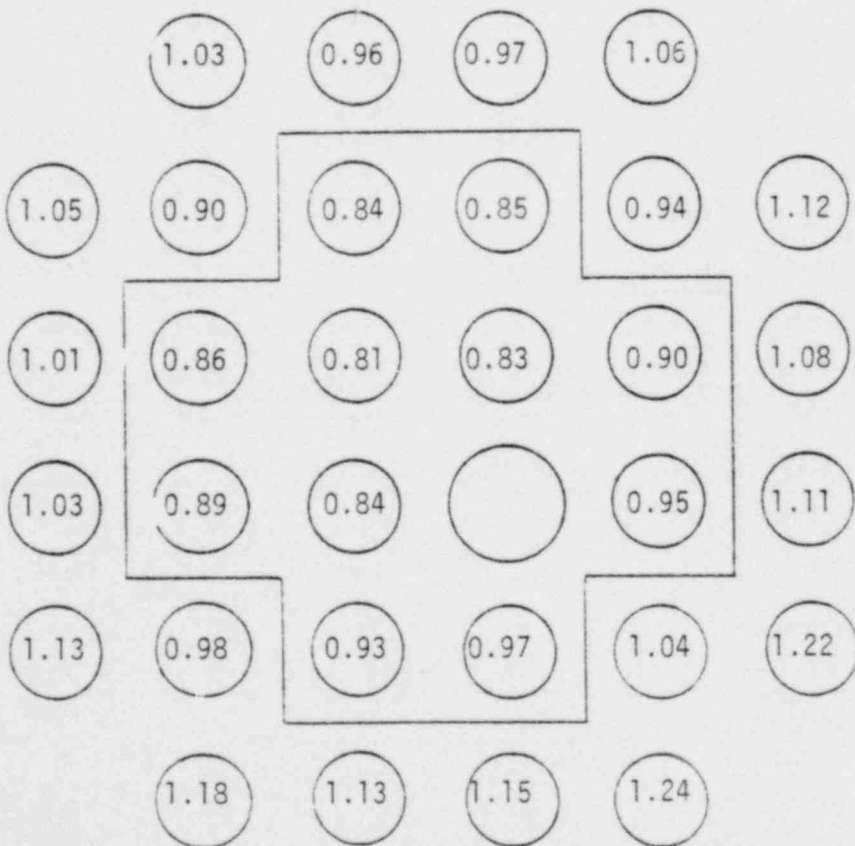
South



Coolant:	Water
Shroud:	Nominal
Enrichment:	2.0 wt% ^{235}U
Configuration:	Nominal

Peaking:	1.53
Tilt:	1.16
Average Power:	15.7 kW/m

South



Coolant:	Water
Shroud:	Thick
Enrichment:	2.0 wt% ^{235}U
Configuration:	Nominal

Peaking:	1.53
Tilt:	1.20
Average Power:	13.7 kW/m

FIGURE 6.5B. Normalized Pin Power Map, Nominal and Thick Shrouds

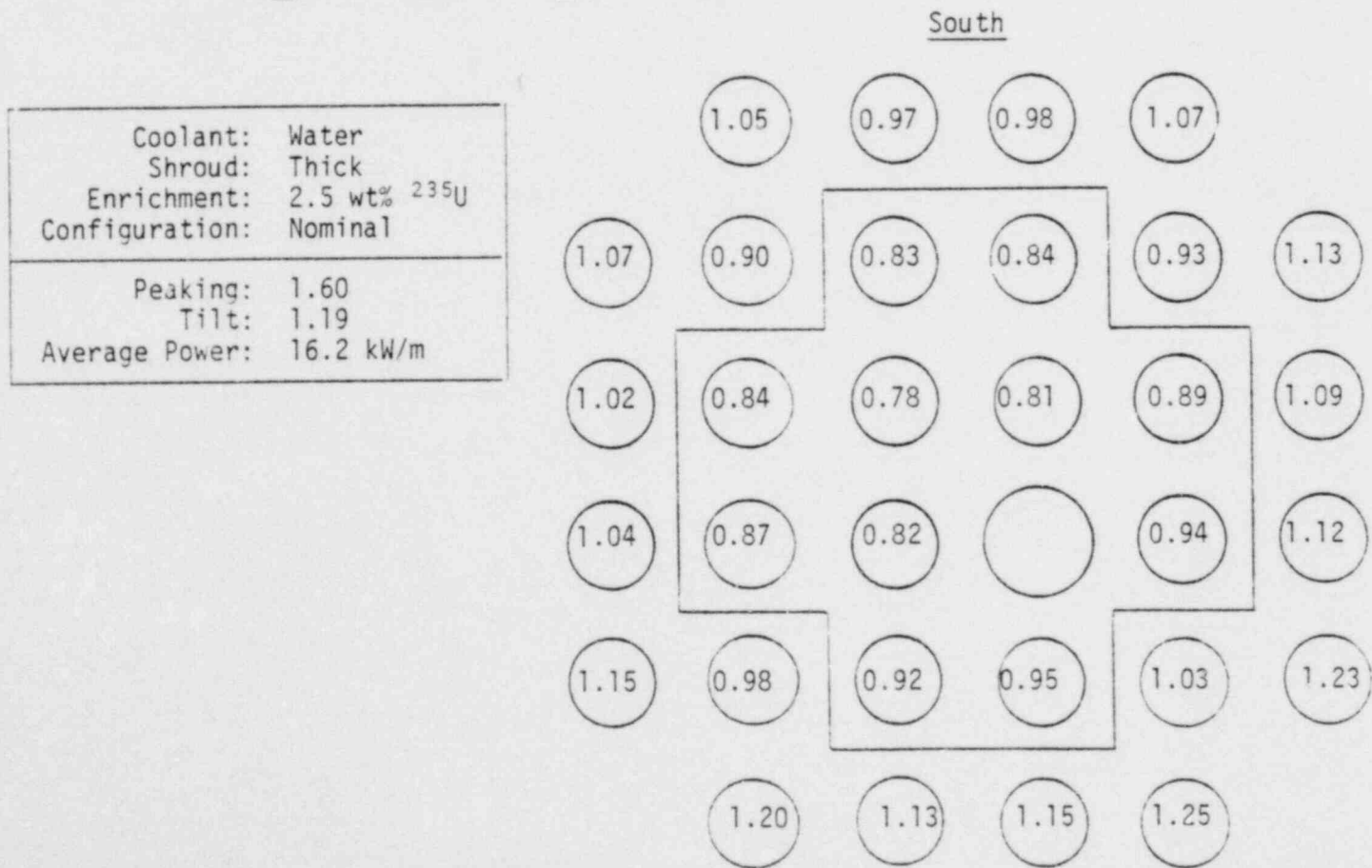
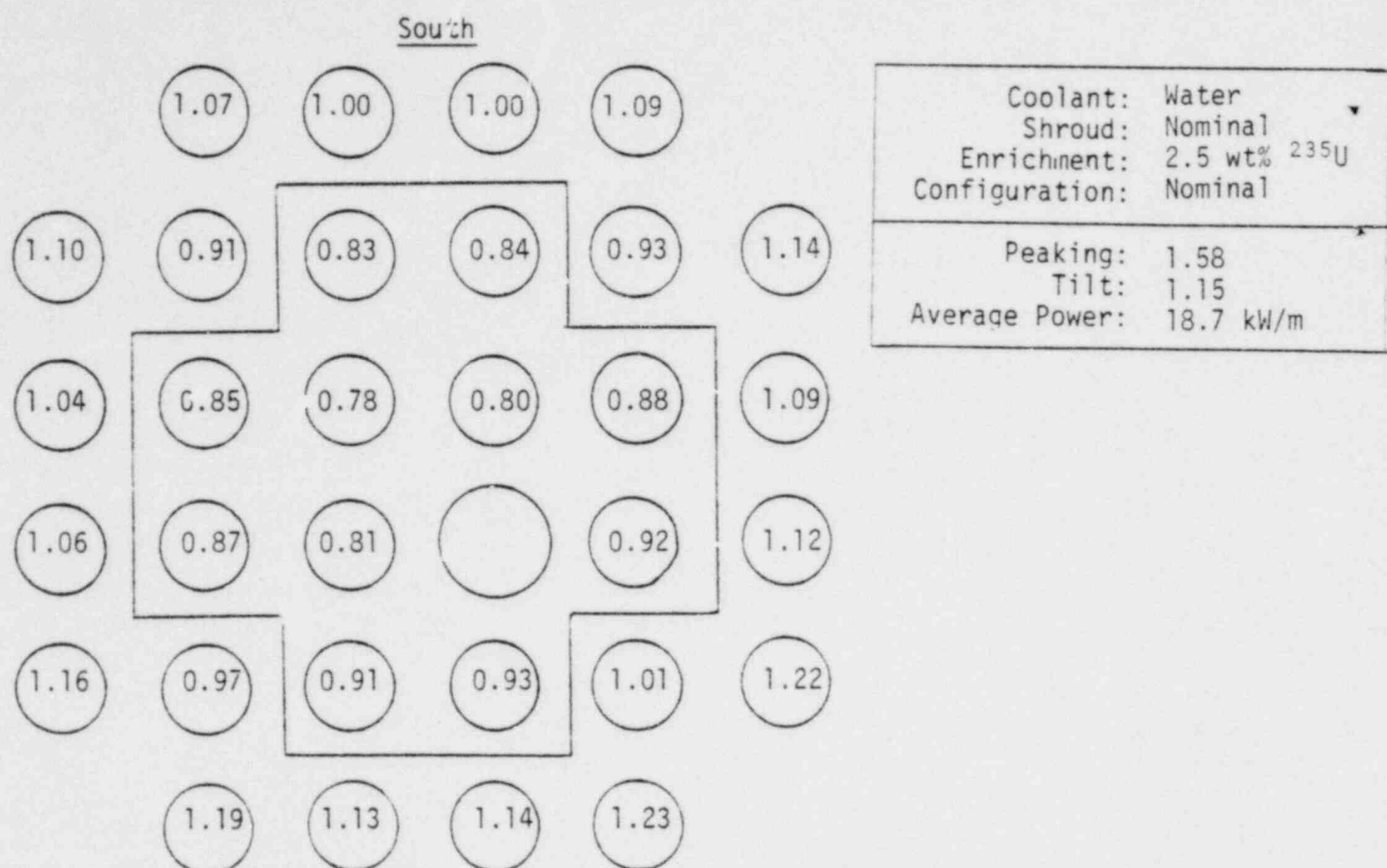


FIGURE 6.5C. Normalized Pin Power Map, Nominal and Thick Shrouds

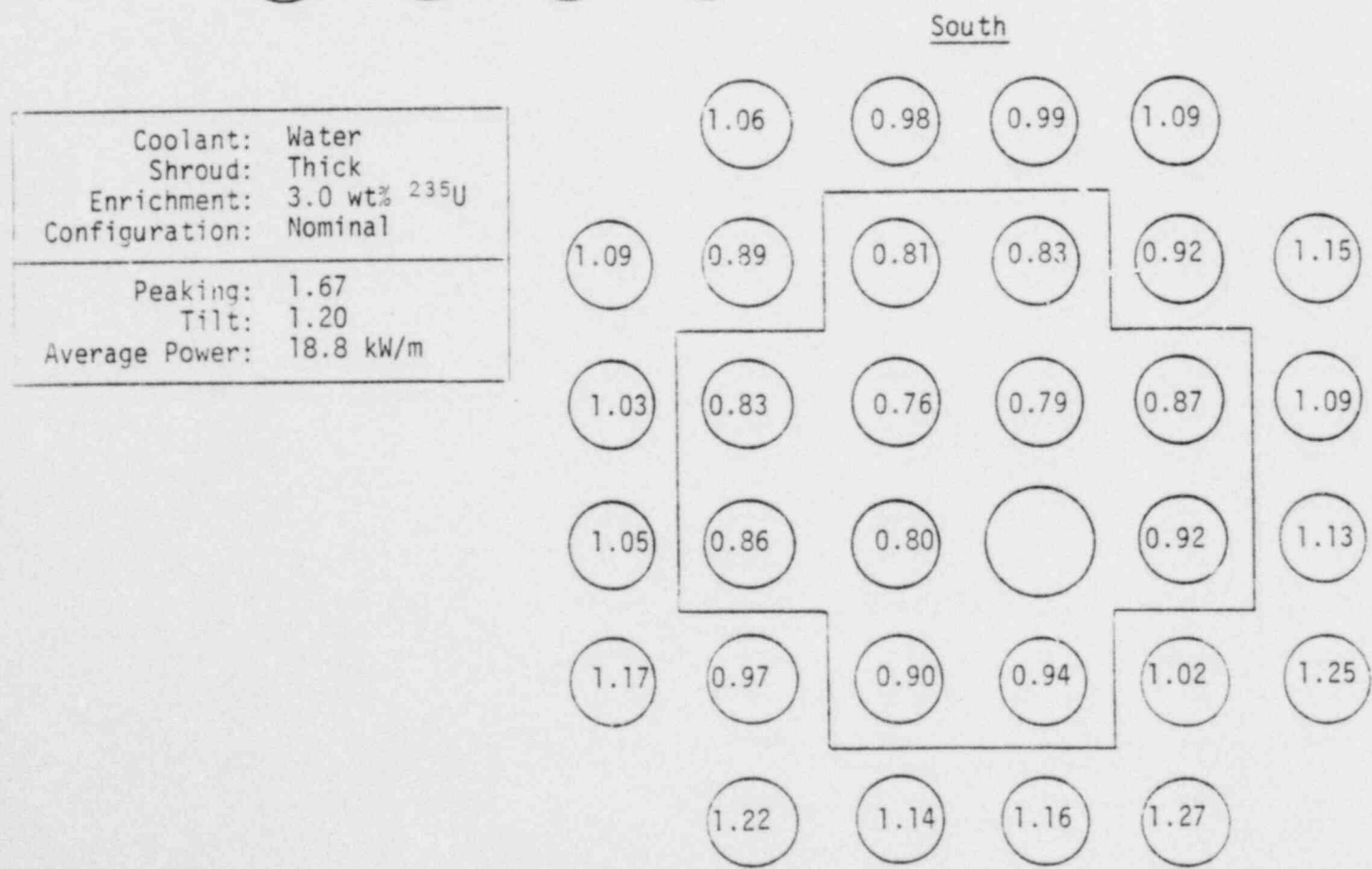
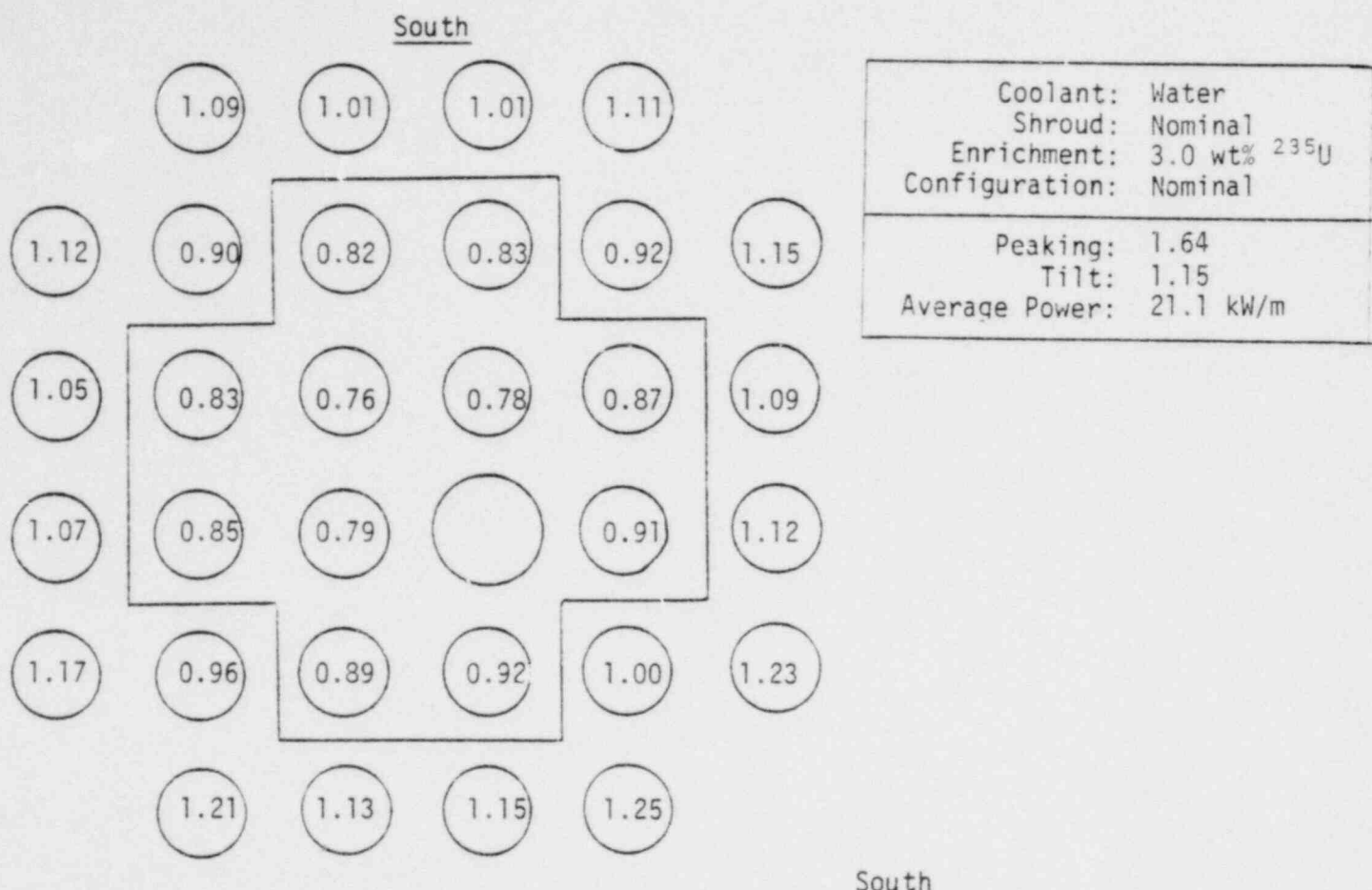
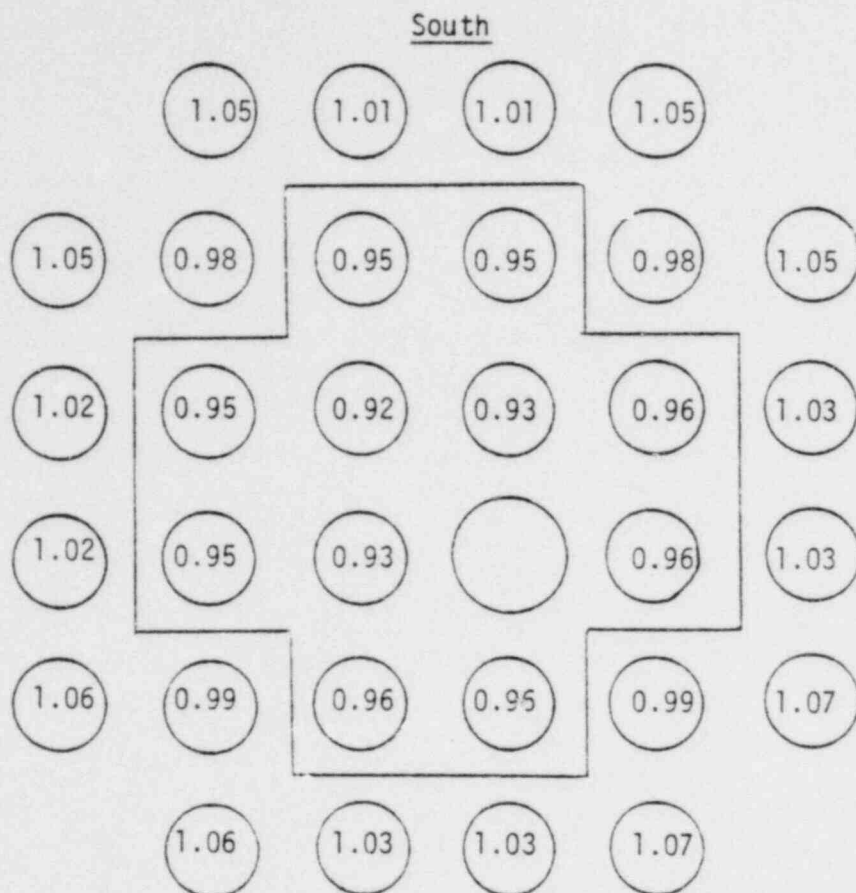
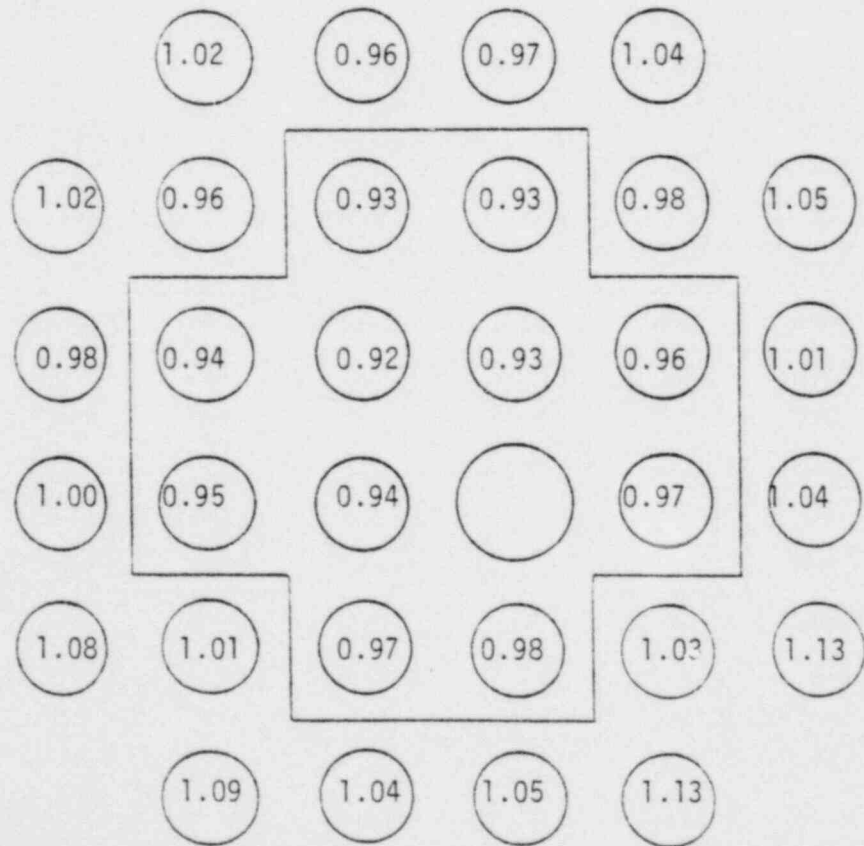


FIGURE 6.5D. Normalized Pin Power Map, Nominal and Thick Shrouds



Coolant:	Steam
Shroud:	Nominal
Enrichment:	2.0 wt% ^{235}U
Configuration:	Nominal
Peaking:	1.16
Tilt:	1.02
Average Power:	16.9 kW/m

South



Coolant:	Steam
Shroud:	Thick
Enrichment:	2.0 wt% ^{235}U
Configuration:	Nominal
Peaking:	1.23
Tilt:	1.11
Average Power:	12.8 kW/m

FIGURE 6.5E. Normalized Pin Power Map, Nominal and Thick Shrouds

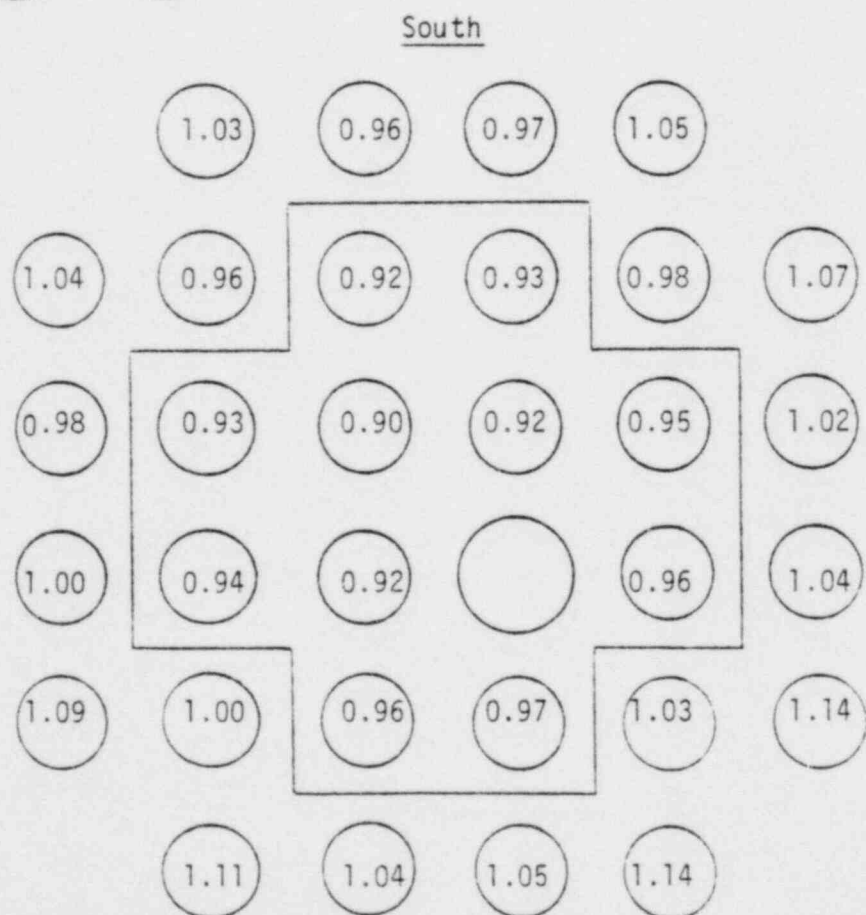
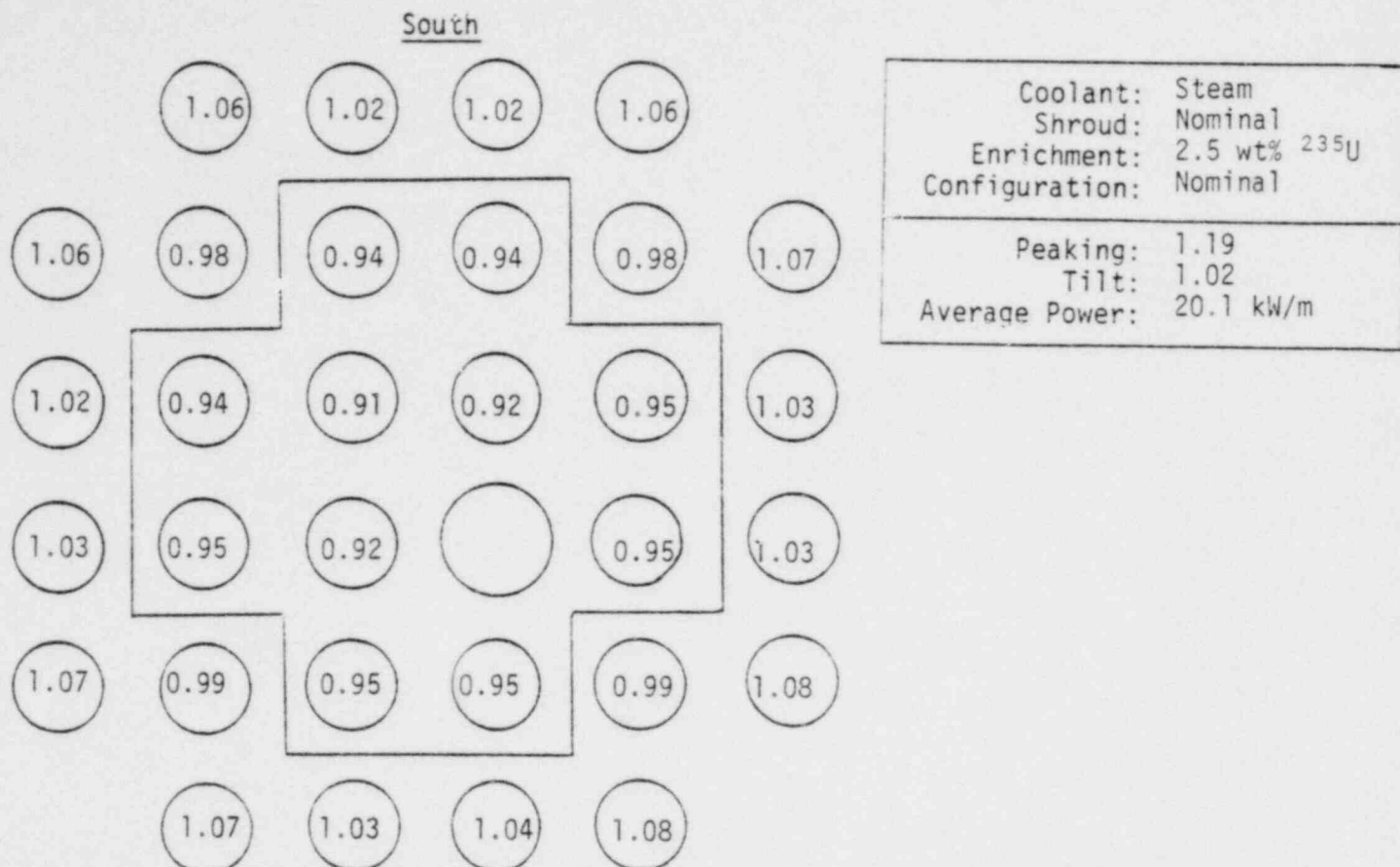


FIGURE 6.5F. Normalized Pin Power Map, Nominal and Thick Shrouds

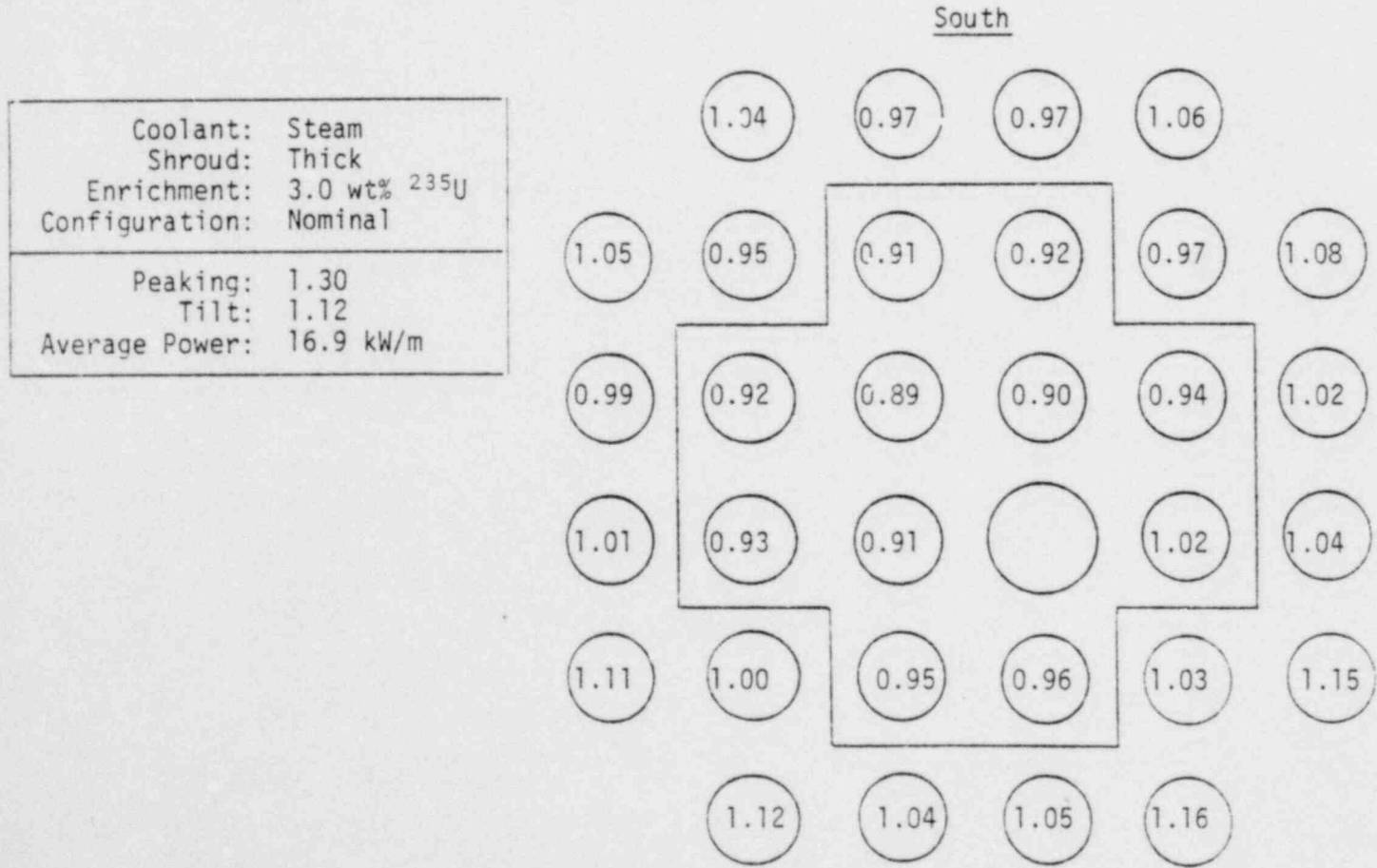
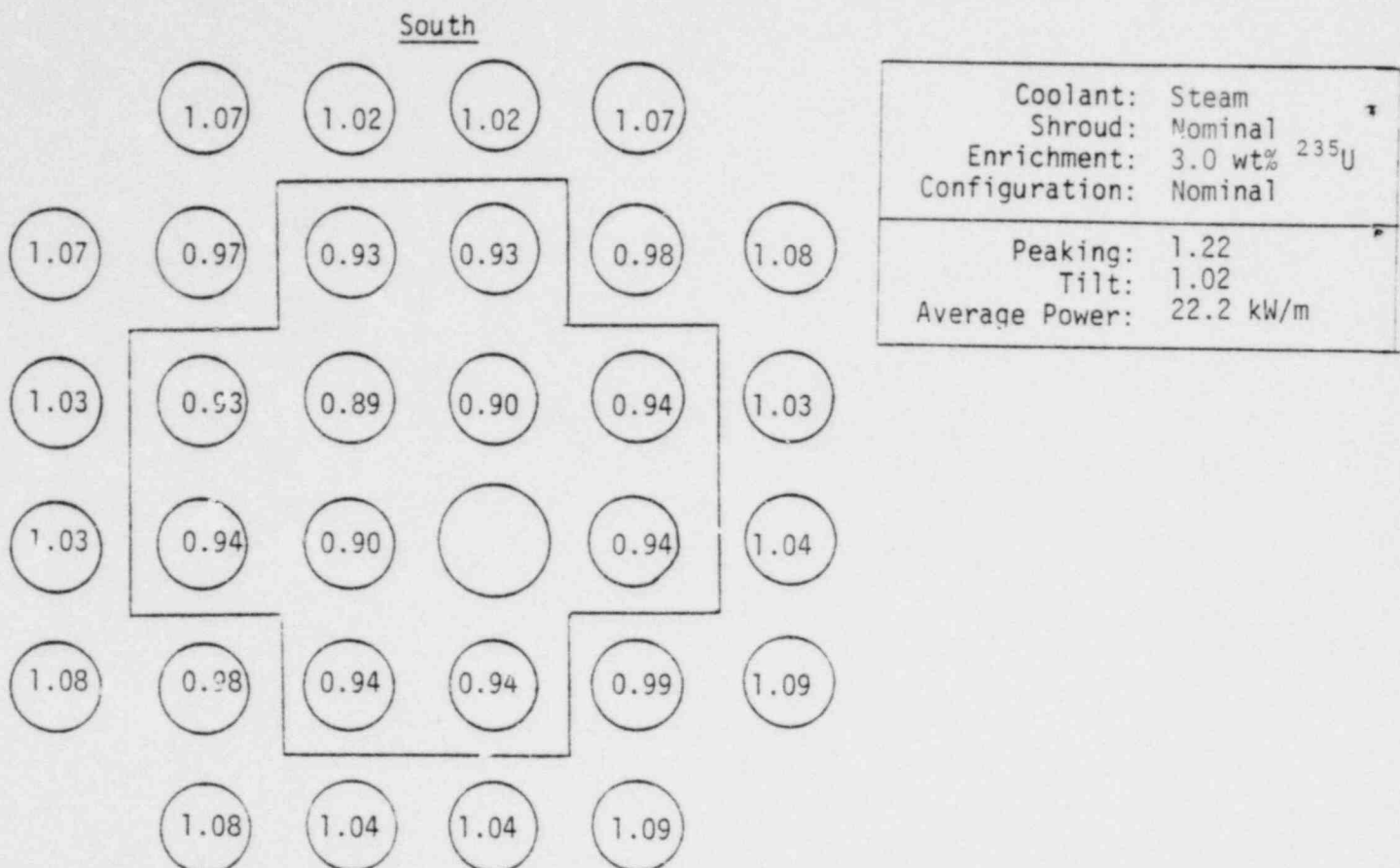


FIGURE 6.6A. Normalized Pin Power Map, Nominal and Hot Configurations

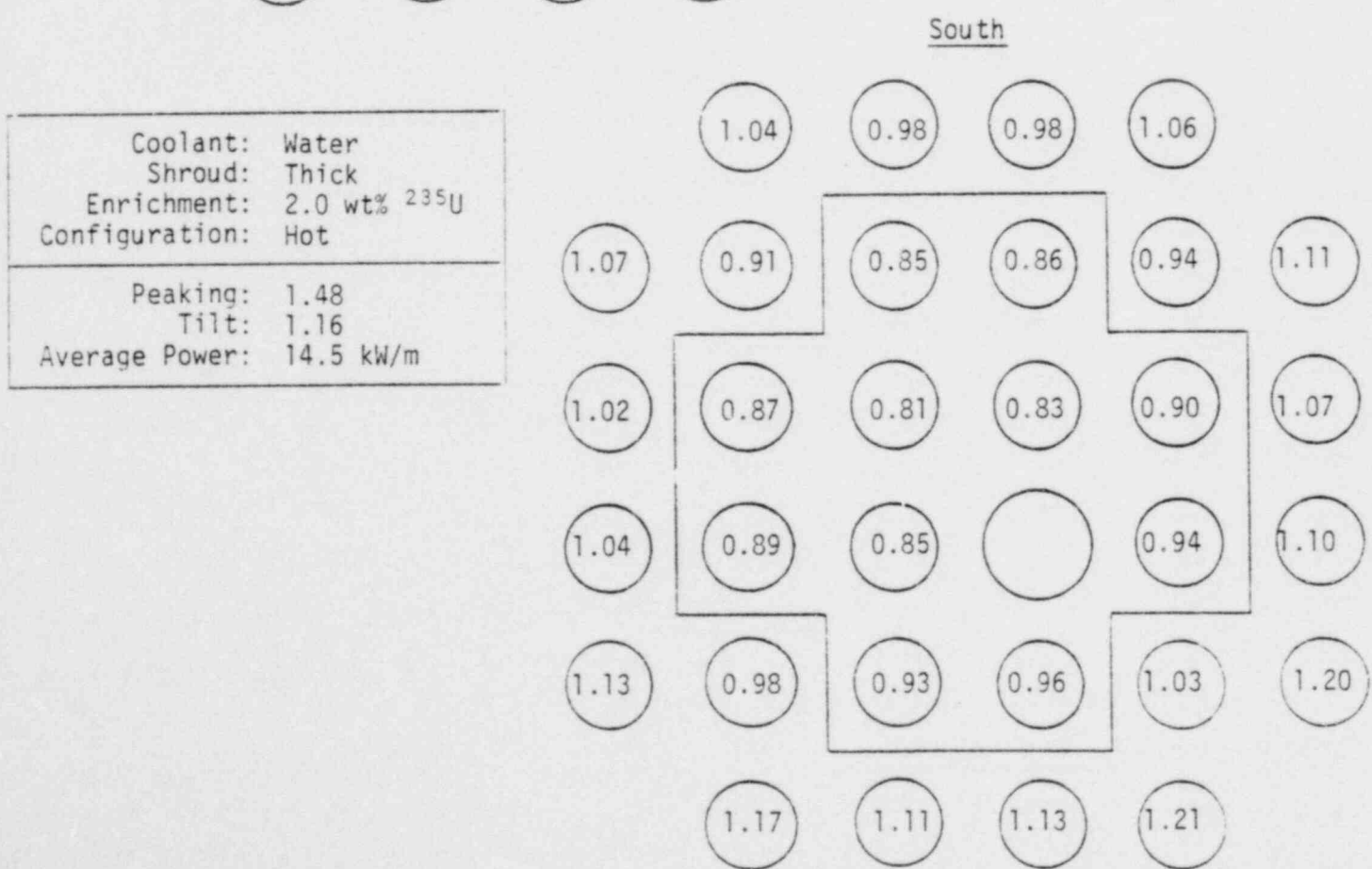
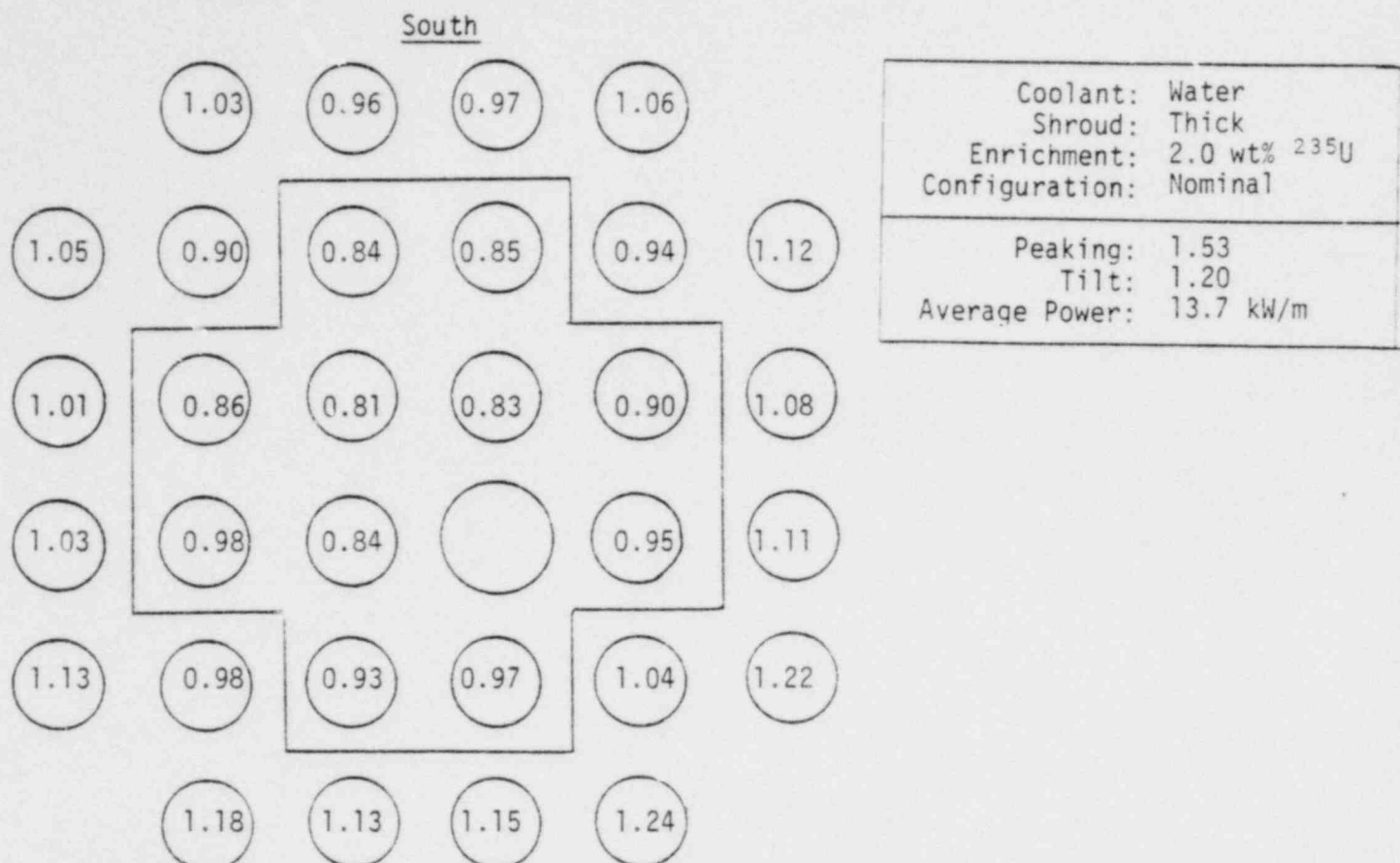
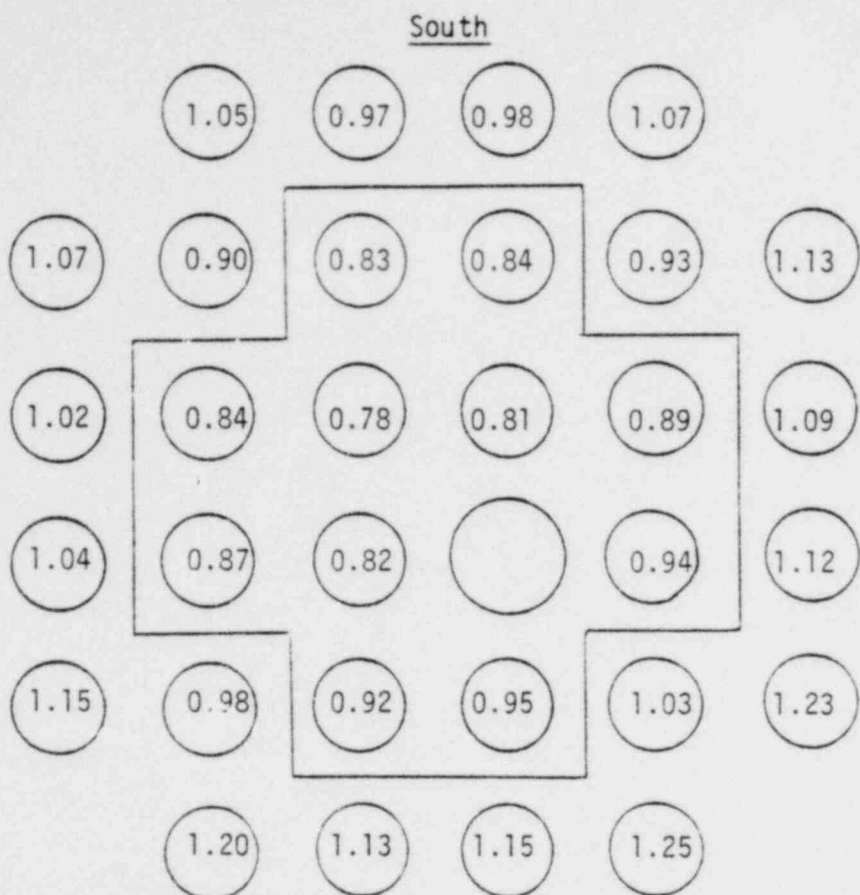


FIGURE 6.6B. Normalized Pin Power Map, Nominal and Hot Configurations



Coolant:	Water
Shroud:	Thick
Enrichment:	2.5 wt% ^{235}U
Configuration:	Nominal
Peaking: 1.60	
Tilt: 1.19	
Average Power: 16.2 kW/m	

South

Coolant:	Water
Shroud:	Thick
Enrichment:	2.5 wt% ^{235}U
Configuration:	Hot
Peaking: 1.53	
Tilt: 1.16	
Average Power: 17.1 kW/m	

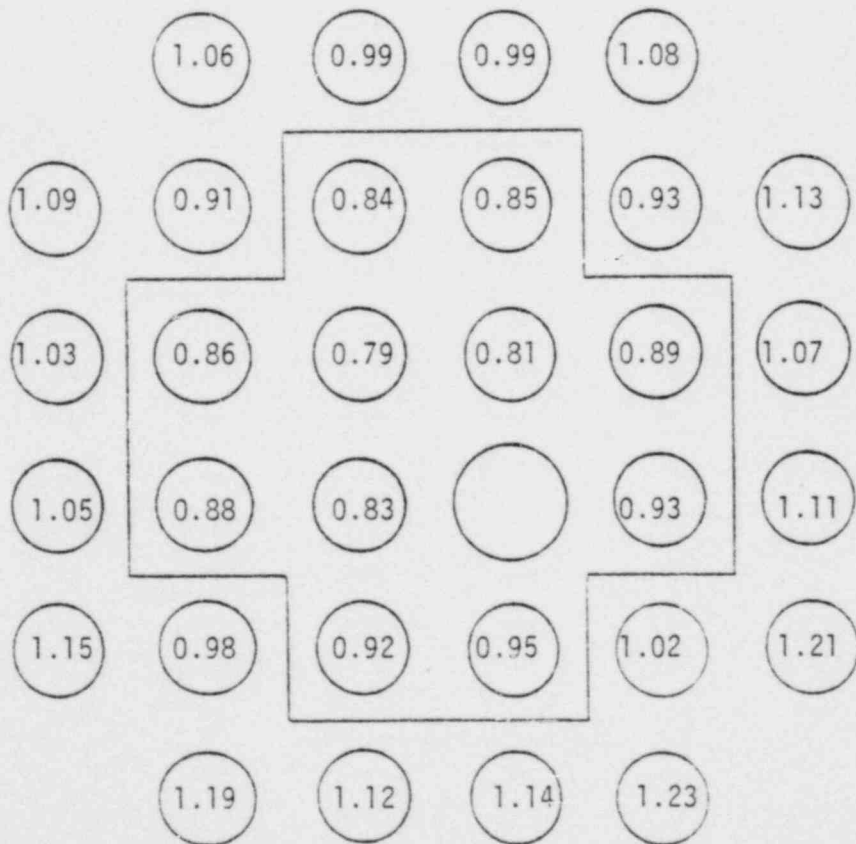


FIGURE 6.6C. Normalized Pin Power Map, Nominal and Hot Configurations

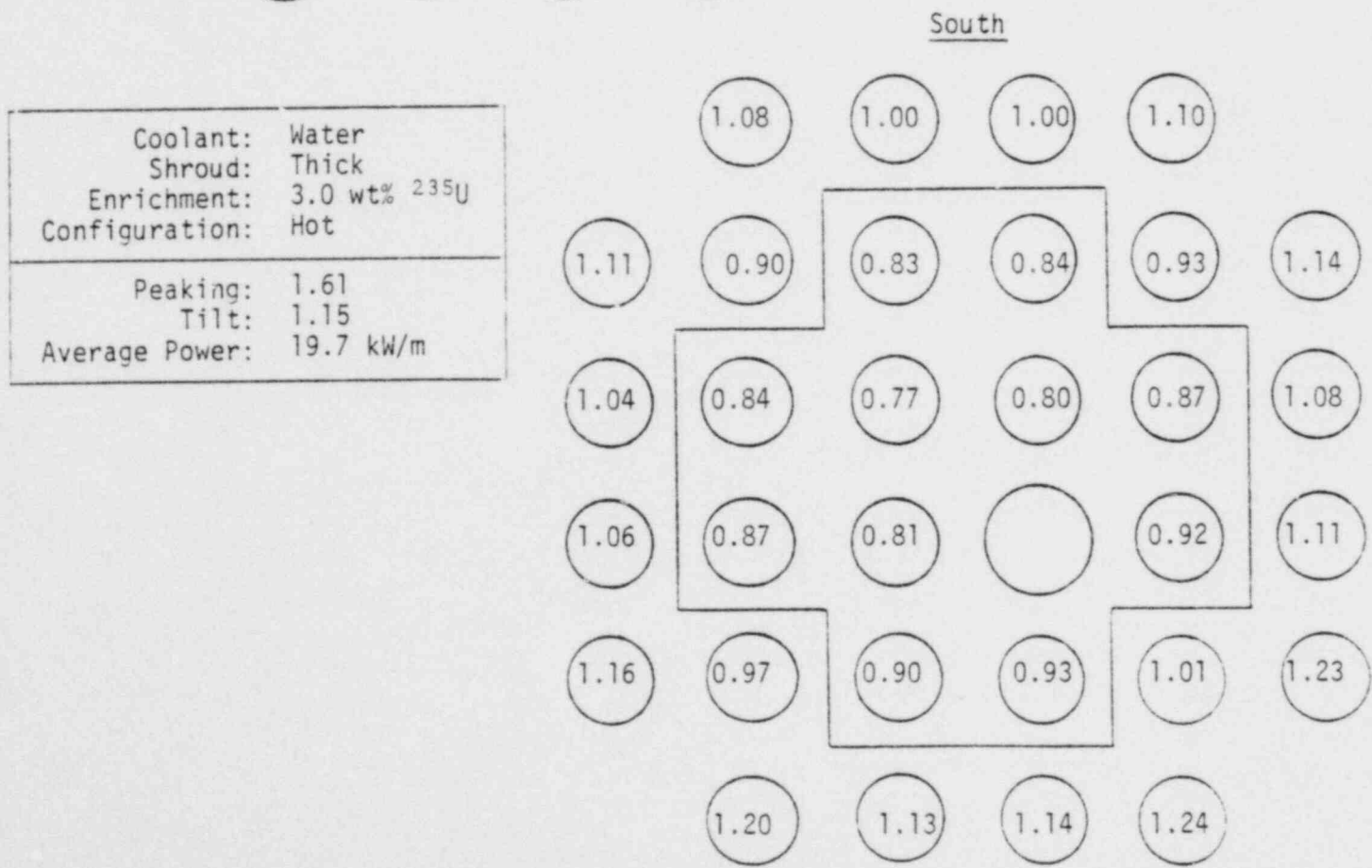
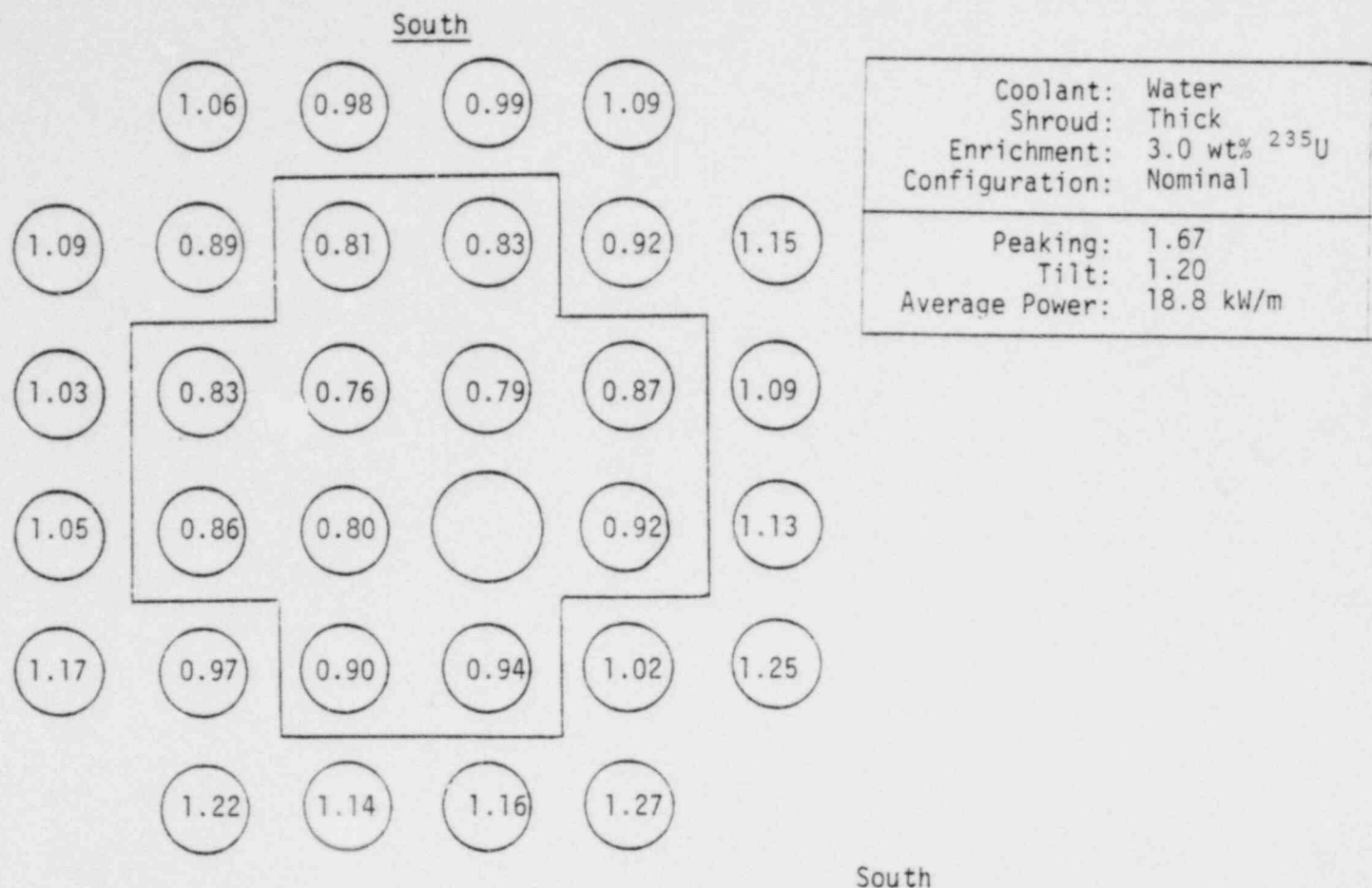
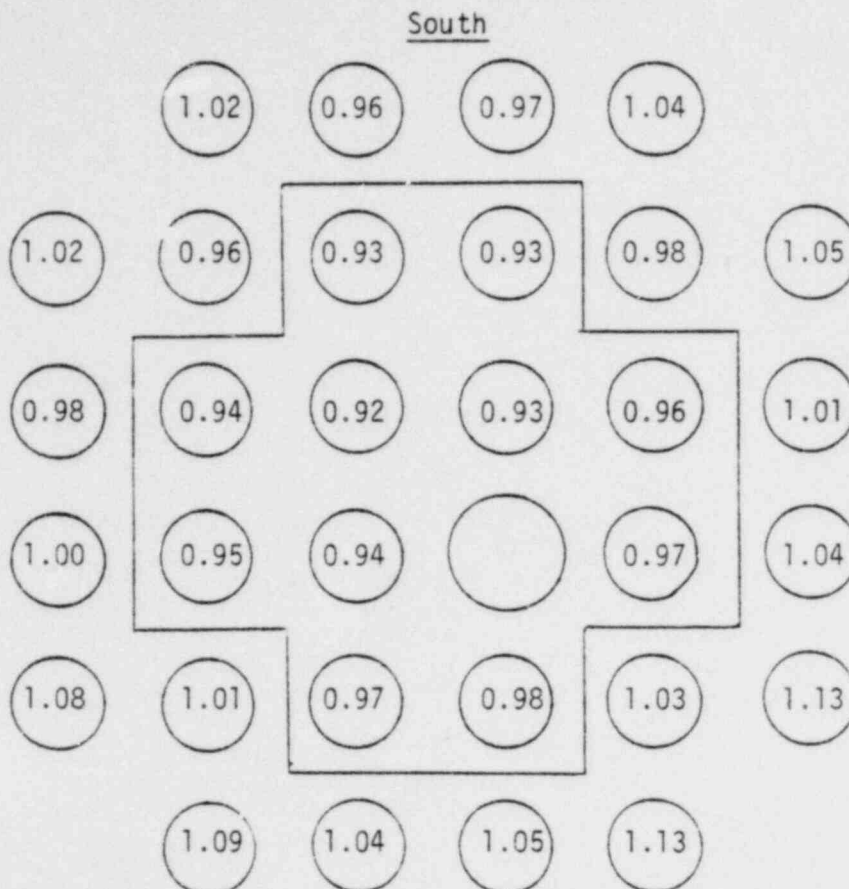
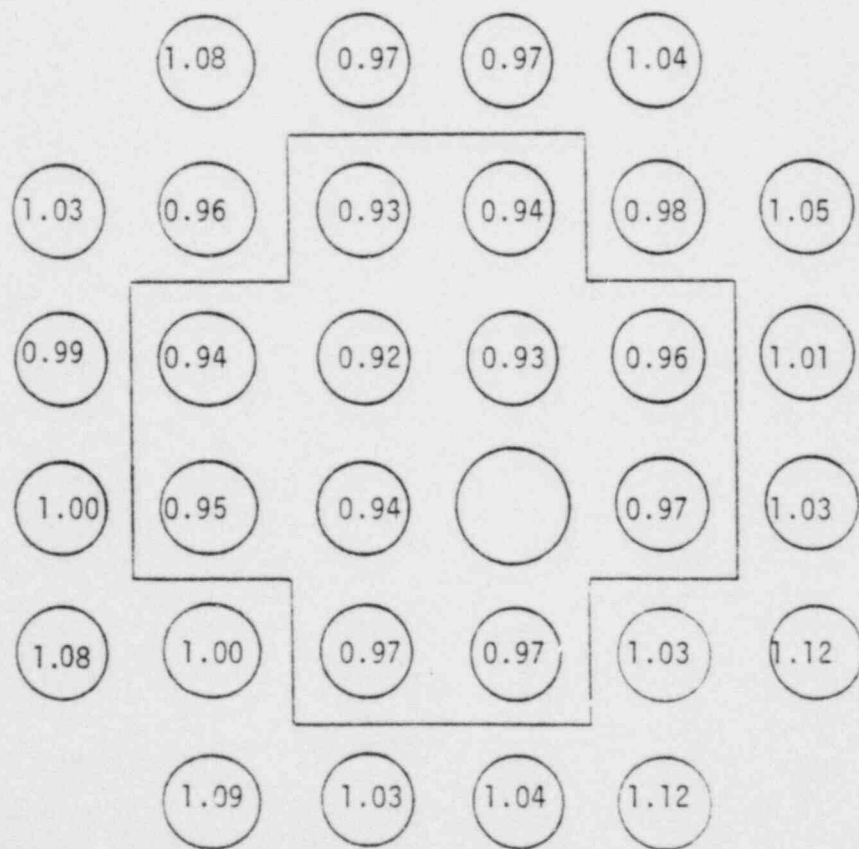


FIGURE 6.6D. Normalized Pin Power Map, Nominal and Hot Configurations



Coolant: Steam
Shroud: Thick
Enrichment: 2.0 wt% ^{235}U
Configuration: Nominal
Peaking: 1.23
Tilt: 1.11
Average Power: 12.8 kW/m

South



Coolant: Steam
Shroud: Thick
Enrichment: 2.0 wt% ^{235}U
Configuration: Hot
Peaking: 1.22
Tilt: 1.09
Average Power: 13.4 kW/m

FIGURE 6.6E. Normalized Pin Power Map, Nominal and Hot Configurations

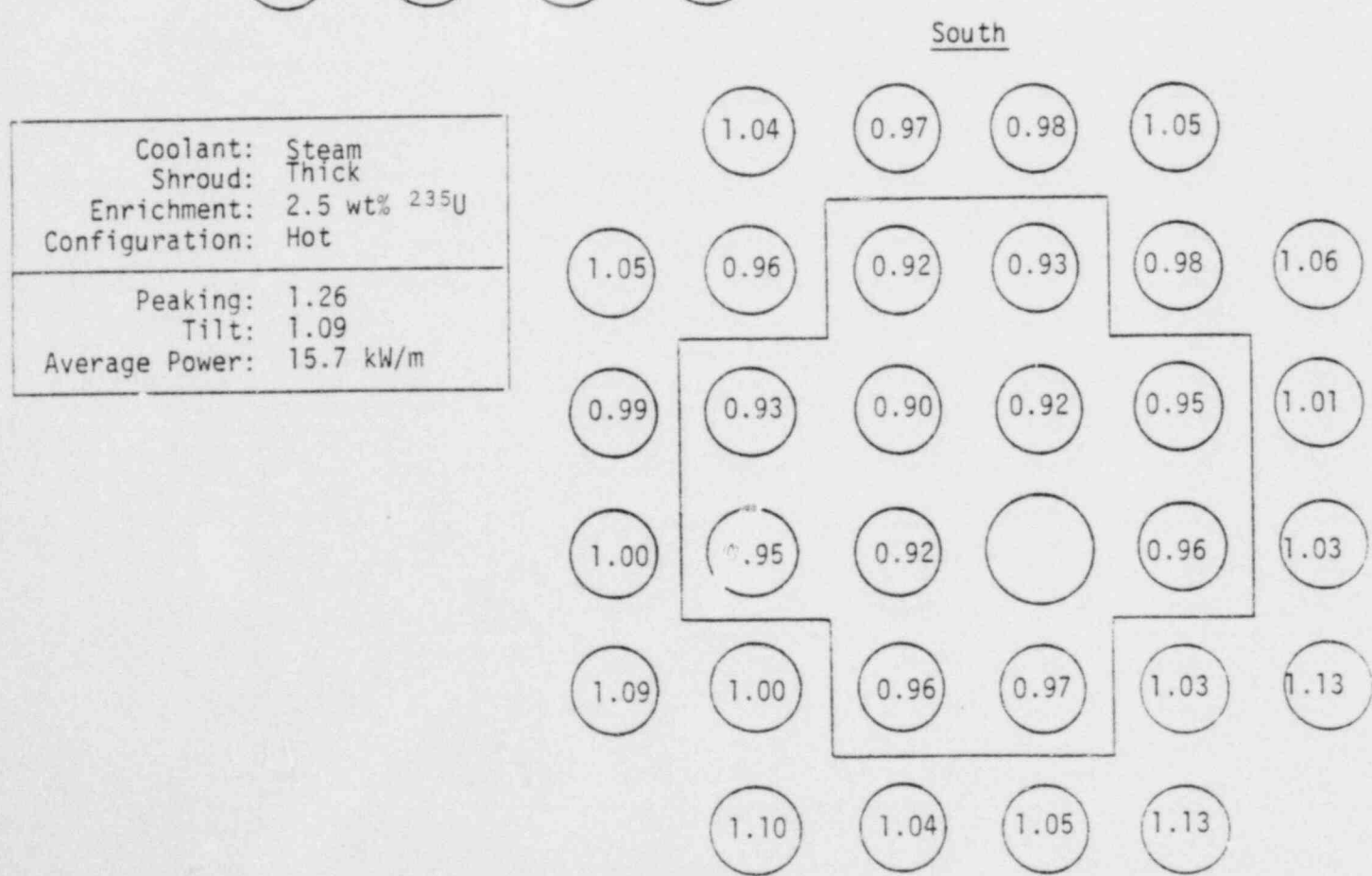
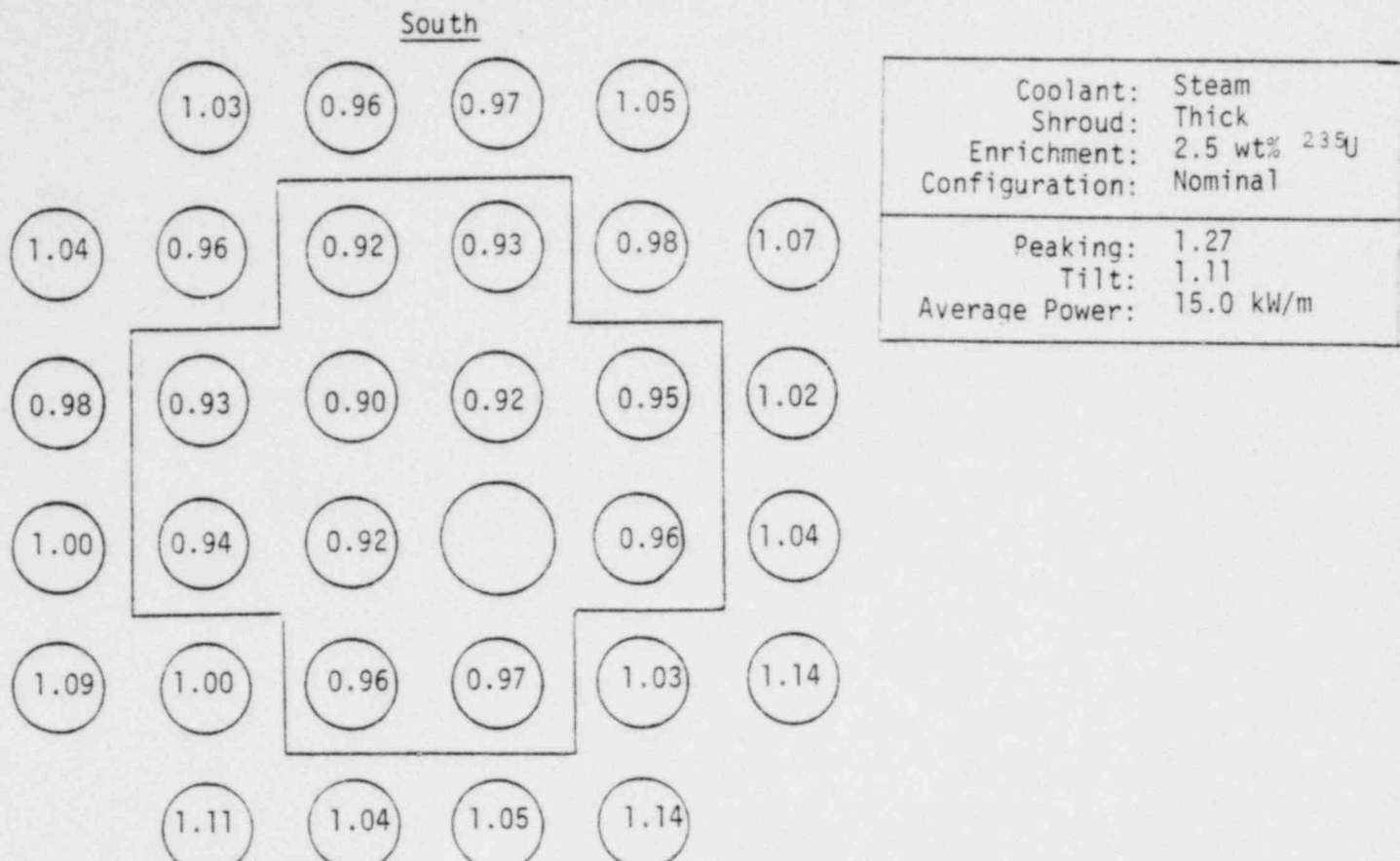
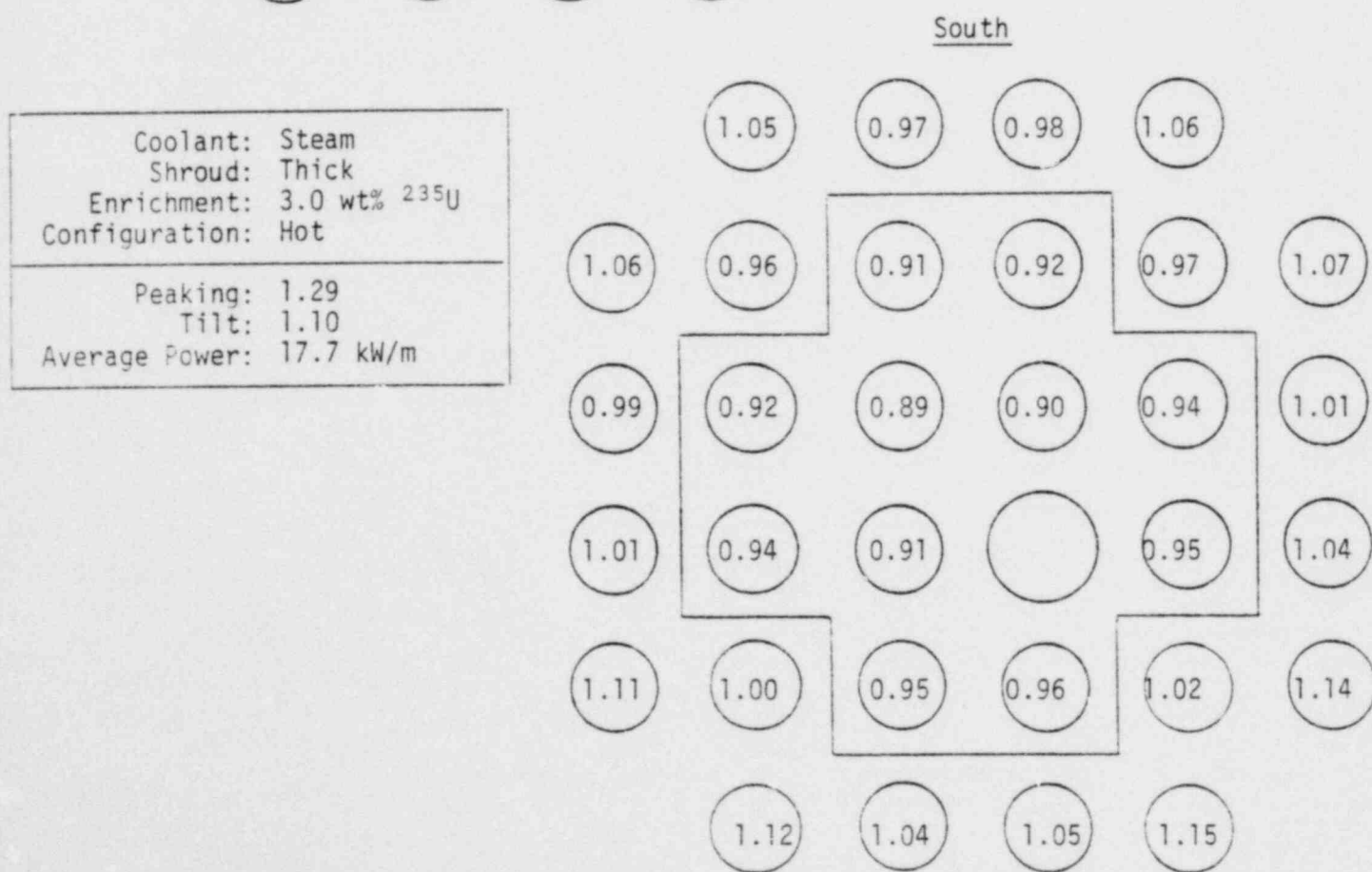
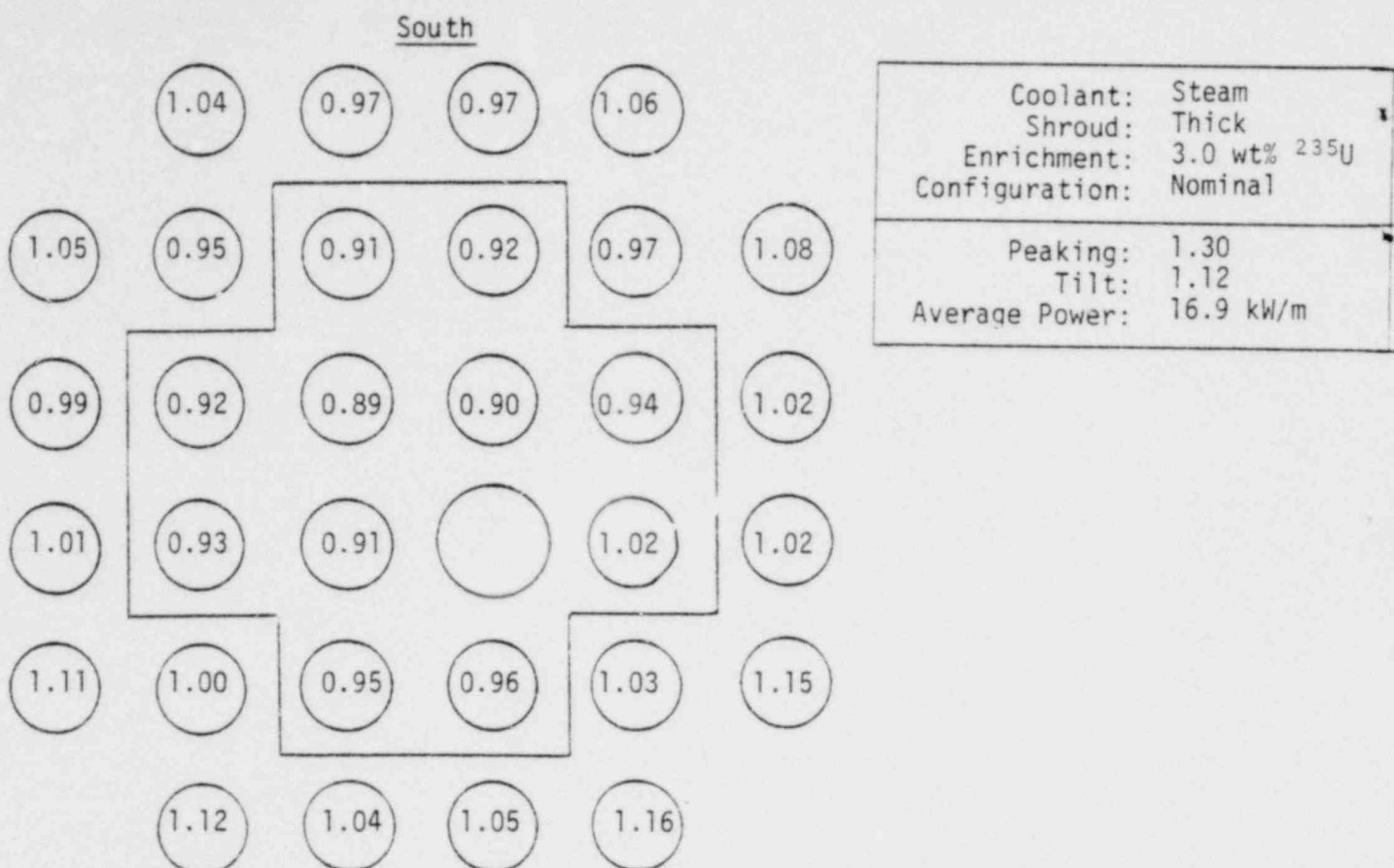


FIGURE 6.6F. Normalized Pin Power Map, Nominal and Hot Configurations



bottom. Figures 6.6A-F compare the nominal fuel configuration and the "hot configuration," both of these with the thick shroud. The nominal configuration has the NRU fuel arranged as in Figure 6.2. The hot configuration replaces two higher exposure driver fuel rods adjacent to the test with two lower exposure rods. This leaves the test surrounded by four of the lowest exposure, hence hottest, driver fuel rods.

Studying Figures 6.5A-F reveals that for the water cases the thick shroud has a slightly larger tilt and more peaking. These same effects are seen in the steam cases but to a greater degree. The comparison of nominal to hot configurations shown in Figures 6.6A-F indicate only a small difference. The water cases have a larger peaking and tilt for the nominal configuration. This minor effect is caused by the more uniform nature of the surrounding rods in the hot configuration. The steam cases also favor a larger tilt and peaking for the nominal configuration but here the effect is hardly detectable.

6.3 AXIAL MODEL AND RESULTS

Axial power distributions for the test region were obtained from R-Z diffusion theory calculations with the test region in the center of the core. In two dimensional geometry, in order to utilize the axial dimension, radial symmetry must be assumed. To obtain proper size and detail this requires the test be located in the center of the model. The calculational model is depicted in Figure 6.7. The fuel in the test region is a homogeneous mixture of fuel, clad, and water or steam. The water hole in the test region is represented explicitly in the center of the test region. The structure material at the top and bottom of the core consists of stainless steel. The driver fuel, etc. region was represented by several zones containing mixtures of the various types of elements. The outside radius given for the shroud is that of the thick shroud. The thin shroud radius is 44.8 mm. Axial burnup effects in the driver fuel were represented by three different exposures in the axial direction. This was done only for the elements closest to the test region.

The absolute power level in the test region is not realistic with this

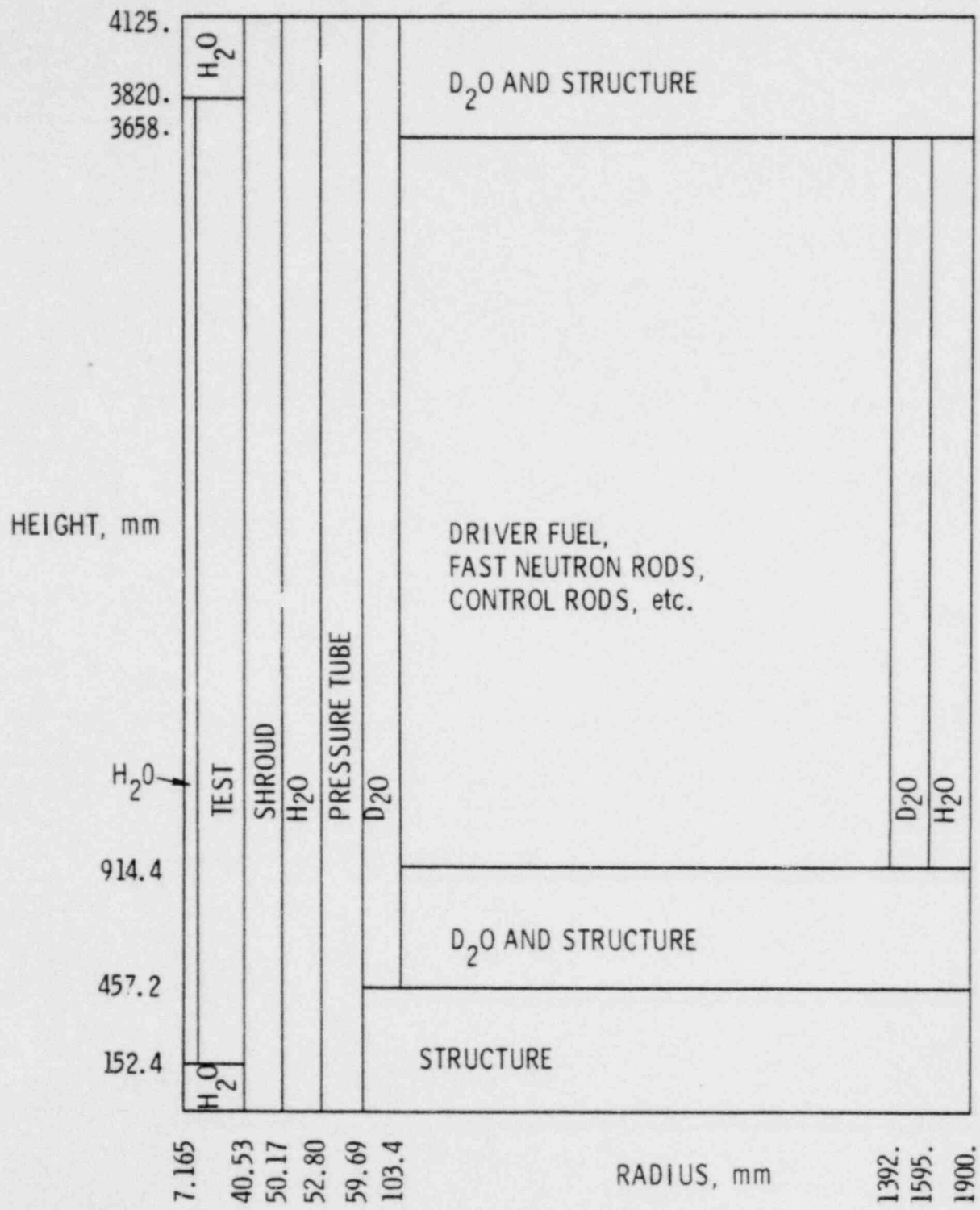


FIGURE 6.7 Axial Model

model because the test region is in the center of the core and the surrounding regions are mixtures of several kinds of elements. However, the power distribution within the test region for various conditions should be valid.

The radial power shape through the test region is shown in Figure 6.8 using the thick shroud. The data shown in Figure 6.8 were taken from the midpoint height of the fuel. Near the ends of the test region the shape is somewhat different.

The axial power shape in the center of the test region is shown in Figure 6.9 for the thin shroud and Figure 6.10 for the thick shroud. The peak power is higher for the water cases than for the steam cases. The data shown on Figures 6.9 and 6.10 assume that the driver fuel exposure is distributed uniformly in the axial dimension. In reality the center portion of the driver fuel is more exposed than the average and the ends are less exposed. The thick-shroud cases were rerun assuming that 22% of the driver fuel at the ends of the rods was at an exposure of 70% of the average, and the central 44% was at an exposure of 115% of the average. The remainder of the fuel was at the average exposure. This was done for the first five rings of driver fuel. The resulting axial power distribution in the first ring of driver fuel is compared to the distribution obtained with a uniform axial exposure in Figure 6.11. The discontinuities in the distributed exposure curve are caused by discrete lengths of different exposures in the model. The effect on the test region of grading the axial exposure is shown in Figures 6.12 and 6.13 using the thick shroud. For the water case the peak power is reduced by 5 1/2%. For the steam case the peak power is reduced by 4%. In addition the average power in the test region is reduced by 1 1/2% when axially graded driver fuel is used in the calculation.

The axial power shape near the center of the test region compared to the average power taken near the edge of the test region is shown in Figure 6.14 for the thick shroud case with water and axially graded fuel. There is very little difference between the two curves.

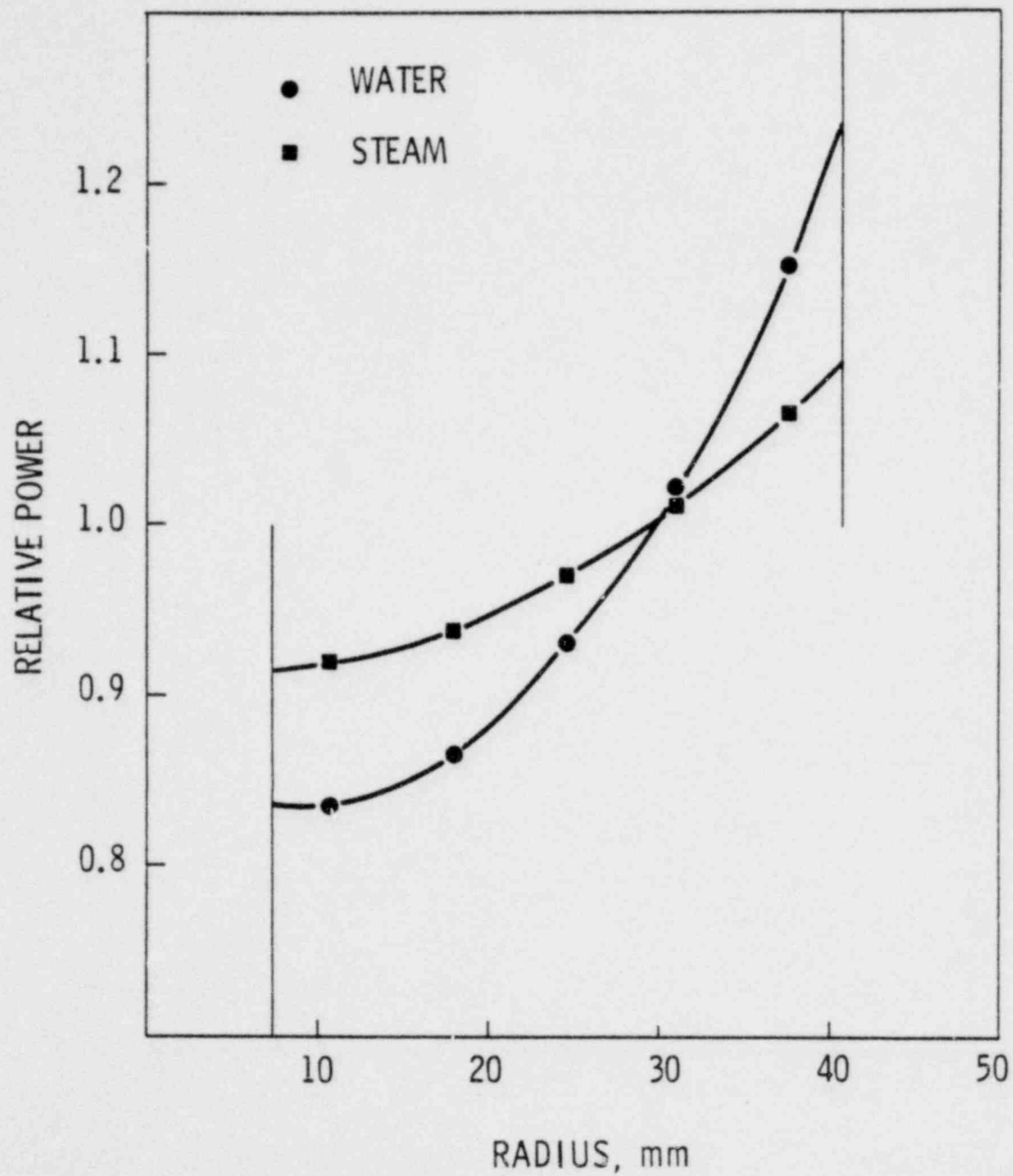


FIGURE 6.8 Normalized Radial Power Distribution From Axial Model,
Thick Shroud

NORMALIZED POWER (LOCAL / AVERAGE)

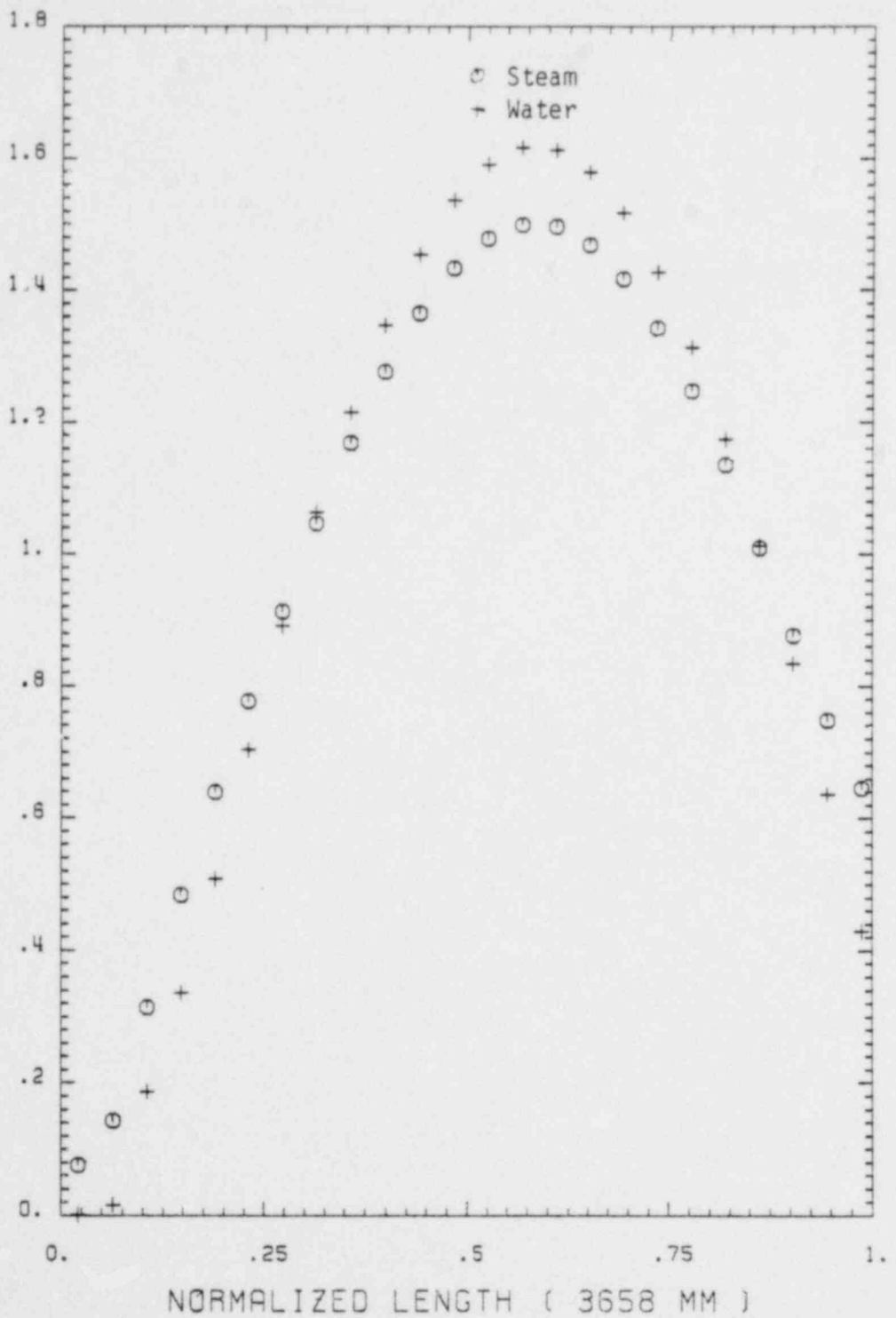


FIGURE 6.9 Normalized Axial Power Distribution - Nominal Shroud,
Uniform Axial Driver Exposure

NORMALIZED POWER (LOCAL / AVERAGE)

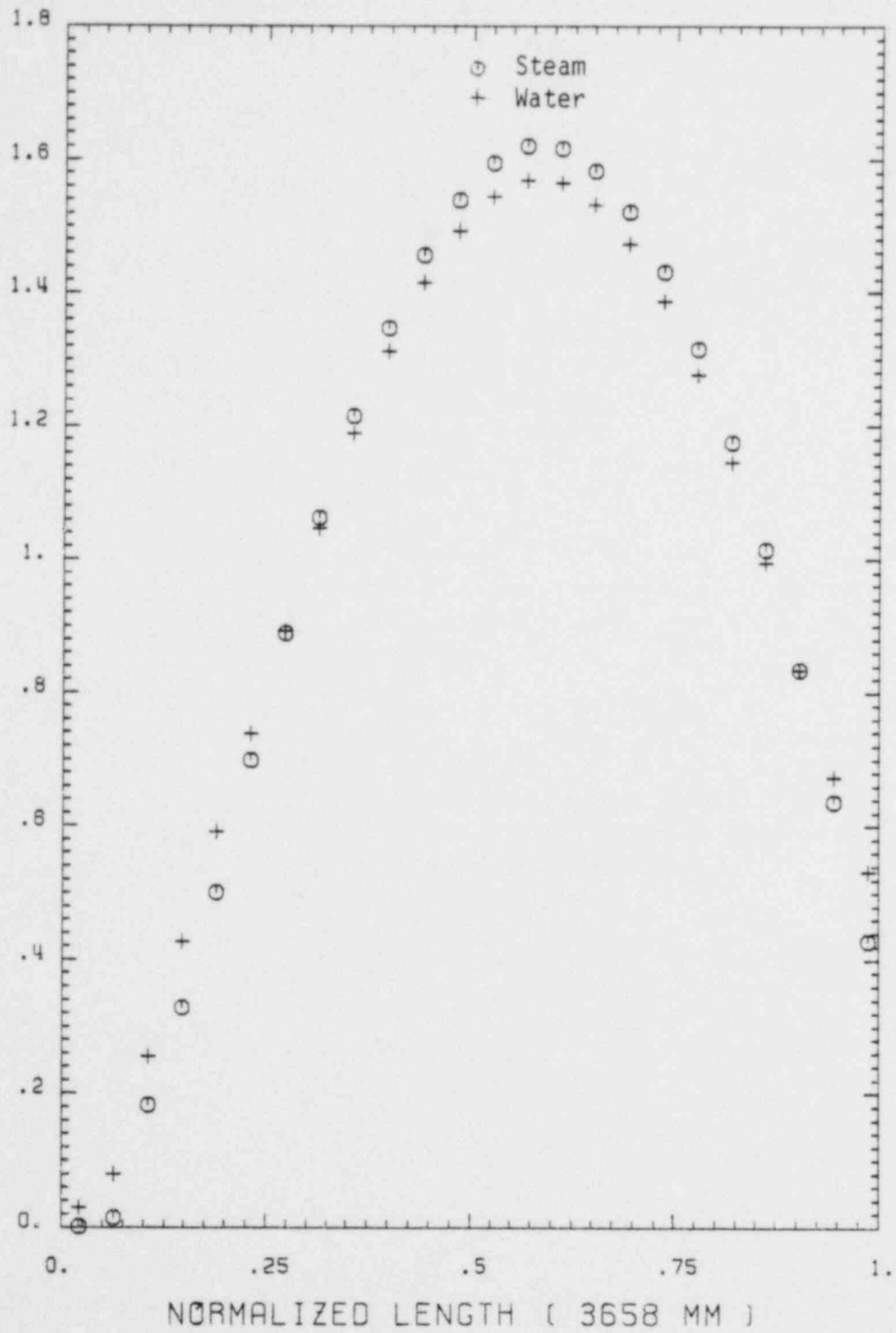


FIGURE 6.10 Normalized Axial Power Distribution - Thick Shroud,
Uniform Axial Driver Exposure

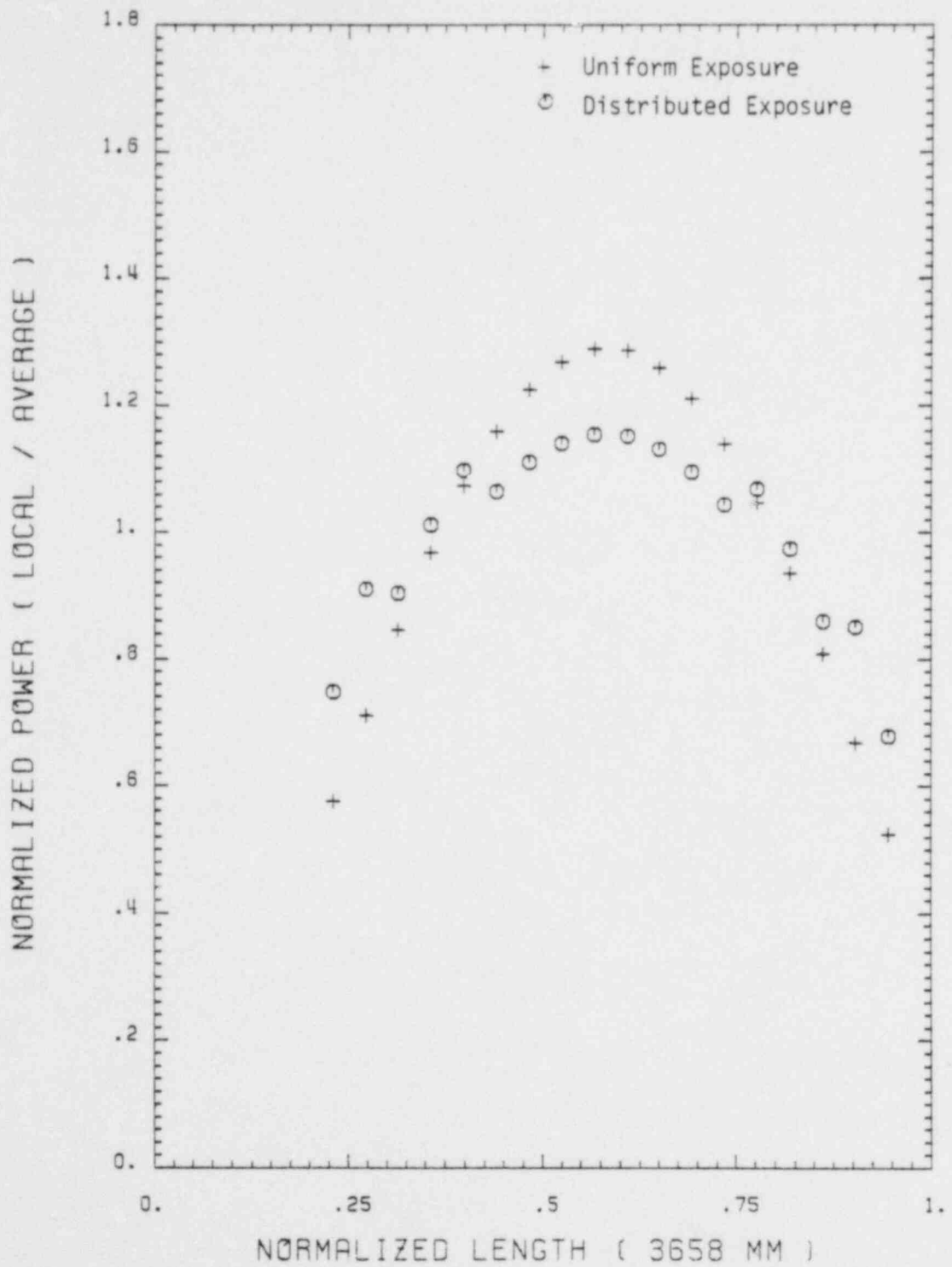


FIGURE 6.11 Normalized Axial Power Distribution - Driver Fuel

NORMALIZED POWER (LOCAL / AVERAGE)

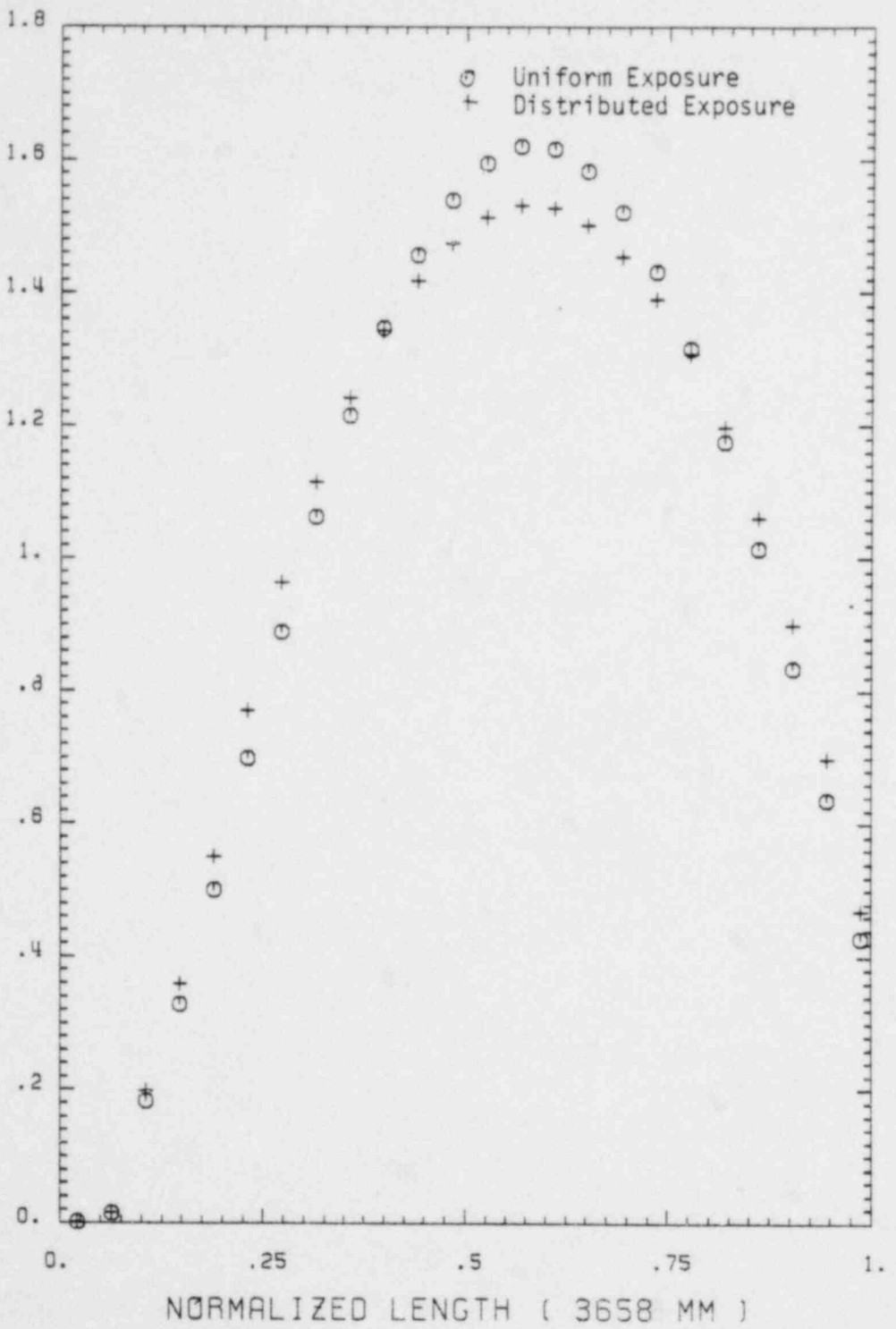


FIGURE 6.12 Normalized Axial Power Distribution - Thick Shroud,
Water Coolant

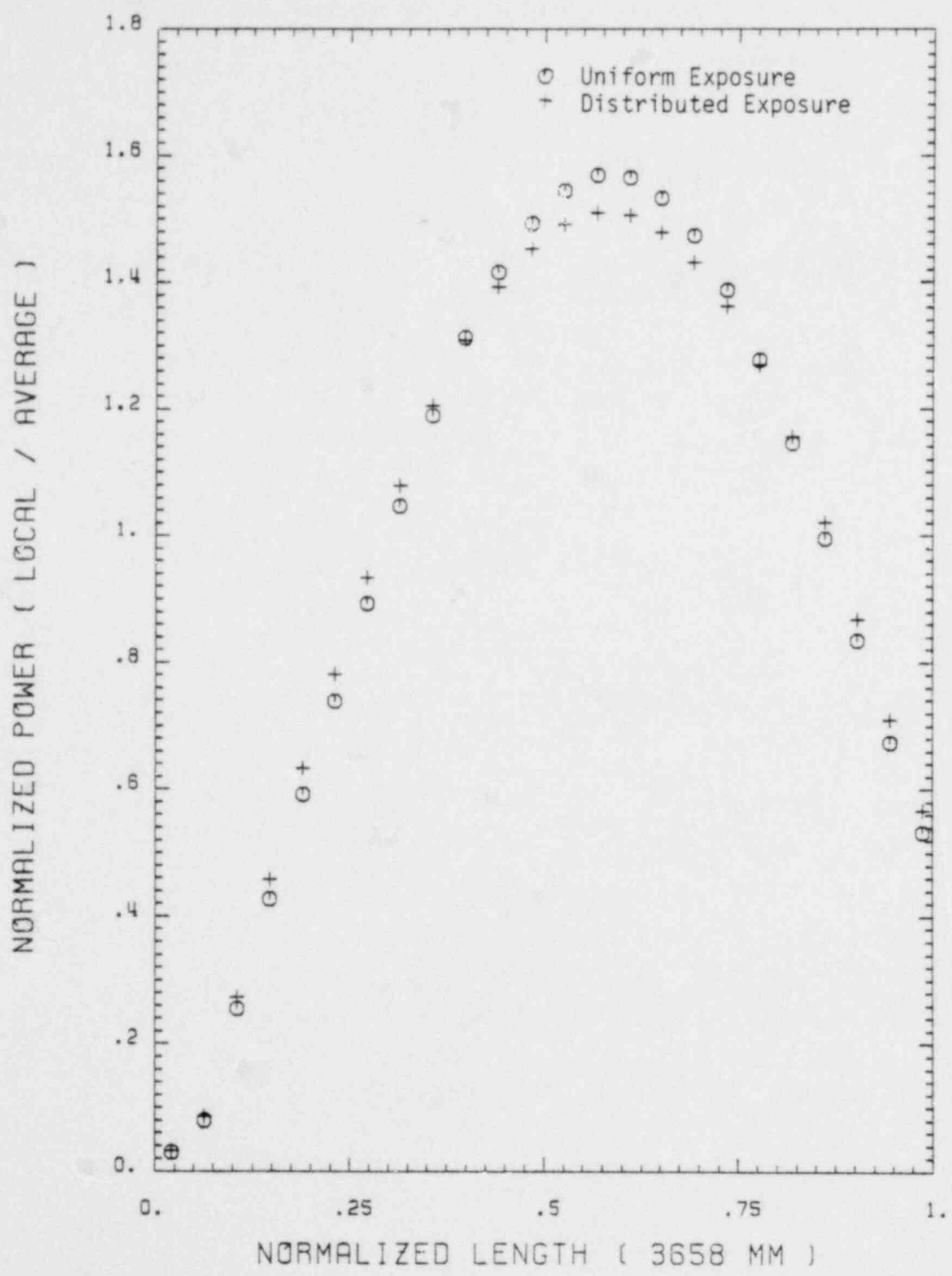


FIGURE 6.13 Normalized Axial Power Distribution - Thick Shroud, Steam Coolant

NORMALIZED POWER (LOCAL / AVERAGE)

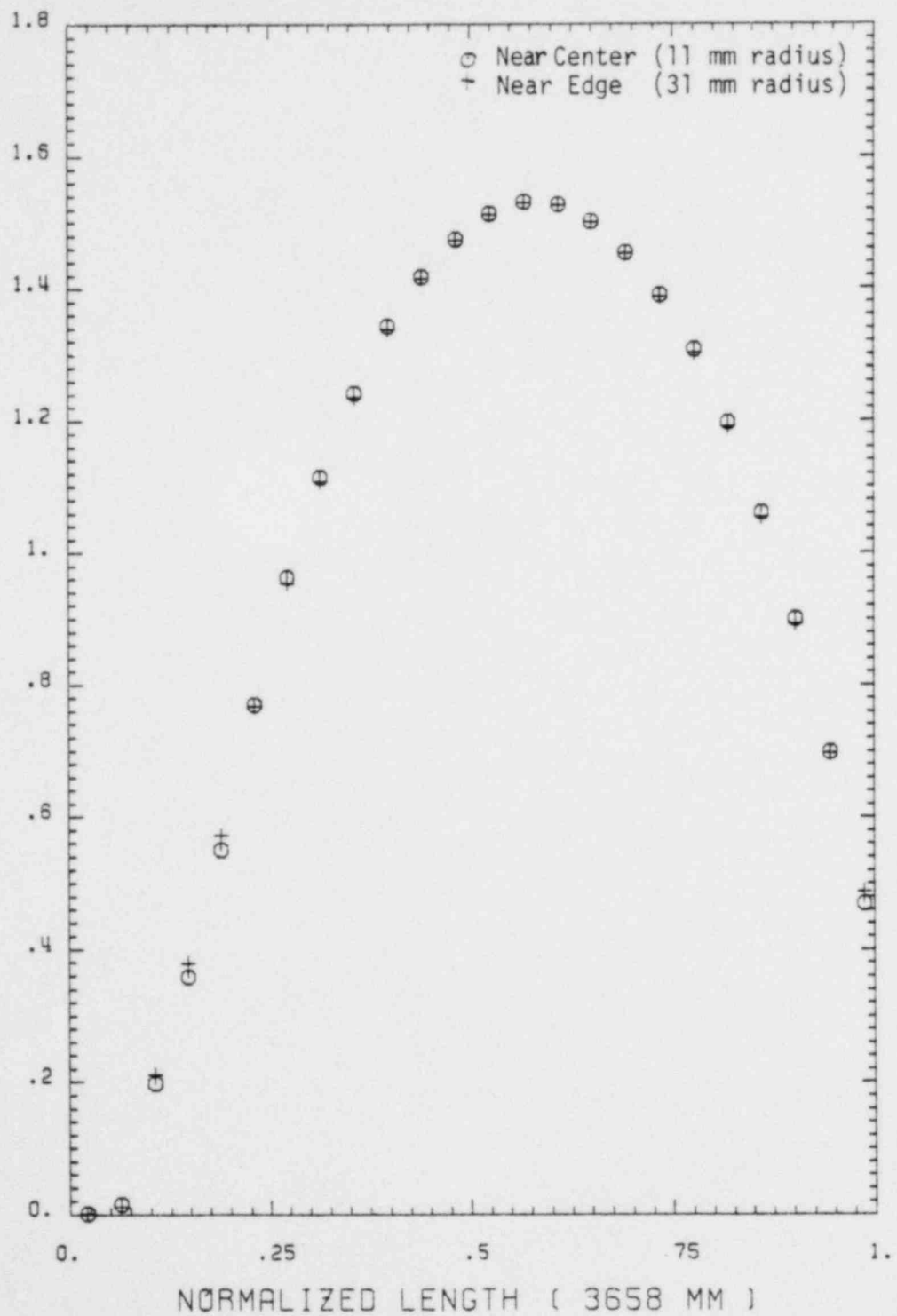


FIGURE 6.14 Normalized Axial Power Distribution - Thick Shroud,
Water Coolant, Distributed Driver Exposure

7.0 SHIELDING

As part of the neutronics support provided to experiment design, a set of shielding calculations were made for post-test examinations in the NRU fuel basin. The examination of the irradiated test fuel requires personnel to work almost directly above the test. For a number of reasons it is preferable to bring the fuel as close to the personnel as possible. Obviously this desire is bounded by radiation safety considerations. The objective of the shielding calculations was to estimate the relation between radiation dose and depth of water, i.e. shield thickness.

The first step in the calculation was to generate fission product source terms. These data were used not only for shielding but also for safety, and gamma scanning considerations. The fission product inventory was estimated using the ORIGEN code. This is a point reactor code which calculates fissile depletion, fission product buildup, radioactive decay and generates an isotopic inventory.

Two cases were considered. The first was for an irradiation conservatively modeling the thermal-hydraulic test sequence. The long irradiation time of this sequence makes it the upper bound of the source term. Even if the same assembly were to be taken through the five shorter material tests, the decay times between the test are sufficient to reduce the radiation source to less than that immediately following the thermal-hydraulics test.

The second case was a lower bound using a lower irradiation power and a shorter total time. This was generated to give the minimum gamma source a gamma scanning examination may have to contend with. The earlier case conservatively over estimated radiation sources and fission product inventories, for gamma scanning requirements this conservatism was not appropriate. Table 7.1 shows the assumptions used in generating the source term estimates for the two cases.

The next step was to perform the radiation transport calculations to estimate the dose rates. The ANISN code was used for this. The results in the form of dose rate vs shield thickness are shown in Figure 7.1.

TABLE 7.1. Primary ORIGEN Input Assumptions

	<u>Time, hr</u>	<u>Power, MW/Test Assembly</u>
Conservative Case	1.0	4.0
	48.0	0.0
	20.0	0.4
Minimum Case	1.0	1.116

These results are for the inspection period following the thermal-hydraulics test. As stated earlier this presents the worst case. The dose rate following the last materials test, assuming the same assembly is used in all the tests, is estimated to be about a fifth of that following the thermal-hydraulic test.

Also included in Figure 7.1 is consideration of additional shielding material. Since the personnel need not have continuous access to the test assembly, such additional material could reduce their total exposure. As can be seen from the figure adding 13 mm of steel cuts the dose rate by roughly a factor of two.

Another means of reducing the dose is to increase the cooling time, the time after irradiation before examination. Figure 7.1 assumes one day cooling, which is felt to be a minimum time to remove the test assembly from the reactor and transfer it into the basin. Increase the cooling time to 30 days yields about a factor of 35 reduction in the dose rate.

The dose estimates presented in Figure 7.1 are from our test only. The basin also contains irradiated AECL material. However, this material is kept at a considerable depth, up to 3.7 m, and therefore the dose from that material will be quite small as compared to that coming from our test.

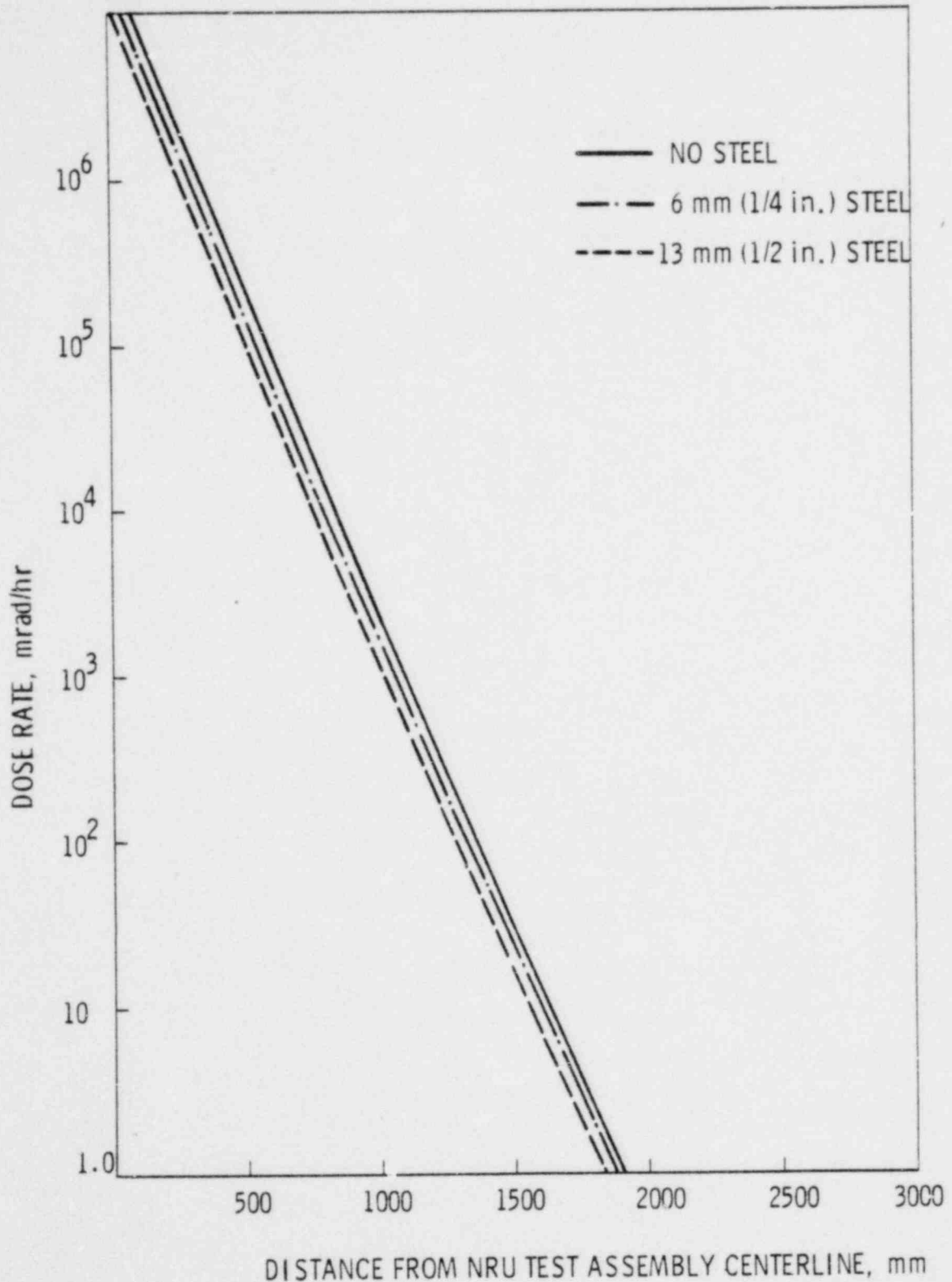


FIGURE 7.1 Dose Rate From NRU Test Assembly as a Function of Distance in Water Filled Pool, Thermal-Hydraulic Test, One Day Cooling

8.0 TRANSIENTS

The majority of neutronics work done in support of the NRU-LOCA project have involved steady state reactor conditions. This is sufficient to supply the answers needed for the majority of the project. However, in some special cases the transient or time dependent behavior of the reactor or the test is desired. Estimates were made of the reactor's response to a sudden voiding of the test loop, the total reactor energy generation following a scram and the decay heat rates for the test assembly as a function of time.

8.1 WATER LOSS FROM THE TEST LOOP

The presence of light water in the test loop during the preconditioning phase acts as a neutron poison. This seemingly unusual effect is a product of the very well thermalized flux of the heavy water reactor. The thermal flux impinging on the light water is degraded by absorption while benefiting little from further moderation. Therefore, there is a concern that if the water were to be lost suddenly from the test loop a sharp positive nuclear reactivity insertion would occur.

The loss of water from the loop is estimated to have a positive reactivity worth of 2.6 mk ($\$0.45$). This is within the acceptable limits established for the NRU reactor. Even though the reactivity increase was acceptable, a series of calculations were performed to further examine the effect. The loss of water in the loop and subsequent replacement with steam results in an increase in reactivity and therefore a power spike. The results of the analysis indicate that the reactor would undergo a 17% maximum increase in total power before the control system could shut the reactor down.

The analysis of the reactor power was made using a point kinetics model with six groups of delayed neutrons. The set of equations were solved using a fourth order Runge-Kutta numerical technique. The numerical values of the nuclear data are displayed in Table 8.1.

The test loop was assumed to drain in a minimum of one second. The positive reactivity insertion was assumed to be linear with time during the water loss up to a maximum positive insertion of $\$0.45$ after one second.

The reactor control system was modeled as inserting a maximum negative reactivity of \$4.5 in two seconds with a cosine shaped insertion. A three tenths of a second delay time was allowed between the detector response and the initiation of control rod motion. The reactor was modeled to scram on any one of three different events: 110% of steady state maximum (135 Mw) power; 5%/second rate change in the log power measurement; or 5 MW/second rate change in the linear power measurement. No time lag existed between the actual occurrence of an event in core and its detection.

The numerical results are displayed in Table 8.2 for the base case. Figure 8.1 shows the reactor power and reactivity for the same case. The calculations indicate that the postulated transient would generate a reactor power increase rising to a peak of 117% of the pretransient power (assumed to be 135 Mw) and decaying to 100% pretransient power about one second after voiding begins.

As an indication of the sensitivity of the water drain rate an analysis was performed in which a \$0.45 step insertion was made in the reactivity. In this case the power rises to 154% of pretransient power. The power and reactivity are shown in Figure 8.2 for this case.

TABLE 8.1. Nuclear Constants for Delayed Neutron Precursors

<u>Group</u>	<u>Fractional Yield</u>	<u>Decay Constant (Seconds -1)</u>
1	.000215	.0124
2	.001424	.0305
3	.001247	.111
4	.002568	.301
5	.000748	1.14
6	.000273	3.01

Prompt Neutron Lifetime - .002 seconds

TABLE 8.2. The Normalized Reactor Power After a Ramp Reactivity Insertion

<u>Time (Seconds)</u>	<u>Reactivity (\$)</u>	<u>Power</u>
0.	0.0	1.0
.1	0.045	1.007
.2	0.090	1.024
.3	0.135	1.051
.4	0.179	1.085
.5	0.206	1.123
.6	0.197	1.157
.7	0.136	1.172
.8	0.009	1.154
.9	-0.187	1.091
1.0	-0.451	0.981

8.2 REACTOR POWER AFTER SCRAM

If some untoward event should happen during the test a reactor scram, or emergency shut down, might be activated. Even with the scram, however, energy generation in the reactor does not immediately cease. The energy generation will have two components, these being the tail off of fission power and decay heat.

Fission power will take a sharp decrease upon control rod insertion. The magnitude of this "prompt drop" is a function of the magnitude and rate of negative reactivity insertion. After the prompt effect the reactor fission power will tail off at an eighty second period. That is it will decrease by a factor of e, the natural logarithm, every eighty seconds. The rate and magnitude of the insertion has no effect on this period. Once the reactor becomes subcritical, fissions are running off delayed neutrons, whose generation rate is fixed.

Decay heat is generated by the radioactive decay in the reactor core. The fission process creates a large number of radioactive isotopes. These

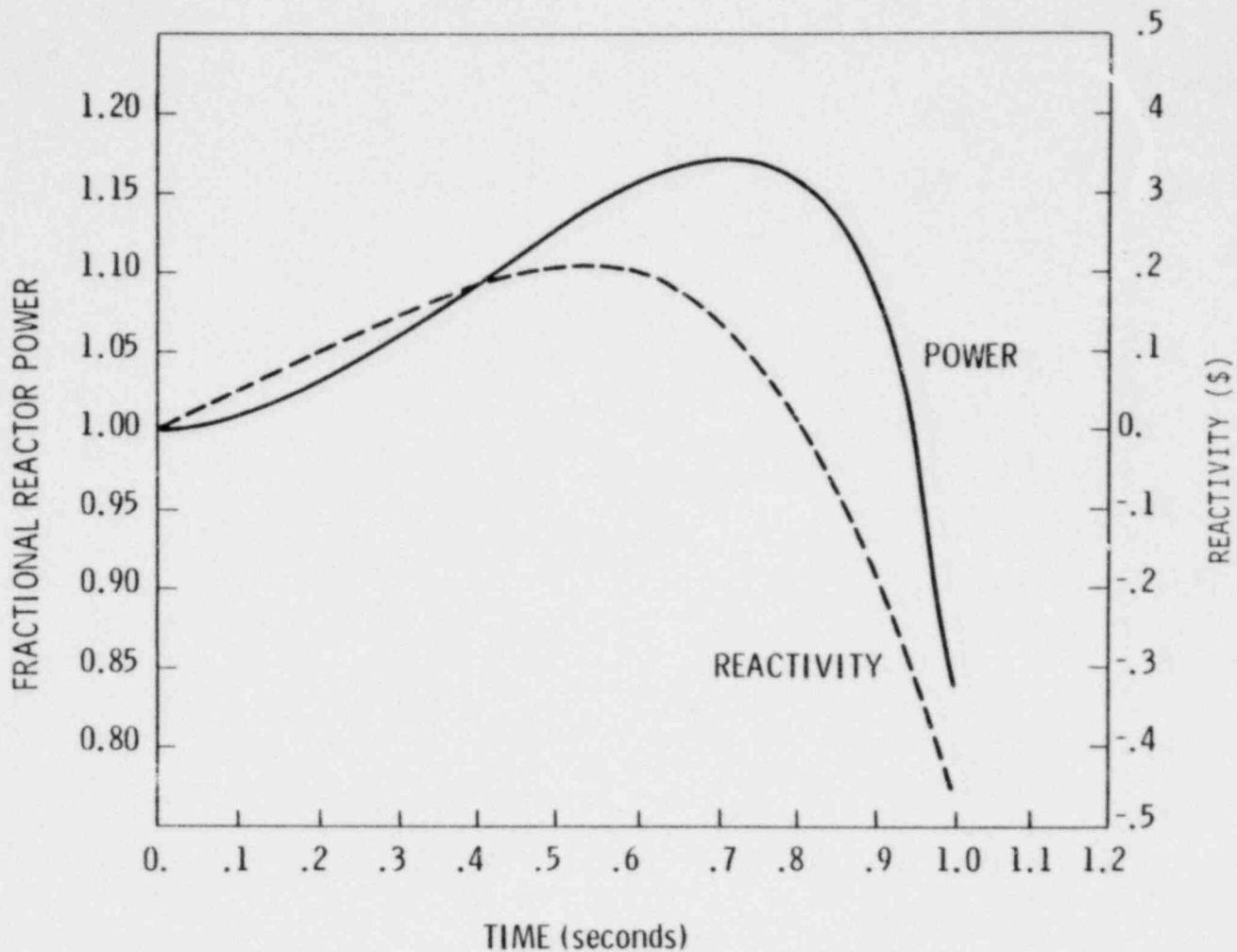


FIGURE 8.1 Ramp Reactivity Insertion

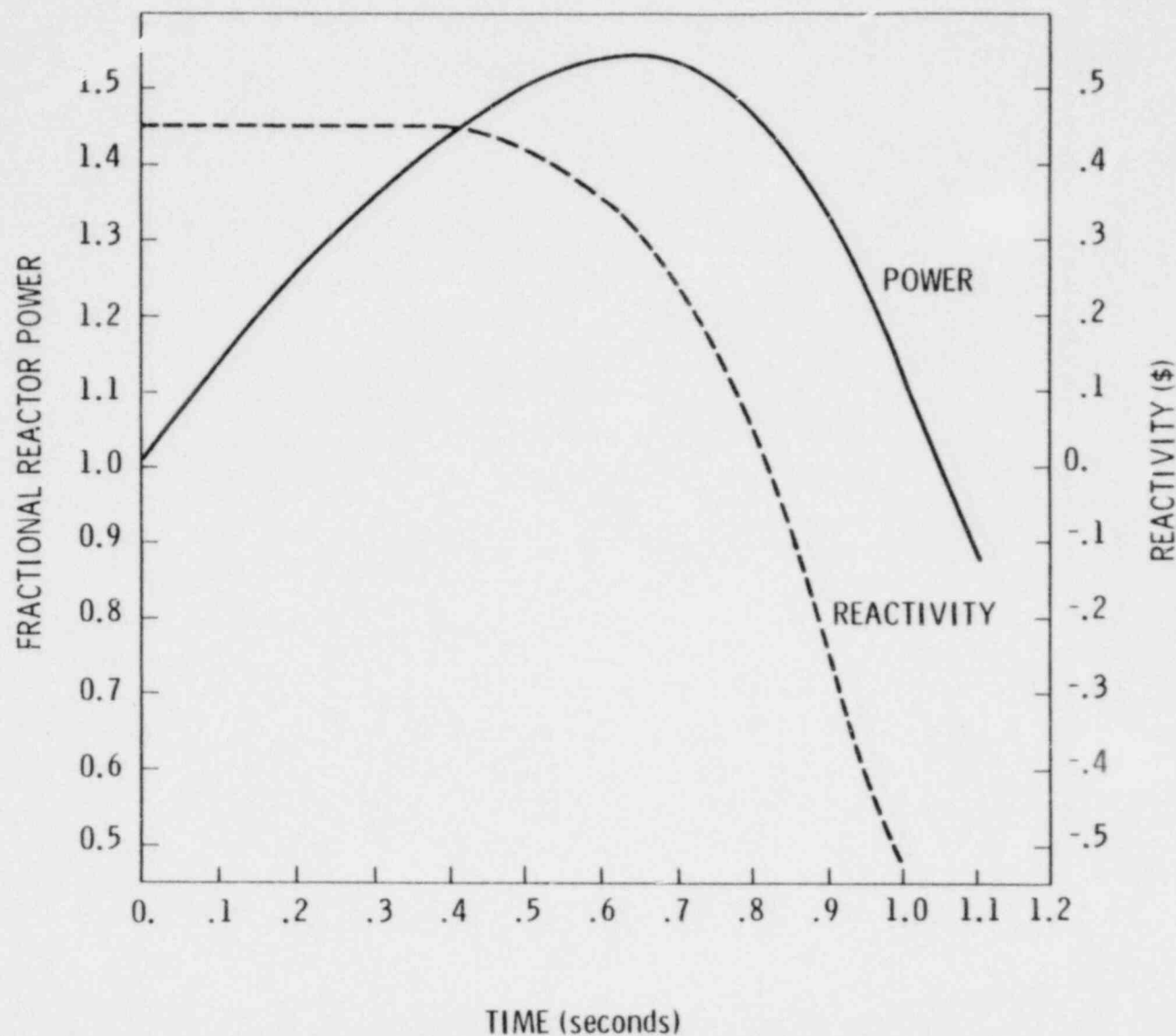


FIGURE 8.2 Step Reactivity Insertion

decay at various rates, giving off radiation which will ultimately appear as heat.

Both of these processes contribute to the total reactor power. We have combined them and the resultant total power is shown in Figure 8.3. In generating this figure it was assumed that \$4.5 worth of control rods were dropped in a two second cosine shaped insertion. This approximates one of two banks of NRU reactor control rods. It was further assumed the reactor has been at power for a sufficient length of time (~100-200 hours minimum) to saturate the fission products.

8.3 DECAY POWER FROM TEST ASSEMBLY

While the preceding material describes the behavior of the reactor as an aggregate it does not strictly apply to the test assembly. The thermal power, from decay heat, for the test assembly can effect the design and operation of post irradiation handling. To estimate the heat generation as a function of time the ORIGEN runs which are shown in Appendix B were used. As part of its prodigious output ORIGEN estimates thermal power. In addition to the thermal power listed in ORIGEN an additional source of heat is supplied by the gamma heating due to the NRU reactor. The gamma heating in the test bundle, from the NRU reactor, is estimated by a ratioing factor. The amount of gamma heating supplied by the reactor to the test bundle, while at full power (see section 9.0), is ratioed down to the reactor at decay power. A weighting factor is then applied to account for the fact that only 7% of the operating power is attributable to gamma heating whereas 50% of decay power comes from gamma heating. The estimates for the test assembly decay heat following the thermal-hydraulics test and one materials test are shown in Figure 8.4. The decay heat in Figure 8.4 includes the gamma heating supplied by the reactor.

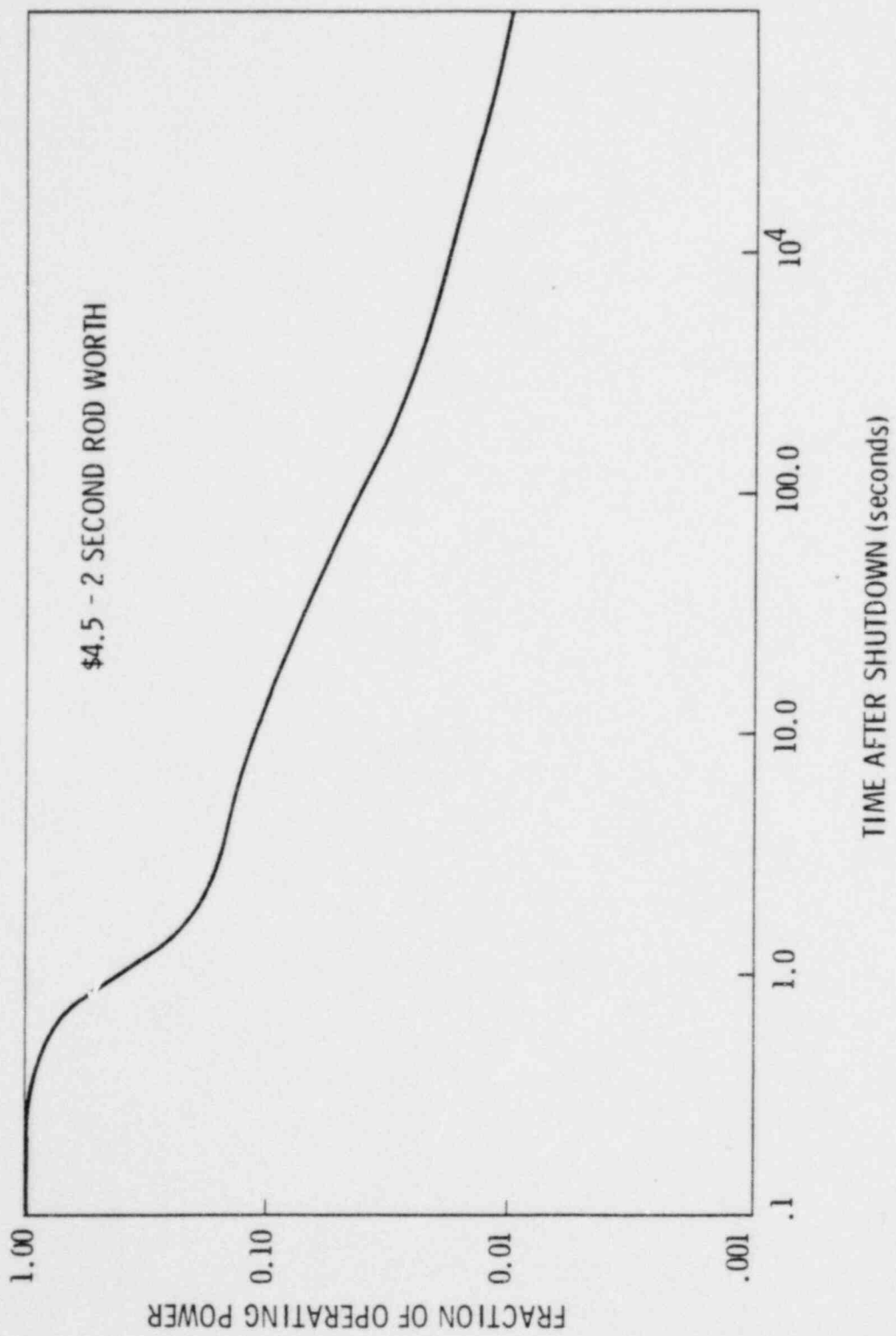


FIGURE 8.3 Total Reactor Power After Scram

DECAY POWER IN TEST

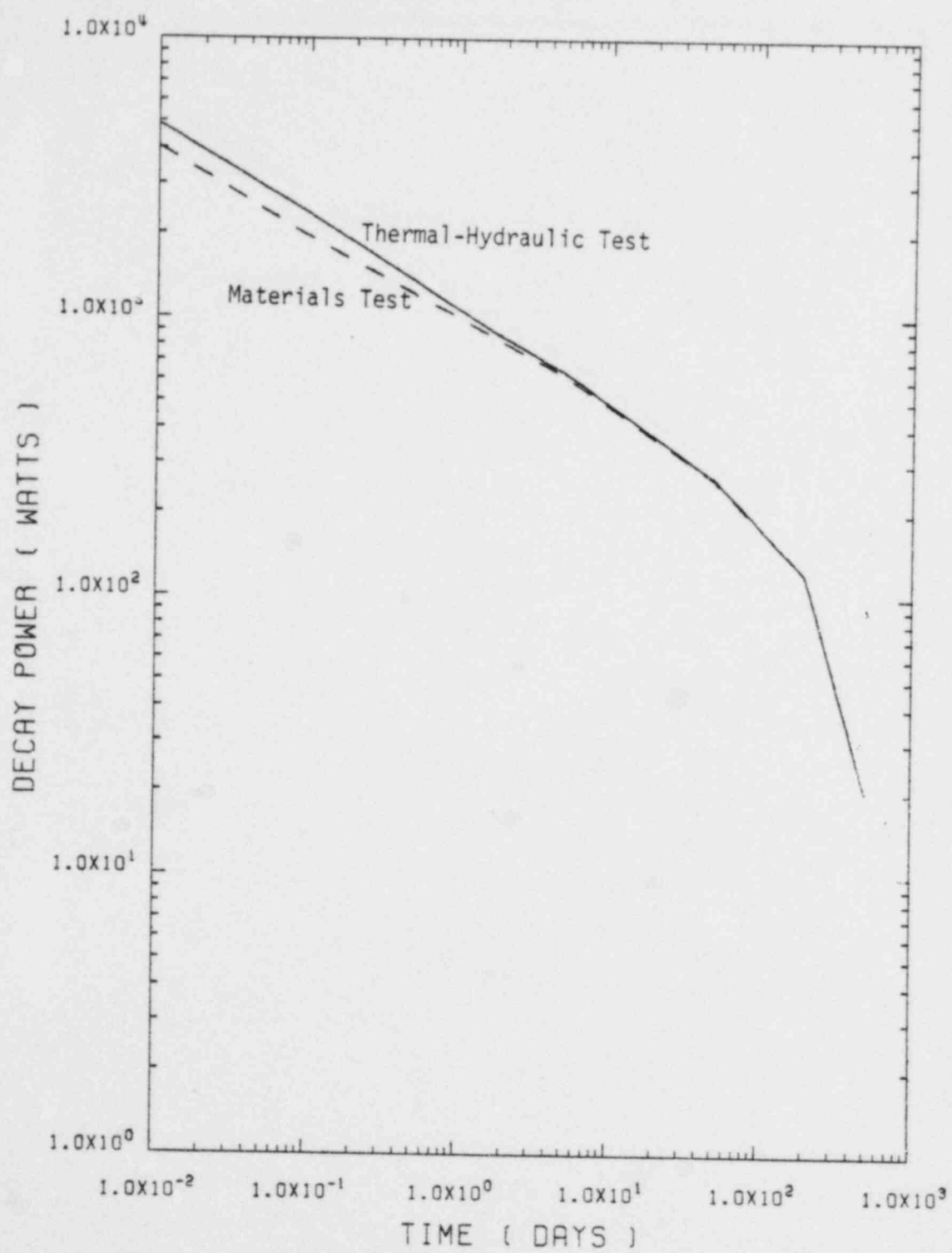


FIGURE 8.4. Test Assembly Decay Heat

9.0 NEUTRON AND GAMMA HEATING

As a consequence of the nuclear fission process neutrons and gamma rays are produced. The interaction of the radiation with structural material and coolant fluids results in energy deposition which appears as heat. The rate of this deposition is usually small, as compared to direct fission heat, but potentially significant.

This section describes the physical process of the neutron and gamma interaction, the neutronics calculations performed to estimate the heating rates, and the results obtained. The calculations were performed before the final reactor model and test specifications were established. However, since the results are generally conservative and the original results did not generate undue concern, the calculations based on the preliminary information was not revised.

9.1 HEATING RATES IN TEST FUEL COOLANT

The neutron and gamma heating in the test fuel coolant is only significant for the water cooled condition. The steam coolant presents too little density for significant interactions. The processes of neutron and gamma interaction are described below.

Neutron

Fission neutrons carry in the form of kinetic energy about 3% of the energy released in the fission process. The majority of this energy is deposited in the reactor core, i.e., fuel, coolant and structure. There are two ways in which that energy deposited will be converted to heat. The first is a local deposition through scattering reactions, atom recoil, and charge particle production. The second is via the process of gamma production, α -transport, and α -absorption.

To determine the amount of heat deposited in the reactor for a single charged particle reaction, each type of reaction must be analyzed independently. For reactions which produce no gamma rays, the energy deposited may be calculated assuming that it is equal to the kinetic energy of the neutron plus the reaction mass difference. For reactions which produce gamma rays,

the average energy carried off by the gamma rays must be subtracted as the gamma energy will be deposited elsewhere in the reactor. For reactions involving β decay, the energy carried off by neutrinos must be taken into account.

In neutron capture reactions, heat is deposited in the reactor due to the recoil of the nucleus following the emission of gamma rays. Neutron scattering reactions also result in a transfer of energy. In this process the particle leaving the reaction site is identical with the incident particle, the net result being that some of the kinetic energy of the incident particle is deposited with the target nucleus.

The total energy deposited in the reactor from the individual neutron reactions may be determined by the use of fluence-to-kerma factors. Fluence is the time integrated flux and kerma is an acronym for the kinetic energy released in materials. The neutron kerma include the energy deposited by the neutrons and charged particles produced by neutron interaction. The kerma factors for neutrons do not include the effects due to collisions after the first collision or energy deposition due to gamma rays produced by a neutron interaction. The assumption that charged particles deposit their energy locally (at the site of the neutron interaction) is an approximation since some charged particles may travel far from the reaction site before all of their kinetic energy is deposited. However, in a steady state case away from a boundary, the average energy deposition from all charged particles is such that this approximation may be made with little error. The microscopic kerma factors may be found by summing over the energy releasing reactions for a particular nuclide

$$KF_i(E) = \sum_j \sigma_{ji}(E) E_j^*(E)$$

where $KF(E)$ is the kerma factor for element i ; $\sigma_{ji}(E)$ is the microscopic cross section for reaction j ; and $E_j^*(E)$ is the energy released by reaction j from a particle with energy E with element i .

The space dependent heating rates, HR_i , in the coolant from neutron interaction may be calculated by use of the fluxes, and the respective group kerma factors from the following relationship:

$$HR_i = \sum_k \sum_{\ell} \Phi_{\ell i} KF_{\ell k} A_{ki}$$

where $\Phi_{\ell i}$ is neutron flux in energy group ℓ at space point i ; $KF_{\ell k}$ is the kerma factor for element k corresponding to flux energy group ℓ ; and A_{ki} is the number density of element k at space point i .

For our particular case, kerma factors were weighted using 20 group rod cell fluxes from ANISN into 4 groups. These 4 group kerma factors were used with the four group fluxes from an ANISN reactor calculation to determine the heating rates in the coolant. The results are plotted in Figure 9.1.

Gamma

Gamma radiation in a reactor is produced in a variety of ways. The most important sources are:

- . Prompt Fission Gammas
- . Fission Product Decay Gammas
- . Neutron Capture
- . Inelastic Scatter

The gammas from prompt fission carry about 7.25 MeV.⁽¹⁾ The fission products will release about 7.63 MeV⁽¹⁾ through decay, and 75% of the gammas will have been released within 10 seconds following fission.⁽¹⁾ If the reactor core has reached equilibrium, it may be assumed that 14.88 MeV, the sum of the delayed plus prompt gammas, are released with each fission. In addition, the gamma energy spectra from both prompt and fission gammas are approximately equal.

Typically from 6 to 8 MeV⁽¹⁾ of gamma energy is produced per capture event. Since about 1.4 neutrons per fission undergo capture, it can be estimated that about 10 MeV of energy is released in the core, due to capture, per fission. This 10 MeV plus the gamma energy generated from other gamma

sources results in an energy release that is approximately equal to 15 MeV due to fission and fission products.

There are three main ways in which gamma rays interact with matter, namely: photoelectric effect, Compton effect, and pair production. These are absorption and scattering processes, thus transport methods may be used to calculate the gamma flux in the reactor core. Each of these processes transfer energy into the form of heat to the core.

Each point in the core is a possible site of gamma production due to one or more of the gamma production processes. However, the gammas produced may be transported a considerable distance before their energy is deposited as heat. Thus the heat distribution is somewhat different from the source distribution, in that, it is flatter and smoother. In addition it would be expected that the capture and decay gamma source would be the highest in the vicinity of the neutron source, that is, where fissions occur. For these reasons, as a first approximation, it was assumed that the gamma flux distribution from fission and fission products is representative of gamma flux distribution in the core due to all sources. In addition, it is assumed that the total energy deposited at a point from all sources, is twice that deposited by the fission and fission product decay gammas since, as noted earlier, the energy release from other processes are approximately equal to that of fission gammas plus fission products decay gammas.

An empirical fit,⁽¹⁾ to the fission spectra measured by Peelle and Maienschein,⁽²⁾ was integrated over each of 16 gamma energy groups, to determine the number of gamma rays in each energy group due to fission and fission product decay. The space and energy dependent gamma source was calculated by multiplying the 16 group spectra times the fission density at each of the space points in the reactor.

This gamma source was used with the preliminary one dimensional model. Using the ANISN code and previously calculated gamma cross sections,⁽³⁾ one dimensional S₈-P₃ gamma transport calculations were made. The resultant space and energy dependent gamma fluxes and associated reaction rates were used to calculate the energy deposited at each space point in the reactor.

Integration over space points gave the energy deposited from the prompt fission and fission product gamma rays. These results were multiplied by two to obtain an approximation for the total gamma energy released.

The calculations yielded an average heating rate in the center of this test cell (in the water pin) and in the water surrounding the shroud. Linear interpretation was used to plot the heating rate across the fuel. The results are plotted in Figure 9-1.

The combined heating rate at the midpoint of the test fuel was estimated to be 7.7 W/g. This estimate is at 135 MW reactor power. Heating rates for lower powers can be approximated by linear scaling.

9.2 GAMMA HEATING IN STRUCTURAL MATERIAL

In estimating the energy deposition in structural materials only gamma rays were considered. Because of the relatively low neutron absorption rates and high densities, neutron heating would be only a small component in the total heating rate of structural materials.

In estimating the heating rates the pressure tube, separating the test from the reactor, and the shroud are of special concern. In order to calculate the gamma heating the gamma sources, gamma transport and rates of deposition must each be determined. The methods used to calculate the heating rates are approximate in nature and the results may be viewed as an upper limit.

Using the approximations noted earlier the total gamma energy deposited per gram of material in the shroud and pressure tube was calculated for three specific cases. The pressure tube was assumed to be two annular rings, the inner of zircaloy and the outer of aluminum.* Two types of shrouds are considered. The first is a zircaloy shroud which was specified in preliminary designs. The second is the stainless steel shroud of later designs. Water

*It was later discovered that both the pressure tube and the outer liner tube are zircaloy. Using the inner zircaloy heating rates for the liner should be conservative.

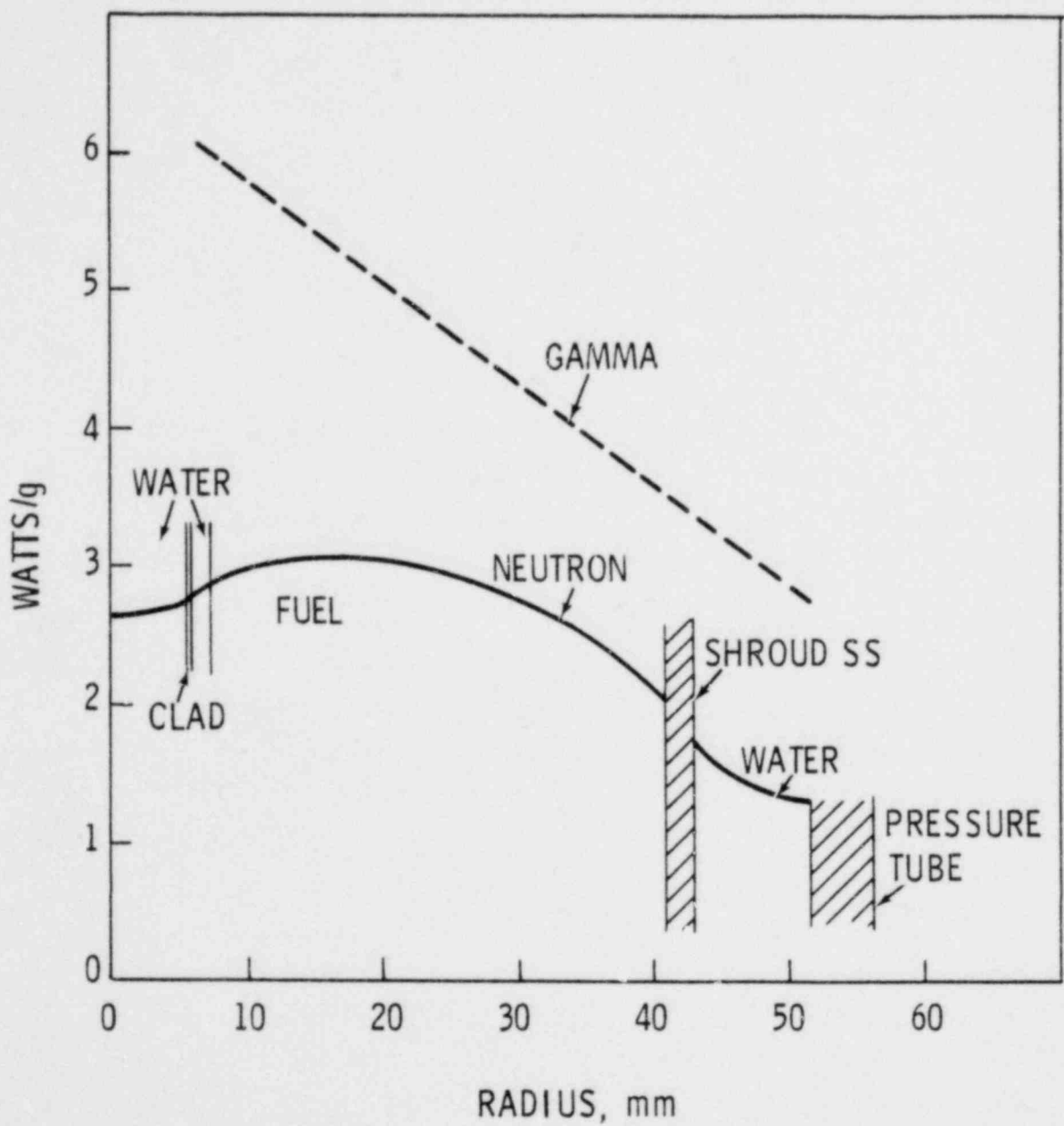


FIGURE 9.1 Neutron and Gamma Deposition in the Water Coolant

was assumed as coolant in the case of the stainless steel shroud. The zircaloy shroud cases were calculated with both steam and water coolant. The results of the calculations are given in Table 9.1.

The differences noted in the heating rates arise from the change in the fission density across the core and the test loop when water replaces steam as a coolant, or stainless steel replaces zircaloy in the shroud. In the zircaloy shroud, water cooled case, 85% of the gamma energy deposited in the shroud came from the test bundle. In the pressure tube, 72% of the energy deposited arose from the test bundle. This gives an indication of the importance of the power level of the test bundle to the gamma heating rates in the surrounding structure.

TABLE 9.1. Gamma Heating Rates (at Full Reactor Power - 135 MW)

<u>Shroud Material</u>	<u>Test Coolant</u>	<u>Shroud Heating Rate</u>	<u>Zr Annulus Heating Rate</u>	<u>Al Annulus Heating Rate</u>
Zr	Water	3.2 W/g	2.4 W/g	2.1 W/g
Zr	Steam	3.7 W/g	2.8 W/g	2.5 W/g
SS	Water	2.1 W/g	1.8 W/g	1.6 W/g

REFERENCES

1. N. M. Schaeffer, Reactor Shielding for Nuclear Engineers, TID-25951, USAEC, 1973.
2. R. W. Peelle and F. C. Maienschein, "Prompt Gamma Rays from Thermal Neutron Fission of Uranium." Nuclear Science and Engineering, 40:485, 1970.
3. M. G. Zimmerman and D. H. Thomsen, A Shielding Calculations System for Plutonium, BNWL-1855, Battelle, Pacific Northwest Laboratories, p. 9, 1975.

APPENDIX A
NEUTRONICS CODE DESCRIPTION

The preliminary neutronics calculations and predictions for the NRU reactor utilized the following computer codes:

1. EGGNIT II

The EGGNIT II Code⁽¹⁾ generates multigroup constants in the energy range from 0 to 10 MeV for either homogeneous mixtures or heterogeneous arrays of cylindrical fuel elements. The thermal group constants are averaged over either (1) Wigner-Wilkins light moderated spectrum, (2) Wilkins heavy moderator spectrum, or (3) Maxwellian distribution. For heterogeneous arrays, the spatial thermal flux is calculated by the P₃ approximation. For epithermal energies, the slowing down distribution is described by either a P₁ or B₁ approximation to the Boltzman equation. Resonance absorption is calculated by the Nordheim method. Nordheim numerical integration method permits treating absorbers and admixed scatterers exactly. An iteration technique is utilized to extend Nordheim's method to multiregion and other complex geometries. Fast fission corrections are calculated by an n-flight collision probability technique.

Other features are: 1) Interference absorption due to a nearby resonance line is permitted, (2) Interference scattering is included, 3) resonance absorption integral contributes to the absorption of several GAM-I fine groups, 4) Dancoff shielding correction is computed for either square or hexagonal lattices.

2. ANISN

ANISN⁽²⁾ solves the one dimensional Boltzman transport equation for neutrons or gamma rays in slab, sphere, or cylinder geometry. The source may be fixed, fission, or a subcritical combination of the two. Criticality search may be performed on any one of several parameters. Cross sections may be weighted using the space and energy dependent flux generated in solving the transport equation.

The solution technique is an advanced discrete ordinates method which represents a generalization of the method originated by G. C. Wick and greatly developed and extended to curvilinear geometry by B. C. Carlson at Los Alamos Scientific Laboratory.

ANISN was designed to solve deep-penetration problems in which angle-dependent spectra are calculated in detail. The principal feature that makes ANISN suitable for such problems is the use of a programming technique with optional data-storage configurations which allows execution of small, intermediate, and extremely large problems. ANISN also includes a technique for handling general anisotropic scattering, pointwise convergence criteria, and alternate step function difference equations that effectively remove the oscillating flux distributions sometimes found in discrete ordinates solutions.

3. 2DBS

2DBS⁽³⁾ is a two dimensional (x-y, R-Z, R-θ, triangular), multi-group diffusion theory code for use in reactor criticality shielding and burnup analysis. The code can be used to:

- Compute k_{eff} and perform criticality searches on buckling, time absorption, reactor composition and reactor dimensions by means of either a flux or adjoint model.
- Compute material burnup using a flexible material shuffling scheme.
- Compute flux distributions for an arbitrary extraneous source.

Since 2DBS was designed for fast reactor calculations a simple modification was performed to allow the user to input the correct removal and transport cross sections for a thermal system.

4. BRT

The original THERMOS code was written by H. C. Honeck⁽⁴⁾ in 1961 at Brookhaven National Laboratory. It is designed to compute the neutron density from the collision probability form of the integral transport-theory matrix equation using either a combination of power

iteration, overrelaxation and extrapolation or straight power iteration. The neutron currents are computed from either the gradient of the scalar flux or the uncollided flux matrix. The flux and current spectra are used to weight point thermal cross sections over an arbitrary thermal energy range for use in multigroup transport or diffusion theory codes.

The first revision of the code at Pacific Northwest Laboratory (PNL) was done by D. R. Skeen and L. J. Page in 1967.⁽⁶⁾ More recently, BRT, or Battelle Revised Thermos was written by C. L. Bennett and W. L. Purcell.⁽⁵⁾ They prepared the previous revisions for release, and also revised the code in mixture expansion, fission cross section averaging, transverse buckling, random access data file, multiple edits, isotropic albedo boundary condition, and neutron current calculations.

5. LEOPARD

The LEOPARD⁽⁷⁾ computer program determines fast and thermal spectra using only basic geometry and temperature data. The code optionally computes fuel depletion effects for a dimensionless reactor and recomputes the spectra before each discrete burnup step.

LEOPARD (abbreviation for Lifetime Evaluating Operations Pertinent to the Analysis of Reactor Designs) is based on the MUFT-SOFOCATE^(8,9) model as modified by Arnold⁽¹⁰⁾ and again by Strawbridge.⁽¹¹⁾

LEOPARD requires only the most basic input data. The reactor geometry, compositions and temperatures are supplied by the user. The code temperature-corrects the input data and computes number densities and three epithermal cross sections (Σ_s for the fuel pellet, Σ_s for the clad and moderator, Σ_s for the homogenized cell) to be used in the spectrum calculations.

LEOPARD assumes that every reactor contains a large array of unit fuel cells arranged in either a square lattice or a hexagonal lattice. Each unit cell contains one cylindrical fuel rod, a metallic clad around the fuel rod, and a moderator. In a real reactor this geometry is adequate within a large fuel bundle, but commonly several percent of the

core is taken up by control rod followers, water slots, assembly cans, structure, etc. LEOPARD accounts for this by allowing a fictitious region to be defined and described in a manner entirely analogous to the description of the "real" regions within the unit fuel cell. Spectrum calculations are then done on an "equivalent" unit cell.

6. CINDER

The temporal concentrations of fission-product nuclei produced in a nuclear reactor are described by a large set of coupled differential equations, each nuclide concentration being determined by a history of gains from direct fission yield, transmutation and radioactive decay from parent nuclei, and losses from its own decay and particle absorption. In 1962 the depletion and fission-product computer program CINDER⁽¹²⁾ was published. It simplified the solution for fission-product concentrations by resolving the complicated nuclide couplings into "linear chains." Each linear chain represents a unique linear path from nuclide to nuclide, resulting in small independent sets of coupled differential equations describing the rate of change of "partial concentrations" of nuclides in each chain. The solution of a large set of coupled differential equations was thus reduced to the solution of a number of small sets of coupled differential equations, each characterized by a single generalized form.

A modified version of the basic CINDER code (EPRI-CINDER)⁽¹³⁾ was developed under the management of the Electric Power Research Institute.

7. ORIGEN

ORIGEN⁽¹⁴⁾ is a versatile point depletion code which solves the equations of radioactive growth and decay for large numbers of isotopes with arbitrary coupling. The code uses the matrix exponential method to solve a large system of coupled, linear, first-order ordinary differential equations with constant coefficients. The general nature of the matrix exponential method permits the treatment of complex decay and transmutation schemes. An extensive library of nuclear data has been

compiled, including half-lives and decay schemes, neutron absorption cross sections, fission yields, disintegration energies, and multigroup phonon release data.

REFERENCES

1. C. R. Richey, EGGNIT: A Multigroup Cross Section Code, BNWL-1203, Pacific Northwest Laboratories, Richland, WA., November 1979.
2. Ward W. Engle, Jr., A Users Manual for ANISN a One Dimensional Discrete Ordinates Transport Code with Anisotropic Scattering, K-1693, Oak Ridge National Laboratory, Oak Ridge, Tennessee, March 30, 1967.
3. D. R. Marr, A User's Manual for 2DFS, A Diffusion Theory Shielding Code, BNWL-1291, Battelle, Pacific Northwest Laboratories, Richland, WA., February 1970.
4. Henry C. Honeck, THERMOS: A Thermalization Transport Theory Code for Reactor Lattice Calculations. Brookhaven National Laboratory, Upton, N.Y., 1961.
5. C. L. Bennett and W. L. Purcell, BRT-1: Battelle Revised THERMOS, BNWL-1434, Battelle, Pacific Northwest Laboratories, Richland, WA., 1970.
6. D. R. Skeen and L. J. Page, THERMOS/Battelle: The Battelle Version of the Thermos Code, BNWL-516, Battelle, Pacific Northwest Laboratories, Richland, WA., 1967.
7. R. F. Barry, LEOPARD-A Spectrum Dependent Non-Spatial Depletion Code for the IBM-7094, WCA9-3269-26, Westinghouse Electric Corporation, Pittsburgh, PA., 1963.
8. H. Bohl, E. Gelbard, and G. Ryan, MUFT-4 - Fast Neutron Spectrum Cor. for the IBM-704, WAPD-TM-72, July 1957.
9. H. Amster and R. Suarez, The Calculation of Thermal Constants Averaged over a Wigner-Wilkins Flux Spectrum: Description of the SOFOCATE Code, WAPD-TM-39, January 1957.
10. W. H. Arnold, Jr., Critical Masses and Lattice Parameters of H₂O-UO₂ Critical Experiments: A Comparison of Theory and Experiment, YAEC-152, November 1959.
11. L. E. Strawbridge, Calculation of Lattice Parameters and Criticality for Uniform Water Moderated Lattices, WCAP-3269-25, September 1953.
12. T. R. England, CINDER-A One-Point Depletion and Fission Product Program, WAPD-TM-334, 1962-Rev. 1964.

13. T. R. England, W. B. Wilson, M. G. Stamatelatos, Fission Product Data for Thermal Reactors, EPRI NP-356, 1976.
14. M. J. Bell, ORIGEN-The ORNL Isotope Generation and Depletion Code, ORNL-4528, 1973.

APPENDIX B

ORIGEN DATA

The ORIGEN code was used to generate fission product source terms and decay heat estimates for the test assembly (see Sections 7.0 and 8.3). In this appendix some of the important input assumptions are given and the fission product inventory by curies is given for three cases. The three cases include the final design power history cases for the thermal hydraulics and materials test and the lower bound irradiation for gamma scanning.

TABLE B.1. ORIGEN Input Assumptions

$THERM = \sqrt{\frac{\pi}{4} \frac{T_0}{T}}$ = 0.5 - The ratio of the neutron reaction rate for a 1/V absorber with a population of neutrons having a Maxwell-Boltzman distribution of energies at absolute temperature, T, to the reaction rate with 2200 m/sec neutrons

T_0 = 293.16°K

T = 922°K = 1200°F

RES = 0.0874

- The ratio of the resonance flux per unit lethargy to the thermal neutron flux

FAST = 0.0

- The ratio of flux above 1 MeV to the fraction of the fission spectrum above 1 MeV, divided by the thermal neutron flux

TABLE B.2 ORIGEN Irradiation Assumptions

	<u>Time, hr</u>	<u>Power, MW/Test Assembly</u>
Thermal-Hydraulics Test	1.0	2.60
	48.0	0.00
	20.0	0.14
Materials Test	1.0	2.60
	24.0	0.00
	1.1	0.14
<u>Minimum Case</u>	1.0	1.12

TABLE B.3. Fuel Isotopes Charged to Reactor

<u>Isotope</u>	<u>Weight in Test Assembly, g</u>
^{234}U	1.24×10^1
^{235}U	1.63×10^3
^{238}U	5.27×10^4
^{16}O	7.28×10^3
^{17}O	2.8
^{18}O	1.49×10^1

The ORIGEN code output shown below may at first appear somewhat odd. The difficulty is caused by the format designing the print out of the time periods. It prints only in integer days, hence the anomalous 0. days on the print out. The proper time spans are 0.01 days, 0.1 days, 0.5 days, and the rest are correct as given.

TABLE B.4. Fission Product Inventory: Materials Test, Curies

10/02/73

NASCITAL DOSE SAVADOCYCLOVIT. CORTES

TABLE B.4 Continued

34519 = THE 31 BOSTON

TABLE B.4 Continued

SEARCHED INDEXED SERIALIZED FILED
SCC 11-26 147330

304

10/02/19

एकलिंग साहोडाची विवादी कृतिशा

TABLE B.4 Continued

DECAY 22113
DECAY 13213, PLATE 4, UD+0124/C4+2-SEC

NUCLEAR RADIODACTIVITY, CURIES
34815 TEST BY NOL

CHARGE	DISCHARGE	0. DV	0. DV	0. DV	1. DV	1. DV	2. DV	5. DV	50. DV	200. DV	500. DV	1000. DV
R4103	+0.0	*0.0	*0.0	*0.0	*0.0	*0.0	*0.0	*0.0	*0.0	*0.0	*0.0	*0.0
R4104	+0.2	2.1*0.03	9.41*0.01	9.19*0.03	9.19*0.00	1.69*0.03	1.72*0.01					
R4104	+0.2	1.41*0.05	1.19*0.03									
R4104	+0.2	*0.0	*0.0	*0.0	*0.0	*0.0	*0.0	*0.0	*0.0	*0.0	*0.0	*0.0
R4104	+0.2	*0.0	*0.0	*0.0	*0.0	*0.0	*0.0	*0.0	*0.0	*0.0	*0.0	*0.0
R4104	+0.2	1.22*0.04	1.53*0.03	1.39*0.14	1.39*0.14	*0.0	*0.0	*0.0	*0.0	*0.0	*0.0	*0.0
R4104	+0.2	1.75*0.03	1.29*0.05	2.26*0.14	2.26*0.14	*0.0	*0.0	*0.0	*0.0	*0.0	*0.0	*0.0
R4104	+0.2	*0.0	*0.0	*0.0	*0.0	*0.0	*0.0	*0.0	*0.0	*0.0	*0.0	*0.0
R4105	+0.2	1.37*0.04	5.37*0.04	*0.0	*0.0	*0.0	*0.0	*0.0	*0.0	*0.0	*0.0	*0.0
R4105	+0.2	1.07*0.04	4.21*0.04	*0.0	*0.0	*0.0	*0.0	*0.0	*0.0	*0.0	*0.0	*0.0
R4105	+0.2	5.52*0.02	5.52*0.02	2.51*0.02	5.51*0.01	8.62*0.00	2.03*0.01	2.67*0.06	*0.0	*0.0	*0.0	*0.0
R4105	+0.2	3.03*0.02	5.53*0.02	2.52*0.02	5.63*0.01	9.65*0.00	2.04*0.01	2.69*0.06	*0.0	*0.0	*0.0	*0.0
R4105	+0.2	2.64*0.02	2.53*0.02	2.55*0.02	2.59*0.02	2.10*0.02	1.35*0.02	3.51*0.01	2.91*0.08	*0.0	*0.0	*0.0
R4105	+0.2	*0.0	*0.0	*0.0	*0.0	*0.0	*0.0	*0.0	*0.0	*0.0	*0.0	*0.0
R4106	+0.2	4.52*0.02	4.22*0.02	*0.0	*0.0	*0.0	*0.0	*0.0	*0.0	*0.0	*0.0	*0.0
R4106	+0.2	6.44*0.01	6.95*0.01	5.94*0.01	6.94*0.01	6.93*0.01	6.92*0.01	6.88*0.01	6.82*0.01	6.76*0.01	6.70*0.01	6.65*0.01
R4106	+0.2	4.22*0.01	3.91*0.01	1.96*0.01	9.05*0.03	1.95*0.04	9.05*0.03	9.99*0.18	*0.0	*0.0	*0.0	*0.0
R4106	+0.2	5.91*0.01	5.95*0.01	5.94*0.01	6.94*0.01	6.93*0.01	6.92*0.01	6.95*0.01	6.93*0.01	6.76*0.01	6.70*0.01	6.65*0.01
R4106	+0.2	*0.0	*0.0	*0.0	*0.0	*0.0	*0.0	*0.0	*0.0	*0.0	*0.0	*0.0
R4107	+0.2	*0.0	*0.0	*0.0	*0.0	*0.0	*0.0	*0.0	*0.0	*0.0	*0.0	*0.0
R4107	+0.2	1.73*0.02	1.42*0.02	2.44*0.00	3.26*0.08	4.59*0.18	*0.0	*0.0	*0.0	*0.0	*0.0	*0.0
R4107	+0.2	5.65*0.01	2.45*0.01	5.04*0.01	6.63*0.02	9.33*0.19	*0.0	*0.0	*0.0	*0.0	*0.0	*0.0
R4107	+0.2	4.66*0.06	4.91*0.05	5.00*0.08	5.02*0.03	5.00*0.08	5.00*0.08	5.00*0.08	5.00*0.08	5.00*0.08	5.00*0.08	5.00*0.08
R4107	+0.2	*0.0	*0.0	*0.0	*0.0	*0.0	*0.0	*0.0	*0.0	*0.0	*0.0	*0.0
R4107	+0.2	1.73*0.01	6.41*0.00	1.89*0.08	1.92*0.08	*0.0	*0.0	*0.0	*0.0	*0.0	*0.0	*0.0
R4107	+0.2	6.73*0.01	6.95*0.00	1.92*0.08	1.92*0.08	*0.0	*0.0	*0.0	*0.0	*0.0	*0.0	*0.0
R4107	+0.2	*0.0	*0.0	*0.0	*0.0	*0.0	*0.0	*0.0	*0.0	*0.0	*0.0	*0.0
R4108	+0.2	1.43*0.13	5.42*0.15	*0.0	*0.0	*0.0	*0.0	*0.0	*0.0	*0.0	*0.0	*0.0
R4108	+0.2	*0.0	*0.0	*0.0	*0.0	*0.0	*0.0	*0.0	*0.0	*0.0	*0.0	*0.0
R4108	+0.2	5.57*0.01	7.65*0.02	*0.0	*0.0	*0.0	*0.0	*0.0	*0.0	*0.0	*0.0	*0.0
R4108	+0.2	8.35*0.05	9.99*0.07	2.99*0.15	*0.0	*0.0	*0.0	*0.0	*0.0	*0.0	*0.0	*0.0
R4108	+0.2	1.52*0.01	1.53*0.01	1.55*0.01	8.46*0.00	4.57*0.00	1.33*0.00	3.30*0.02				
R4108	+0.2	1.57*0.01	1.55*0.01	1.53*0.01	8.46*0.00	4.57*0.00	1.33*0.00	3.31*0.02				
R4108	+0.2	*0.0	*0.0	*0.0	*0.0	*0.0	*0.0	*0.0	*0.0	*0.0	*0.0	*0.0
R4108	+0.2	*0.0	*0.0	*0.0	*0.0	*0.0	*0.0	*0.0	*0.0	*0.0	*0.0	*0.0
R4108	+0.2	2.35*0.01	*0.0	*0.0	*0.0	*0.0	*0.0	*0.0	*0.0	*0.0	*0.0	*0.0
R4108	+0.2	*0.0	*0.0	*0.0	*0.0	*0.0	*0.0	*0.0	*0.0	*0.0	*0.0	*0.0
R4109	+0.2	5.17*0.09	5.16*0.09	5.16*0.09	5.14*0.13	5.10*0.09	4.51*0.09	2.99*0.09	2.99*0.09	2.99*0.09	2.99*0.09	2.99*0.09
R4109	+0.2	5.74*0.04	5.72*0.10	6.71*0.12	6.70*0.10	6.59*0.10	6.63*0.10	5.46*0.10	5.49*0.10	5.49*0.10	5.49*0.10	5.49*0.10
R4109	+0.2	*0.0	*0.0	*0.0	*0.0	*0.0	*0.0	*0.0	*0.0	*0.0	*0.0	*0.0
R4109	+0.2	4.37*0.02	5.37*0.02	5.37*0.02	5.13*0.03	4.13*0.03	2.04*0.04	2.33*0.06	*0.0	*0.0	*0.0	*0.0
R4109	+0.2	1.47*0.01	1.42*0.01	2.42*0.01	1.25*0.02	3.37*0.03	1.54*0.04	1.87*0.06	*0.0	*0.0	*0.0	*0.0
R4109	+0.2	1.47*0.01	1.53*0.01	2.40*0.01	2.00*0.02	4.42*0.03	2.15*0.04	2.47*0.05	*0.0	*0.0	*0.0	*0.0
R4109	+0.2	1.60*0.02	1.62*0.03	1.63*0.00	1.57*0.00	1.57*0.00	1.37*0.00	1.04*0.00	1.62*0.02	1.55*0.08	1.41*0.20	*0.0
R4109	+0.2	5.35*0.13	6.34*0.13	5.86*0.14	1.86*0.17	6.45*0.22	*0.0	*0.0	*0.0	*0.0	*0.0	*0.0
R4109	+0.2	*0.0	*0.0	*0.0	*0.0	*0.0	*0.0	*0.0	*0.0	*0.0	*0.0	*0.0
R4110	+0.2	4.44*0.03	4.44*0.03	4.14*0.00	3.03*0.00	9.15*0.01	9.53*0.02	2.81*0.17	*0.0	*0.0	*0.0	*0.0
R4110	+0.2	4.64*0.05	4.64*0.05	4.50*0.00	3.51*0.00	1.03*0.00	1.01*0.01	3.32*0.17	*0.0	*0.0	*0.0	*0.0
R4110	+0.2	*0.0	*0.0	*0.0	*0.0	*0.0	*0.0	*0.0	*0.0	*0.0	*0.0	*0.0
R4110	+0.2	5.73*0.01	2.93*0.02	*0.0	*0.0	*0.0	*0.0	*0.0	*0.0	*0.0	*0.0	*0.0

TABLE B.4 Continued

Richard A. Gershon

כטב-טבנער צדקה

64 / 2004

עיכריה אוניברסיטאי, כוונת

TABLE B.4 Continued

માર્ગ માર્ગ
સંક્ષિપ્ત

244 *Journal of Clinical Endocrinology*

eL/e0/01

ACUTE RADIACTIVITY, CURIOS

TABLE B.4 Continued

$$S = \frac{1}{2} \int d^4x \sqrt{-g} (R - 2\Lambda) + \frac{1}{2} \int d^4x \sqrt{-g} (\partial_\mu \phi) \partial^\mu \phi - \frac{1}{2} \int d^4x \sqrt{-g} \phi (R_{\mu\nu} - g_{\mu\nu} R)$$

64 / 20 / 04

NUCLEAR RADIOACTIVITY, CUSIES

TABLE B.4 Continued

DECA 321035

גָּמְנִי, מִלְּגָמָד,

10/02/79

SOCIOLOGICAL AND DEMOCRATIC CULTURES

TABLE B.4 Continued

DECAY MODES
DATA SHEET
NUCLEAR DATA
DECAY FLUXES 4.06+012V/C4**2+3EC

10/02/79

BASIS # TEST BUNDLE
NUCLEAR RADIACTIVITY, CURIES

CHARGE	DISCHARGE	0. DY	1. DY	2. DY	3. DY	4. DY	5. DY	200. DY	500. DY	1000. DY
94147	0.0	0.0	0.0	0.0	0.0	0.0	0.0	0.0	0.0	0.0
CE148	*0.1	*0.3+005	1.82+035	*0.0	*0.0	*0.0	*0.0	*0.0	*0.0	*0.0
P2148	*0.0	2.03+031	2.15+031	6.72+019	*0.0	*0.0	*0.0	*0.0	*0.0	*0.0
H149	*0.0	*0.0	*0.0	*0.0	*0.0	*0.0	*0.0	*0.0	*0.0	*0.0
CH149	*0.0	4.54+036	4.53+0	2.53+006	4.50+006	4.46+006	4.33+005	4.19+006	3.99+006	3.86+013
P4149	*0.0	3.31+005	3.91+035	3.35+005	3.67+005	3.45+005	3.04+005	2.77+005	2.23+007	1.34+011
S4149	*0.0	*0.0	*0.0	*0.0	*0.0	*0.0	*0.0	*0.0	*0.0	*0.0
P4149	*0.0	1.34+033	1.25+031	1.31+016	*0.0	*0.0	*0.0	*0.0	*0.0	*0.0
N2149	*0.0	4.42+002	4.32+032	1.98+002	4.67+003	4.59+002	4.45+005	4.05+016	3.93+001	3.76+025
P4149	*0.0	2.77+002	2.71+032	2.71+002	2.45+002	2.10+002	1.53+002	5.93+001	4.51+005	1.76+025
S4149	*0.0	*0.0	*0.0	*0.0	*0.0	*0.0	*0.0	*0.0	*0.0	*0.0
N2150	*0.0	*0.0	*0.0	*0.0	*0.0	*0.0	*0.0	*0.0	*0.0	*0.0
P4150	*0.0	*0.0	*0.0	*0.0	*0.0	*0.0	*0.0	*0.0	*0.0	*0.0
S4150	*0.0	*0.0	*0.0	*0.0	*0.0	*0.0	*0.0	*0.0	*0.0	*0.0
N2151	*0.0	5.11+002	2.22+032	1.25+001	4.44+015	*0.0	*0.0	*0.0	*0.0	*0.0
P4151	*0.0	1.05+002	1.07+032	1.65+002	1.26+032	2.38+001	5.18+001	8.71+000	2.13+011	0.0
S4151	*0.0	5.09+003	3.12+035	3.46+003	6.66+003	5.87+003	7.02+013	9.00+003	9.31+003	9.22+003
E4151	*0.0	*0.0	*0.0	*0.0	*0.0	*0.0	*0.0	*0.0	*0.0	*0.0
N2152	*0.0	*0.0	*0.0	*0.0	*0.0	*0.0	*0.0	*0.0	*0.0	*0.0
P4152	*0.0	*0.0	*0.0	*0.0	*0.0	*0.0	*0.0	*0.0	*0.0	*0.0
S4152	*0.0	4.37+004	4.24+035	3.55+008	1.74+018	7.51+009	1.22+002	5.71+012	0.0	0.0
E4152	*0.0	7.41+012	7.41+012	7.41+012	7.41+012	7.41+012	7.41+012	7.35+012	7.18+012	6.65+012
S4153	*0.0	*0.0	*0.0	*0.0	*0.0	*0.0	*0.0	*0.0	*0.0	*0.0
E4153	*0.0	1.75+002	2.23+012	2.54+006	*0.0	*0.0	*0.0	*0.0	*0.0	*0.0
S4153	*0.0	4.51+001	4.55+001	4.59+001	3.81+001	3.19+001	2.24+001	7.75+000	9.18+007	0.0
E4153	*0.0	*0.0	*0.0	*0.0	*0.0	*0.0	*0.0	*0.0	*0.0	*0.0
S4153	*0.0	1.05+018	1.05+018	1.05+018	1.05+018	1.05+018	1.05+018	9.18+019	2.46+019	2.55+020
E4154	*0.0	9.15+001	1.05+000	1.05+000	1.05+000	1.05+000	1.05+000	0.0	0.0	0.0
S4154	*0.0	*0.0	*0.0	*0.0	*0.0	*0.0	*0.0	*0.0	*0.0	*0.0
E4154	*0.0	1.65+004	1.65+004	1.56+006	1.56+006	1.48+006	1.68+008	1.67+008	1.64+008	1.77+008
S4155	*0.0	*0.0	*0.0	*0.0	*0.0	*0.0	*0.0	*0.0	*0.0	*0.0
E4155	*0.0	5.57+002	5.53+032	5.35+002	3.35+002	3.35+002	3.33+002	3.18+002	2.72+002	1.94+002
S4155	*0.0	*0.0	*0.0	*0.0	*0.0	*0.0	*0.0	*0.0	*0.0	*0.0
E4156	*0.0	7.35+030	7.35+030	6.27+000	3.09+010	1.28+000	2.17+011	1.07+003	0.0	0.0
S4156	*0.0	4.25+031	4.27+031	4.53+001	5.27+001	5.62+001	5.63+001	6.95+001	6.19+002	6.05+005
E4156	*0.0	*0.0	*0.0	*0.0	*0.0	*0.0	*0.0	*0.0	*0.0	*0.0
S4156	*0.0	*0.0	*0.0	*0.0	*0.0	*0.0	*0.0	*0.0	*0.0	*0.0
E4157	*0.0	9.27+000	1.27+026	1.56+003	1.56+003	1.66+012	3.68+025	0.0	0.0	0.0
S4157	*0.0	5.42+000	5.42+000	5.50+000	5.50+000	5.32+000	4.45+000	1.65+002	5.13+003	4.55+021
E4157	*0.0	*0.0	*0.0	*0.0	*0.0	*0.0	*0.0	*0.0	*0.0	*0.0
S4157	*0.0	*0.0	*0.0	*0.0	*0.0	*0.0	*0.0	*0.0	*0.0	*0.0
E4158	*0.0	1.65+001	1.65+001	1.59+001	1.59+001	1.48+014	0.0	0.0	0.0	0.0
S4158	*0.0	*0.0	*0.0	*0.0	*0.0	*0.0	*0.0	*0.0	*0.0	*0.0
E4158	*0.0	1.17+000	1.17+000	1.17+000	1.17+000	1.17+000	1.17+000	0.0	0.0	0.0
S4159	*0.0	*0.0	*0.0	*0.0	*0.0	*0.0	*0.0	*0.0	*0.0	*0.0
E4159	*0.0	5.57+004	5.57+004	5.36+006	5.34+006	5.52+006	5.46+006	5.31+009	3.44+009	3.44+010
S4159	*0.0	*0.0	*0.0	*0.0	*0.0	*0.0	*0.0	*0.0	*0.0	*0.0
E4159	*0.0	*0.0	*0.0	*0.0	*0.0	*0.0	*0.0	*0.0	*0.0	*0.0

TABLE B.4 Continued

DECAY MODES
•134m, 232U, 232Th, FLUX 4.06+0124/C4+2+3FC

10/02/79

NUCLEUS RADICABILITY, CURIES
BASIS = TEST BUNDLE

CHARGE	DISCARGE	0. DY	1. DY	2. DY	5. DY	50. DY	200. DY	500. DY	1000. DY
G0151	* 0.1	9.04+002	6.04+003	1.74+013	* 0.0	* 0.0	* 0.0	* 0.0	* 0.0
T0151	* 0.2	0.67+003	0.87+003	0.57+003	5.24+003	5.65+003	4.18+003	4.55+003	4.05+024
DY151	* 0.2	* 0.0	* 0.0	* 0.0	* 0.0	* 0.0	* 0.0	* 0.0	* 0.0
G0152	* 0.2	4.53+002	1.73+002	5.11+006	0.02+024	* 0.0	* 0.0	* 0.0	* 0.0
T0152	* 0.2	0.42+002	3.12+002	1.10+005	2.37+022	* 0.0	* 0.0	* 0.0	* 0.0
DY152	* 0.2	* 0.0	* 0.0	* 0.0	* 0.0	* 0.0	* 0.0	* 0.0	* 0.0
G0153	* 0.2	* 0.0	* 0.0	* 0.0	* 0.0	* 0.0	* 0.0	* 0.0	* 0.0
T0153	* 0.2	2.14+002	5.14+003	1.37+005	* 0.0	* 0.0	* 0.0	* 0.0	* 0.0
DY153	* 0.2	7.53+007	7.37+007	3.47+007	2.11+007	5.87+008	4.54+009	2.10+012	* 0.0
G0154	* 0.2	* 0.0	* 0.0	* 0.0	* 0.0	* 0.0	* 0.0	* 0.0	* 0.0
T0154	* 0.2	2.57+005	2.55+005	2.59+003	1.74+003	1.25+003	0.05+004	0.93+005	5.16+019
DY154	* 0.2	* 0.0	* 0.0	* 0.0	* 0.0	* 0.0	* 0.0	* 0.0	* 0.0
G0155	* 0.2	2.89+005	1.02+003	* 0.0	* 0.0	* 0.0	* 0.0	* 0.0	* 0.0
T0155	* 0.2	7.12+003	6.55+003	3.47+008	1.95+004	5.42+011	4.13+014	1.82+023	* 0.0
DY155	* 0.2	* 0.0	* 0.0	* 0.0	* 0.0	* 0.0	* 0.0	* 0.0	* 0.0
G0156	* 0.2	1.00+004	1.00+004	2.35+009	9.05+003	8.13+009	0.57+019	3.61+013	* 0.0
T0156	* 0.2	4.05+021	4.05+021	4.05+021	4.05+021	4.05+021	4.05+021	4.05+021	4.05+021
H0156	* 0.2	5.25+010	3.93+010	3.93+010	2.77+009	4.31+009	5.70+009	5.53+013	* 0.0
E0156	* 0.2	* 0.0	* 0.0	* 0.0	* 0.0	* 0.0	* 0.0	* 0.0	* 0.0
E0157	* 0.2	* 0.0	* 0.0	* 0.0	* 0.0	* 0.0	* 0.0	* 0.0	* 0.0
T0157	* 0.2	4.37+005	1.27+005	4.59+004	2.44+004	1.51+004	6.16+003	3.54+003	3.36+002
									5.74+001
									1.23+001
									4.61+000

TABLE B.5. Fission Product Inventory: Thermal-Hydraulics Test, Curries

DECAY PERIODS
•15000, 3.944000
DECAY PERIODS
•15000, 3.944000

09/12/79

NUCLEO RADICACTIVITY, CURRIES

BASIS = TEST BUNDLE

CHARGE	DISCHARGE	0. DY	1. DY	2. DY	3. DY	4. DY	5. DY	200. DY	500. DY	1000. DY
1 3	*0.0	3.23+003	3.23+003	3.23+003	3.23+003	3.23+003	3.23+003	3.21+003	3.21+003	3.21+003
2 4 72	*0.0	7.41+003	7.41+003	7.41+003	7.41+003	7.41+003	7.41+003	7.35+010	7.35+010	7.35+010
3 4 72	*0.0	4.91+003	5.00+003	5.00+003	5.00+003	5.00+003	5.00+003	4.96+003	4.96+003	4.96+003
4 6 72	*0.0	5.28+003	5.28+003	5.28+003	5.28+003	5.28+003	5.28+003	5.24+010	5.24+010	5.24+010
GE 72	*0.0	*0.0	*0.0	*0.0	*0.0	*0.0	*0.0	*0.0	*0.0	*0.0
GA 73	*0.0	1.23+001	1.21+001	8.90+002	2.24+002	4.19+003	1.01+004	5.31+009	*0.0	*0.0
3E 73	*0.0	*0.0	*0.0	*0.0	*0.0	*0.0	*0.0	*0.0	*0.0	*0.0
3A 74	*0.0	4.10+001	1.15+001	1.35+006	*0.0	*0.0	*0.0	*0.0	*0.0	*0.0
3L 74	*0.0	*0.0	*0.0	*0.0	*0.0	*0.0	*0.0	*0.0	*0.0	*0.0
3A 75	*0.0	9.51+001	6.47+003	2.02+022	*0.0	*0.0	*0.0	*0.0	*0.0	*0.0
GE 75	*0.0	9.15+001	1.04+032	3.23+022	*0.0	*0.0	*0.0	*0.0	*0.0	*0.0
3E 75	*0.0	9.51+001	8.71+001	2.91+001	2.24+003	5.04+006	2.63+011	*0.0	*0.0	*0.0
4.5 75	*0.0	*0.0	*0.0	*0.0	*0.0	*0.0	*0.0	*0.0	*0.0	*0.0
GA 76	*0.0	2.97+000	2.21+005	*0.0	*0.0	*0.0	*0.0	*0.0	*0.0	*0.0
3E 76	*0.0	*0.0	*0.0	*0.0	*0.0	*0.0	*0.0	*0.0	*0.0	*0.0
4.5 76	*0.0	3.64+007	6.55+007	6.11+007	6.31+007	6.61+007	6.46+007	5.74+008	5.02+020	*0.0
3E 76	*0.0	*0.0	*0.0	*0.0	*0.0	*0.0	*0.0	*0.0	*0.0	*0.0
3E 77	*0.0	7.93+000	1.22+004	*0.0	*0.0	*0.0	*0.0	*0.0	*0.0	*0.0
3E 77	*0.0	3.12+000	3.11+000	2.72+000	1.51+000	7.24+001	1.66+001	2.01+003	*0.0	*0.0
4.5 77	*0.0	4.11+000	4.11+000	4.06+000	3.74+000	3.22+000	2.22+000	6.30+001	2.51+009	*0.0
3E 77	*0.0	1.23+002	1.23+002	1.22+002	1.12+002	9.67+003	6.67+003	1.89+003	7.52+012	*0.0
3E 77	*0.0	*0.0	*0.0	*0.0	*0.0	*0.0	*0.0	*0.0	*0.0	*0.0
3E 77	*0.0	2.35+001	2.12+001	7.67+000	6.29+002	2.89+004	3.52+009	6.34+024	*0.0	*0.0
4.5 78	*0.0	*0.0	*0.0	*0.0	*0.0	*0.0	*0.0	*0.0	*0.0	*0.0
4.5 78	*0.0	2.35+001	2.35+001	1.65+001	5.99+001	4.21+003	1.19+007	9.77+022	*0.0	*0.0
SE 78	*0.0	*0.0	*0.0	*0.0	*0.0	*0.0	*0.0	*0.0	*0.0	*0.0
4.9 79	*0.0	6.46+001	2.22+001	1.02+003	5.52+023	*0.0	*0.0	*0.0	*0.0	*0.0
3E 79	*0.0	6.66+001	3.44+001	1.79+003	9.74+023	*0.0	*0.0	*0.0	*0.0	*0.0
3E 79	*0.0	3.22+006	3.23+003	3.24+006	3.24+006	3.24+006	3.24+006	3.24+006	3.24+006	3.24+006
3E 79	*0.0	1.41+002	1.19+015	*0.0	*0.0	*0.0	*0.0	*0.0	*0.0	*0.0
4.5 80	*0.0	*0.0	*0.0	*0.0	*0.0	*0.0	*0.0	*0.0	*0.0	*0.0
SE 80	*0.0	1.15+002	1.11+002	7.86+003	1.72+003	2.58+004	5.77+006	6.50+011	*0.0	*0.0
3E 80	*0.0	1.45+002	1.14+002	6.42+003	1.84+003	2.76+004	6.19+006	6.97+011	*0.0	*0.0
K2 80	*0.0	*0.0	*0.0	*0.0	*0.0	*0.0	*0.0	*0.0	*0.0	*0.0
K2 81	*0.0	*0.0	*0.0	*0.0	*0.0	*0.0	*0.0	*0.0	*0.0	*0.0
K2 81	*0.0	4.44+000	1.31+007	*0.0	*0.0	*0.0	*0.0	*0.0	*0.0	*0.0
K2 81	*0.0	9.99+000	8.45+000	1.75+000	1.59+003	2.51+007	6.23+015	*0.0	*0.0	*0.0
SE 81	*0.0	1.67+002	1.01+002	3.51+000	2.30+003	3.72+007	9.24+015	*0.0	*0.0	*0.0
3E 81	*0.0	*0.0	*0.0	*0.0	*0.0	*0.0	*0.0	*0.0	*0.0	*0.0
3E 81	*0.0	4.61+002	2.53+003	3.77+009	*0.0	*0.0	*0.0	*0.0	*0.0	*0.0
3E 82	*0.0	2.54+002	2.59+002	2.30+002	1.90+002	1.50+002	9.38+003	2.28+003	1.41+012	*0.0
3E 82	*0.0	*0.0	*0.0	*0.0	*0.0	*0.0	*0.0	*0.0	*0.0	*0.0
K2 82	*0.0	*0.0	*0.0	*0.0	*0.0	*0.0	*0.0	*0.0	*0.0	*0.0
K2 82	*0.0	5.45+002	6.04+002	*0.0	*0.0	*0.0	*0.0	*0.0	*0.0	*0.0
SE 83	*0.0	4.61+002	9.53+003	3.77+009	*0.0	*0.0	*0.0	*0.0	*0.0	*0.0
3E 83	*0.0	2.62+002	1.75+002	9.85+000	5.00+007	1.20+015	*0.0	*0.0	*0.0	*0.0
3E 83	*0.0	5.73+002	5.73+002	5.27+002	2.07+001	6.57+001	6.60+004	6.71+013	*0.0	*0.0
3E 83	*0.0	5.45+002	5.45+002	5.05+002	2.17+001	5.25+003	2.94+012	*0.0	*0.0	*0.0
K2 83	*0.0	*0.0	*0.0	*0.0	*0.0	*0.0	*0.0	*0.0	*0.0	*0.0

TABLE B.5 Continued

DECAY PERIODS
0.154ns, 0.0000, FLUX = 3.90+012V/CY**2-SEC
PERIODS

NUCLIDE RADIODACTIVITY, CURIES
BASIS = TEST BUNDLE

	CHARGE	DISCHARGE	0.2Y	0. DY	1. DY	2. DY	5. DY	50. DY	200. DY	500. DY	1000. DY
CE 54	.00	1.04+003	5.31+001	0.01+011	0.0	0.0	0.0	0.0	0.0	0.0	0.0
39 54	.00	2.25+001	4.23+000	1.35+006	0.0	0.0	0.0	0.0	0.0	0.0	0.0
32 64	.00	1.64+003	8.85+002	5.29+001	1.87+004	2.85+011	6.67+025	0.0	0.0	0.0	0.0
KF 54	.00	.00	.00	.00	.00	.00	.00	.00	.00	.00	.00
3E 55	.00	1.51+003	2.63+004	0.0	0.0	0.0	0.0	0.0	0.0	0.0	0.0
38 55	.00	1.51+003	5.63+001	5.34+012	0.0	0.0	0.0	0.0	0.0	0.0	0.0
KF 55	.00	1.42+002	1.53+003	9.58+002	2.10+002	3.29+001	7.50+001	8.89+006	0.0	0.0	0.0
KF 55	.00	7.94+002	1.00+001	1.04+001	1.12+001	1.14+001	1.15+001	1.14+001	1.11+001	1.05+001	0.63+002
Q3 55	.00	.00	.00	.00	.00	.00	.00	.00	.00	.00	.00
32 60	.00	2.00+003	3.05+012	0.0	0.0	0.0	0.0	0.0	0.0	0.0	0.0
EE 56	.00	.00	.00	.00	.00	.00	.00	.00	.00	.00	.00
33 56	.00	3.34+002	2.34+006	0.0	0.0	0.0	0.0	0.0	0.0	0.0	0.0
43 56	.00	1.95+003	1.95+003	1.95+003	1.95+003	1.91+002	1.80+003	1.65+003	1.51+004	1.20+006	1.77+011
Q3 56	.00	.00	.00	.00	.00	.00	.00	.00	.00	.00	.00
34 56	.00	2.95+003	5.53+002	0.0	0.0	0.0	0.0	0.0	0.0	0.0	0.0
38 57	.00	2.45+003	2.63+003	9.06+002	4.22+000	5.93+003	1.17+005	9.10+026	0.0	0.0	0.0
KF 57	.00	1.71+010	1.72+010	1.78+010	1.86+010	1.80+010	1.80+010	1.80+010	1.80+010	1.80+010	1.80+010
33 57	.00	2.05+010	1.94+010	1.14+010	1.09+011	5.76+013	1.54+015	3.46+023	0.0	0.0	0.0
54 57	.00	.00	.00	.00	.00	.00	.00	.00	.00	.00	.00
32 58	.00	4.24+003	2.55+015	0.0	0.0	0.0	0.0	0.0	0.0	0.0	0.0
KF 58	.00	4.21+003	3.93+003	2.53+003	2.10+002	1.11+001	2.92+002	5.31+010	0.0	0.0	0.0
33 58	.00	4.21+003	4.16+003	2.55+003	2.42+002	1.24+001	3.26+002	5.93+010	0.0	0.0	0.0
54 58	.00	.00	.00	.00	.00	.00	.00	.00	.00	.00	.00
34 59	.00	5.45+003	2.47+003	1.59+010	0.0	0.0	0.0	0.0	0.0	0.0	0.0
KF 59	.00	5.45+003	5.45+003	1.05+001	5.84+011	4.95+025	0.0	0.0	0.0	0.0	0.0
32 59	.00	1.49+002	1.19+002	1.20+002	1.19+002	1.19+002	1.17+002	1.17+002	6.17+001	4.35+000	1.53+004
32 59	.00	.00	.00	.00	.00	.00	.00	.00	.00	.00	.00
34 60	.00	5.34+003	7.51+005	0.0	0.0	0.0	0.0	0.0	0.0	0.0	0.0
KF 60	.00	5.44+003	2.32+012	0.0	0.0	0.0	0.0	0.0	0.0	0.0	0.0
32 60	.00	7.41+001	7.42+001	7.42+001	7.42+001	7.42+001	7.42+001	7.42+001	7.32+001	7.15+001	6.94+001
KF 60	.00	2.12+005	2.04+005	1.26+004	1.47+009	1.00+010	4.63+013	4.76+020	0.0	0.0	0.0
32 60	.00	1.52+001	1.52+001	1.70+001	2.27+001	2.49+001	3.93+001	5.82+001	7.15+001	6.94+001	6.94+001
ZF 61	.00	.00	.00	.00	.00	.00	.00	.00	.00	.00	.00
KF 61	.00	4.10+003	0.0	0.0	0.0	0.0	0.0	0.0	0.0	0.0	0.0
32 61	.00	5.42+003	1.74+009	0.0	0.0	0.0	0.0	0.0	0.0	0.0	0.0
KF 61	.00	5.42+003	5.83+025	5.00+003	2.51+003	1.05+003	1.90+002	1.23+002	0.0	0.0	0.0
32 61	.00	5.54+003	3.52+003	3.13+003	1.86+003	6.86+002	1.22+002	1.27+002	1.24+002	7.28+001	3.62+001
KF 61	.00	6.63+001	9.47+001	0.0	0.0	0.0	0.0	0.0	0.0	0.0	0.0
ZF 61	.00	.00	.00	.00	.00	.00	.00	.00	.00	.00	.00
KF 62	.00	2.22+003	0.0	0.0	0.0	0.0	0.0	0.0	0.0	0.0	0.0
32 62	.00	0.39+003	0.0	0.0	0.0	0.0	0.0	0.0	0.0	0.0	0.0
KF 62	.00	0.26+003	5.93+005	3.59+005	2.91+002	1.35+001	2.93+010	0.0	0.0	0.0	0.0
32 62	.00	0.61+003	0.73+003	5.97+003	1.65+003	2.03+002	2.12+000	1.61+006	0.0	0.0	0.0
KF 62	.00	0.0	0.0	0.0	0.0	0.0	0.0	0.0	0.0	0.0	0.0
ZF 62	.00	5.71+002	0.0	0.0	0.0	0.0	0.0	0.0	0.0	0.0	0.0
KF 63	.00	7.22+003	0.0	0.0	0.0	0.0	0.0	0.0	0.0	0.0	0.0
32 63	.00	7.23+003	2.11+003	2.80+002	5.94+024	0.0	0.0	0.0	0.0	0.0	0.0
KF 63	.00	6.11+003	6.03+003	5.27+003	1.21+003	2.38+002	1.78+000	0.0	0.0	0.0	0.0

TABLE B.5 Continued

DECAY PERIODS
154n, BURNUP = 0.000, FLUX = 3.90+012V/cm²-sec

09/12/79

NUCLINE RADIONACTIVITY, CURIES
BASIS = TEST BUNDLE

CHARGE	DISC/TANGE	0. DY	1. DY	2. DY	3. DY	4. DY	5. DY	50. DY	200. DY	500. DY	1000. DY
ZR 93	*0.0	1.07+005	1.15+005	1.34+005	1.46+005	1.56+005	1.56+005	1.56+005	1.56+005	1.56+005	1.56+005
Y3 931	*0.0	1.20+009	1.21+013	1.35+013	2.05+009	3.04+009	5.14+009	1.16+008	1.29+007	1.29+007	2.03+006
Y1 23	*0.0	*0.0	*0.0	*0.0	*0.0	*0.0	*0.0	*0.0	*0.0	*0.0	*0.0
X9 34	*0.0	1.19+002	1.00	1.00	1.00	1.00	1.00	1.00	1.00	1.00	1.00
Y3 34	*0.0	2.97+005	1.00	1.00	1.00	1.00	1.00	1.00	1.00	1.00	1.00
S4 34	*0.0	0.42+003	3.03+003	4.20+003	3.03+001	1.45+007	3.05+016	*0.0	*0.0	*0.0	*0.0
Y 34	*0.0	0.42+003	4.20+003	*0.0	*0.0	*0.0	*0.0	*0.0	*0.0	*0.0	*0.0
Z3 34	*0.0	*0.0	*0.0	*0.0	*0.0	*0.0	*0.0	*0.0	*0.0	*0.0	*0.0
Z3 95	*0.0	1.34+003	*0.0	*0.0	*0.0	*0.0	*0.0	*0.0	*0.0	*0.0	*0.0
Si 95	*0.0	3.41+003	2.10+032	*0.0	*0.0	*0.0	*0.0	*0.0	*0.0	*0.0	*0.0
Y 95	*0.0	7.37+003	3.12+003	1.24+001	1.02+015	*0.0	*0.0	*0.0	*0.0	*0.0	*0.0
Z4 95	*0.0	1.42+002	1.24+002	1.25+002	1.24+002	1.23+002	1.19+002	7.12+001	1.06+001	6.91+003	6.91+003
Y3 454	*0.0	3.67+001	3.40+001	4.25+001	5.72+001	7.43+001	1.63+000	1.61+000	1.55+000	1.14+001	1.14+001
Y3 35	*0.0	2.25+000	2.25+000	2.49+000	3.44+000	4.61+000	6.89+000	1.34+001	5.89+001	2.60+001	6.31+003
Y1 35	*0.0	*0.0	*0.0	*0.0	*0.0	*0.0	*0.0	*0.0	*0.0	*0.0	*0.0
Y 35	*0.0	7.52+003	9.81+001	1.37+015	*0.0	*0.0	*0.0	*0.0	*0.0	*0.0	*0.0
Y 96	*0.0	*0.0	*0.0	*0.0	*0.0	*0.0	*0.0	*0.0	*0.0	*0.0	*0.0
Z4 30	*0.0	*0.0	*0.0	*0.0	*0.0	*0.0	*0.0	*0.0	*0.0	*0.0	*0.0
Y3 36	*0.0	4.53+001	4.53+001	4.50+001	3.22+001	2.24+001	1.09+001	1.24+002	9.11+017	1.00	1.00
Y1 36	*0.0	*0.0	*0.0	*0.0	*0.0	*0.0	*0.0	*0.0	*0.0	*0.0	*0.0
Y 36	*0.0	*0.0	*0.0	*0.0	*0.0	*0.0	*0.0	*0.0	*0.0	*0.0	*0.0
Y 47	*0.0	1.01+005	*0.0	*0.0	*0.0	*0.0	*0.0	*0.0	*0.0	*0.0	*0.0
Z4 47	*0.0	5.17+003	5.05+003	4.63+003	3.13+003	1.92+003	7.21+002	3.43+001	2.44+018	2.44+018	2.44+018
Y3 471	*0.0	4.91+003	4.45+003	4.25+003	3.01+003	1.84+003	9.93+002	3.68+001	2.76+018	2.76+018	2.76+018
N3 47	*0.0	5.11+003	5.10+003	4.37+003	3.30+003	1.95+003	7.24+002	3.68+001	3.10+018	3.10+018	3.10+018
Y1 37	*0.0	*0.0	*0.0	*0.0	*0.0	*0.0	*0.0	*0.0	*0.0	*0.0	*0.0
Z4 36	*0.0	6.00+003	9.22+001	2.89+018	*0.0	*0.0	*0.0	*0.0	*0.0	*0.0	*0.0
N3 361	*0.0	6.00+003	9.22+001	2.89+018	*0.0	*0.0	*0.0	*0.0	*0.0	*0.0	*0.0
Y1 36	*0.0	7.61+001	6.25+001	1.67+001	4.29+003	2.41+007	7.63+010	*0.0	*0.0	*0.0	*0.0
Y1 38	*0.0	*0.0	*0.0	*0.0	*0.0	*0.0	*0.0	*0.0	*0.0	*0.0	*0.0
Y1 48	*0.0	*0.0	*0.0	*0.0	*0.0	*0.0	*0.0	*0.0	*0.0	*0.0	*0.0
Yd 39	*0.0	7.20+003	1.13+032	6.25+015	*0.0	*0.0	*0.0	*0.0	*0.0	*0.0	*0.0
Y1 49	*0.0	2.29+003	2.25+003	2.23+003	2.02+003	1.79+003	1.39+003	6.62+002	9.30+003	6.22+019	6.22+019
TC 394	*0.0	1.01+003	1.62+003	1.70+003	1.74+003	1.67+003	1.33+003	6.31+002	5.94+003	5.94+003	5.94+003
TC 37	*0.0	1.56+005	1.57+005	1.75+005	2.46+005	3.35+005	4.8d+005	7.74+005	1.03+004	1.03+004	1.03+004
QU 49	*0.0	*0.0	*0.0	*0.0	*0.0	*0.0	*0.0	*0.0	*0.0	*0.0	*0.0
Y3100	*0.0	*0.0	*0.0	*0.0	*0.0	*0.0	*0.0	*0.0	*0.0	*0.0	*0.0
TC100	*0.0	*0.0	*0.0	*0.0	*0.0	*0.0	*0.0	*0.0	*0.0	*0.0	*0.0
TC101	*0.0	*0.0	*0.0	*0.0	*0.0	*0.0	*0.0	*0.0	*0.0	*0.0	*0.0
H3100	*0.0	*0.0	*0.0	*0.0	*0.0	*0.0	*0.0	*0.0	*0.0	*0.0	*0.0
H3101	*0.0	*0.0	*0.0	*0.0	*0.0	*0.0	*0.0	*0.0	*0.0	*0.0	*0.0
H3102	*0.0	*0.0	*0.0	*0.0	*0.0	*0.0	*0.0	*0.0	*0.0	*0.0	*0.0
H3103	*0.0	*0.0	*0.0	*0.0	*0.0	*0.0	*0.0	*0.0	*0.0	*0.0	*0.0
H3104	*0.0	*0.0	*0.0	*0.0	*0.0	*0.0	*0.0	*0.0	*0.0	*0.0	*0.0
TC102	*0.0	2.44+003	3.22+003	6.85+000	9.12+012	*0.0	*0.0	*0.0	*0.0	*0.0	*0.0
TC103	*0.0	2.03+003	9.91+003	4.71+001	1.73+010	5.71+020	*0.0	*0.0	*0.0	*0.0	*0.0
QU102	*0.0	*0.0	*0.0	*0.0	*0.0	*0.0	*0.0	*0.0	*0.0	*0.0	*0.0
QU103	*0.0	3.54+003	2.25+003	5.59+001	9.47+017	*0.0	*0.0	*0.0	*0.0	*0.0	*0.0
TC104	*0.0	3.55+003	1.03+003	4.73+001	8.17+017	*0.0	*0.0	*0.0	*0.0	*0.0	*0.0
TC105	*0.0	2.03+003	1.03+001	3.42+001	9.67+001	9.50+001	4.10+001	2.97+000	1.56+002	2.97+000	2.97+000
QU105	*0.0	2.03+003	1.03+001	3.55+001	9.77+001	9.51+001	4.10+001	2.97+000	1.55+002	2.97+000	2.97+000

TABLE B.5 Continued

DECAY PERIODS
15^{mu}m, SURFACE

0.000, PLUX 3.90+012V/CMAA2=3EC

09/12/79

NUCLIDE RADIONACTIVITY, CURIES
3AISIS # TEST HUNDLE

CHARGE	DISCHARGE	0. DRY	0. DRY	1. DRY	1. DRY	2. DRY	2. DRY	5. DRY	5. DRY	200. DRY	500. DRY	1000. DRY
RH103	*0.0	*0.0	*0.0	*0.0	*0.0	*0.0	*0.0	*0.0	*0.0	*0.0	*0.0	*0.0
HJ104	*0.0	2.04+003	9.91+003	*0.0	*0.0	*0.0	*0.0	*0.0	*0.0	*0.0	*0.0	*0.0
TC104	*0.0	2.04+003	1.52+003	3.01+000	2.14+009	1.91+021	*0.0	*0.0	*0.0	*0.0	*0.0	*0.0
RJ104	*0.0	*0.0	*0.0	*0.0	*0.0	*0.0	*0.0	*0.0	*0.0	*0.0	*0.0	*0.0
RH104	*0.0	3.54+004	3.63+005	5.25+014	*0.0	*0.0	*0.0	*0.0	*0.0	*0.0	*0.0	*0.0
RH104	*0.0	4.62+005	4.43+005	6.27+014	*0.0	*0.0	*0.0	*0.0	*0.0	*0.0	*0.0	*0.0
PJ104	*0.0	*0.0	*0.0	*0.0	*0.0	*0.0	*0.0	*0.0	*0.0	*0.0	*0.0	*0.0
TC105	*0.0	1.07+003	3.37+004	*0.0	*0.0	*0.0	*0.0	*0.0	*0.0	*0.0	*0.0	*0.0
RJ105	*0.0	1.07+003	4.21+004	*0.0	*0.0	*0.0	*0.0	*0.0	*0.0	*0.0	*0.0	*0.0
RH105	*0.0	1.07+003	9.97+002	7.12+002	1.59+002	2.44+001	5.76+001	7.57+006	*0.0	*0.0	*0.0	*0.0
RH105	*0.0	1.07+003	1.53+003	7.14+002	1.59+002	2.45+001	5.78+031	7.59+006	*0.0	*0.0	*0.0	*0.0
RH105	*0.0	4.59+002	4.61+002	4.77+002	4.57+002	5.77+002	2.39+002	5.98+001	5.24+008	*0.0	*0.0	*0.0
PJ105	*0.0	*0.0	*0.0	*0.0	*0.0	*0.0	*0.0	*0.0	*0.0	*0.0	*0.0	*0.0
TC106	*0.0	4.52+002	4.22+002	*0.0	*0.0	*0.0	*0.0	*0.0	*0.0	*0.0	*0.0	*0.0
RJ106	*0.0	1.36+000	1.35+000	1.36+000	1.36+000	1.36+000	1.36+000	1.36+000	1.36+000	1.36+000	1.36+000	1.36+000
RJ106	*0.0	2.13+000	2.39+001	2.39+001	2.39+001	2.39+001	2.39+001	2.39+001	2.39+001	2.39+001	2.39+001	2.39+001
RJ106	*0.0	6.52+000	1.55+000	1.36+000	1.36+000	1.36+000	1.36+000	1.36+000	1.36+000	1.36+000	1.36+000	1.36+000
PJ106	*0.0	*0.0	*0.0	*0.0	*0.0	*0.0	*0.0	*0.0	*0.0	*0.0	*0.0	*0.0
RJ107	*0.0	2.25+002	2.11+001	1.08+006	*0.0	*0.0	*0.0	*0.0	*0.0	*0.0	*0.0	*0.0
RH107	*0.0	2.25+002	1.72+032	2.33+000	3.93+008	5.53+018	*0.0	*0.0	*0.0	*0.0	*0.0	*0.0
PJ107	*0.0	4.25+001	3.52+001	6.94+001	8.04+009	1.13+018	*0.0	*0.0	*0.0	*0.0	*0.0	*0.0
PJ107	*0.0	4.05+004	9.71+039	9.82+008	9.82+008	9.82+008	9.82+008	9.82+008	9.82+008	9.82+008	9.82+008	9.82+008
AG107	*0.0	*0.0	*0.0	*0.0	*0.0	*0.0	*0.0	*0.0	*0.0	*0.0	*0.0	*0.0
RJ108	*0.0	7.74+001	5.42+000	1.05+000	*0.0	*0.0	*0.0	*0.0	*0.0	*0.0	*0.0	*0.0
RJ108	*0.0	7.74+001	8.92+000	1.92+008	*0.0	*0.0	*0.0	*0.0	*0.0	*0.0	*0.0	*0.0
PJ108	*0.0	*0.0	*0.0	*0.0	*0.0	*0.0	*0.0	*0.0	*0.0	*0.0	*0.0	*0.0
AG108	*0.0	5.20+013	5.43+015	*0.0	*0.0	*0.0	*0.0	*0.0	*0.0	*0.0	*0.0	*0.0
CC108	*0.0	*0.0	*0.0	*0.0	*0.0	*0.0	*0.0	*0.0	*0.0	*0.0	*0.0	*0.0
CC108	*0.0	3.57+001	7.64+033	*0.0	*0.0	*0.0	*0.0	*0.0	*0.0	*0.0	*0.0	*0.0
PJ109	*0.0	1.05+005	1.97+003	9.97+015	*0.0	*0.0	*0.0	*0.0	*0.0	*0.0	*0.0	*0.0
PJ109	*0.0	2.01+001	2.75+001	2.49+001	1.52+001	6.20+000	2.39+000	5.93+002	*0.0	*0.0	*0.0	*0.0
AG109	*0.0	2.01+001	2.75+001	2.49+001	1.52+001	6.21+000	2.39+000	5.94+002	*0.0	*0.0	*0.0	*0.0
AG109	*0.0	*0.0	*0.0	*0.0	*0.0	*0.0	*0.0	*0.0	*0.0	*0.0	*0.0	*0.0
CQ109	*0.0	*0.0	*0.0	*0.0	*0.0	*0.0	*0.0	*0.0	*0.0	*0.0	*0.0	*0.0
RH110	*0.0	2.53+001	*0.0	*0.0	*0.0	*0.0	*0.0	*0.0	*0.0	*0.0	*0.0	*0.0
PJ110	*0.0	*0.0	*0.0	*0.0	*0.0	*0.0	*0.0	*0.0	*0.0	*0.0	*0.0	*0.0
AG110	*0.0	1.17+007	1.17+007	1.17+007	1.17+007	1.16+007	1.16+007	1.15+007	1.15+007	1.15+007	1.15+007	1.15+007
AG110	*0.0	1.95+003	5.03+000	3.10+000	2.44+009	2.66+000	2.66+000	1.97+000	1.97+000	1.97+000	1.97+000	1.97+000
CC110	*0.0	*0.0	*0.0	*0.0	*0.0	*0.0	*0.0	*0.0	*0.0	*0.0	*0.0	*0.0
PJ111	*0.0	2.13+001	2.07+001	1.57+001	4.69+002	1.03+002	5.03+004	5.76+008	*0.0	*0.0	*0.0	*0.0
PJ111	*0.0	2.25+001	1.43+001	3.60+001	3.77+002	8.31+003	4.04+004	4.63+008	*0.0	*0.0	*0.0	*0.0
AG111	*0.0	2.28+001	1.53+001	3.22+001	4.92+002	5.30+004	6.09+008	*0.0	*0.0	*0.0	*0.0	*0.0
AG111	*0.0	7.92+000	7.65+000	7.51+000	7.51+000	7.51+000	7.51+000	7.51+000	7.51+000	7.51+000	7.51+000	7.51+000
CC111	*0.0	*0.0	*0.0	*0.0	*0.0	*0.0	*0.0	*0.0	*0.0	*0.0	*0.0	*0.0
PJ112	*0.0	7.25+000	7.25+000	7.57+000	6.13+000	4.22+000	1.92+000	1.75+000	1.75+000	1.75+000	1.75+000	1.75+000
AG112	*0.0	*0.0	*0.0	*0.0	*0.0	*0.0	*0.0	*0.0	*0.0	*0.0	*0.0	*0.0
CC112	*0.0	5.73+001	2.97+032	*0.0	*0.0	*0.0	*0.0	*0.0	*0.0	*0.0	*0.0	*0.0
PJ113	*0.0	*0.0	*0.0	*0.0	*0.0	*0.0	*0.0	*0.0	*0.0	*0.0	*0.0	*0.0

TABLE B.5 Continued

 DECAY PERIODS
 .154ns, 3.947ns, 0.44ns, FLUX 3.90+0124/cm**2*sec

09/12/79

 NUCLEIDE RADIODACTIVITY, CURIES
 BASIS ■ TEST DUNBLE

CHARGE	DISCHARGE	0. DY	0. DY	1. DY	2. DY	5. DY	200. DY	500. DY	1000. DY
A4113+	.00	3.73+000	1.55+002	*.00	*.00	*.00	*.00	*.00	*.00
A4113+	.00	3.18+001	2.33+001	6.64+000	1.38+000	5.99+002	6.88+006	*.00	*.00
C2113+	.00	2.12+010	2.15+010	2.15+010	2.15+010	2.14+010	2.13+010	2.10+010	1.87+010
C2113+	.00	*.00	*.00	*.00	*.00	*.00	*.00	*.00	*.00
T4113	.00	*.00	*.00	*.00	*.00	*.00	*.00	*.00	*.00
P2114	.00	1.45+001	2.25+011	1.24+017	*.00	*.00	*.00	*.00	*.00
A2114	.00	1.45+001	2.31+031	1.28+017	*.00	*.00	*.00	*.00	*.00
C2114	.00	*.00	*.00	*.00	*.00	*.00	*.00	*.00	*.00
T4114+	.00	6.36+019	6.36+019	6.38+018	6.39+018	6.34+018	6.12+018	5.94+018	5.54+019
T4114	.00	6.35+016	6.32+015	5.16+016	6.16+016	6.16+016	5.91+016	5.37+016	5.10+019
S4114	.00	*.00	*.00	*.00	*.00	*.00	*.00	*.00	*.00
P2115	.00	1.24+001	2.05+035	*.00	*.00	*.00	*.00	*.00	*.00
A2115+	.00	3.46+001	1.05+035	*.00	*.00	*.00	*.00	*.00	*.00
C2115+	.00	6.93+000	5.02+030	6.27+002	1.52+010	1.96+021	*.00	*.00	*.00
T4115+	.00	2.01+002	2.02+032	2.04+002	2.02+002	2.01+002	1.97+002	1.48+002	9.10+003
C2115	.00	4.32+001	4.33+030	4.24+000	3.75+000	3.21+000	2.35+000	9.25+001	7.75+007
T4115+	.00	5.71+000	5.74+030	5.59+000	3.92+000	3.48+000	2.57+000	1.01+000	6.46+007
T4115	.00	*.00	*.00	*.00	*.00	*.00	*.00	*.00	*.00
S4115	.00	*.00	*.00	*.00	*.00	*.00	*.00	*.00	*.00
A2116	.00	1.25+001	2.50+001	5.72+017	*.00	*.00	*.00	*.00	*.00
C2115	.00	*.00	*.00	*.00	*.00	*.00	*.00	*.00	*.00
T4116+	.00	3.45+001	2.79+034	5.29+005	3.62+008	3.16+012	2.96+020	*.00	*.00
C2116	.00	6.93+005	2.35+025	*.00	*.00	*.00	*.00	*.00	*.00
S4116	.00	*.00	*.00	*.00	*.00	*.00	*.00	*.00	*.00
A2117	.00	1.31+001	1.50+034	*.00	*.00	*.00	*.00	*.00	*.00
C2117	.00	2.12+006	2.05+035	1.32+006	1.67+007	1.62+006	1.21+010	5.12+017	*.00
C2117	.00	1.35+001	1.22+001	6.5b+000	4.1v+001	1.28+002	1.25+005	1.17+014	*.00
T4117	.00	1.35+001	1.50+031	1.07+001	1.37+003	5.57+002	6.21+005	5.96+014	*.00
T4117	.00	6.12+030	5.57+030	7.42+031	3.15+032	6.19+035	4.03+014	1.09+012	1.17+013
S4117	.00	1.44+012	1.32+012	1.39+012	1.36+012	1.35+012	1.26+012	1.09+012	1.46+017
C2118	.00	1.31+001	1.07+031	1.71+030	4.94+004	1.86+008	2.65+017	*.00	*.00
T4118	.00	1.44+006	1.43+037	2.03+016	*.00	*.00	*.00	*.00	*.00
T4118	.00	1.51+001	1.07+031	1.71+030	4.94+004	1.87+008	2.66+017	*.00	*.00
S4118	.00	*.03	*.00	*.00	*.00	*.00	*.00	*.00	*.00
C2119	.00	7.15+001	1.77+031	5.29+016	*.00	*.00	*.00	*.00	*.00
C2119	.00	7.15+001	2.65+030	3.30+004	1.51+021	2.05+023	*.00	*.00	*.00
T4119	.00	1.43+001	1.07+031	9.51+002	2.23+011	1.15+024	1.61+004	1.59+004	1.42+005
T4119	.00	1.13+001	5.61+031	5.39+003	1.26+012	1.60+004	1.60+004	*.00	*.00
S4119	.00	1.55+004	1.59+034	1.61+004	*.00	*.00	*.00	*.00	*.00
T4120	.00	1.53+001	7.15+034	*.00	*.00	*.00	*.00	*.00	*.00
S4120	.00	*.00	*.00	*.00	*.00	*.00	*.00	*.00	*.00
T4121	.00	7.75+001	3.73+034	*.00	*.00	*.00	*.00	*.00	*.00
T4121	.00	7.73+001	1.45+033	*.00	*.00	*.00	*.00	*.00	*.00
S4121	.00	*.00	*.00	*.00	*.00	*.00	*.00	*.00	*.00

B-17

TABLE B.5 Continued

DECAY PERIODS
15H⁻, BURNUPS 0.04D, FLUX 3.90+012V/CM²*2=3EC

09/12/79

NUCLIDE RADIOACTIVITY, CURIES
MASTS # TEST BUNDLE

CHARGE	DISCHARGE	0. DY	1. DY	2. DY	5. DY	50. DY	200. DY	500. DY	1000. DY
S4121	*0.0	1.04+001	1.04+001	9.57+000	7.71+000	5.67+000	3.06+000	4.82+001	4.38+013
S5121	*0.2	*0.0	*0.0	*0.0	*0.0	*0.0	*0.0	*0.0	*0.0
T4122	*0.0	1.49+001	*0.0	*0.0	*0.0	*0.0	*0.0	*0.0	*0.0
S4122	*0.0	*0.0	*0.0	*0.0	*0.0	*0.0	*0.0	*0.0	*0.0
S4122*	*0.0	5.49+006	5.47+007	2.81+016	*0.0	*0.0	*0.0	*0.0	*0.0
S5122	*0.0	7.55+005	7.53+005	7.37+006	6.67+005	5.90+006	4.60+006	2.19+006	3.18+011
TE122	*0.0	*0.0	*0.0	*0.0	*0.0	*0.0	*0.0	*0.0	*0.0
T4123*	*0.0	1.49+001	1.15+006	*0.0	*0.0	*0.0	*0.0	*0.0	*0.0
14123	*0.0	1.52+000	*0.0	*0.0	*0.0	*0.0	*0.0	*0.0	*0.0
S4123*	*0.0	1.21+030	1.28+001	5.92+005	2.26+011	3.29+022	*0.0	*0.0	*0.0
S5123	*0.0	1.65+001	1.68+001	1.68+001	1.67+001	1.66+001	1.64+001	1.27+001	5.55+002
S5123*	*0.0	*0.0	*0.0	*0.0	*0.0	*0.0	*0.0	*0.0	*0.0
TE123*	*0.0	0.41+016	6.91+016	6.91+016	6.87+016	6.83+016	6.71+016	5.14+016	2.11+016
T4123	*0.0	*0.0	*0.0	*0.0	*0.0	*0.0	*0.0	*0.0	*0.0
T4124	*0.0	2.02+001	*0.0	*0.0	*0.0	*0.0	*0.0	*0.0	*0.0
S4124	*0.0	*0.0	*0.0	*0.0	*0.0	*0.0	*0.0	*0.0	*0.0
S5124	*0.0	1.69+007	5.00+010	*0.0	*0.0	*0.0	*0.0	*0.0	*0.0
S5124*	*0.0	1.10+007	1.10+007	1.09+007	1.09+007	1.09+007	1.09+007	6.17+008	3.41+010
TE124	*0.0	*0.0	*0.0	*0.0	*0.0	*0.0	*0.0	*0.0	*0.0
T4125	*0.0	9.51+000	3.40+030	3.23+004	4.31+022	*0.0	*0.0	*0.0	*0.0
S4125	*0.0	1.70+000	1.69+000	1.64+000	1.58+000	1.47+000	1.19+000	4.27+002	6.71+007
S5125	*0.0	1.14+002	1.15+032	1.20+002	1.24+002	1.30+002	1.41+002	1.63+002	2.46+002
S5125*	*0.0	2.01+035	5.13+035	3.26+005	7.66+005	1.07+004	1.69+004	3.76+004	4.24+003
TE125	*0.0	*0.0	*0.0	*0.0	*0.0	*0.0	*0.0	*0.0	*0.0
T4126	*0.0	1.54+006	1.59+006	1.59+006	1.59+006	1.59+006	1.59+006	1.59+006	1.59+006
S4126	*0.0	3.06+002	2.93+013	1.60+006	1.59+005	1.59+006	1.59+005	1.59+006	1.59+006
S5126	*0.0	2.53+007	2.55+037	2.63+007	2.93+007	3.30+007	3.38+007	5.80+007	1.49+006
TE126	*0.0	*0.0	*0.0	*0.0	*0.0	*0.0	*0.0	*0.0	*0.0
T4127	*0.0	2.19+005	1.60+017	3.17+017	*0.0	*0.0	*0.0	*0.0	*0.0
S4127	*0.0	1.54+002	1.45+002	5.99+001	2.94+000	5.60+002	2.03+005	9.70+016	*0.0
S5127	*0.0	3.44+001	3.21+001	3.02+001	3.51+001	3.22+001	2.69+001	1.57+001	5.02+003
TE127	*0.0	4.00+002	4.05+002	5.10+002	7.10+002	9.42+002	1.35+001	2.19+001	1.60+001
T4127	*0.0	1.91+001	1.43+031	2.05+001	2.44+001	2.54+001	2.30+001	1.38+001	2.61+001
S4127	*0.0	*0.0	*0.0	*0.0	*0.0	*0.0	*0.0	*0.0	*0.0
S5127	*0.0	3.71+002	3.67+002	3.67+001	3.67+001	3.67+001	3.67+001	3.67+001	3.67+001
S5127*	*0.0	5.13+001	5.05+001	4.57+001	2.16+001	6.33+000	1.31+000	5.13+003	0.00+000
TE127	*0.0	*0.0	*0.0	*0.0	*0.0	*0.0	*0.0	*0.0	*0.0
T4128	*0.0	5.25+002	2.44+002	6.60+004	7.66+011	1.64+019	*0.0	*0.0	*0.0
S4128	*0.0	*0.0	*0.0	*0.0	*0.0	*0.0	*0.0	*0.0	*0.0
S5128	*0.0	1.13+003	1.01+035	2.25+002	2.96+001	7.09+005	4.23+012	*0.0	*0.0
TE128	*0.0	*0.0	*0.0	*0.0	*0.0	*0.0	*0.0	*0.0	*0.0
T4129	*0.0	1.07+005	1.07+005	2.04+002	2.17+002	2.99+001	0.25+001	5.69+006	*0.0
S4129	*0.0	5.62+009	5.05+000	5.94+000	6.52+009	6.60+000	6.11+000	2.44+000	2.53+004
S5129	*0.0	9.05+002	9.07+002	9.53+002	2.40+002	3.87+001	4.84+000	1.56+000	7.35+002
TE129	*0.0	1.04+007	1.05+007	1.74+007	1.97+007	2.04+007	2.05+007	2.07+007	2.00+007
T4129	*0.0	7.36+010	7.53+010	7.36+010	6.75+010	6.19+010	4.77+010	9.67+012	2.19+017
S4129	*0.0	*0.0	*0.0	*0.0	*0.0	*0.0	*0.0	*0.0	*0.0
S5129	*0.0	2.39+003	5.12+003	5.00+014	*0.0	*0.0	*0.0	*0.0	*0.0

TABLE B.5 Continued

0. מ.מ., פלחה 3. 90+013/4/C/M+n2+9EC
DECA E81CC

69 / 12 / 79

NUCLIDE RADIODACTIVITY, CURIES MASSES & TEST BUNDLES

TABLE B.5 Continued

PURENE .154²⁰, DURUMS 0.140, FLUX = 3.90+012V/CN**2=3EC

09/12/79

NUCLIDE RADIACTIVITY, CURIES
BASIS = TEST HANDLE

CHARGE	DISCHARGE	0. DY	0. DY	1. DY	2. DY	3. DY	5. DY	200. DY	500. DY	2000. DY	5000. DY	10000. DY
9A157	.0.0	*.00	*.00	*.00	*.00	*.00	*.00	*.00	*.00	*.00	*.00	*.00
T158	.0.0	0.02+003	0.02	0.01	0.01	0.01	0.01	0.01	0.01	0.01	0.01	0.01
AE159	.0.0	0.02+003	3.82+003	1.94+001	1.22+009	2.18+022	0.0	0.0	0.0	0.0	0.0	0.0
CS154	.0.0	0.02+003	6.37+003	6.32+002	2.64+003	5.01+010	1.73+023	0.0	0.0	0.0	0.0	0.0
DA155	.0.0	.0.0	.0.0	.0.0	.0.0	.0.0	.0.0	.0.0	.0.0	.0.0	.0.0	.0.0
T159	.0.0	0.4+003	0.0	0.0	0.0	0.0	0.0	0.0	0.0	0.0	0.0	0.0
AE153	.0.0	0.42+003	0.32+005	0.03	0.03	0.0	0.0	0.0	0.0	0.0	0.0	0.0
CS153	.0.0	1.63+003	2.05+003	2.25+001	1.26+019	0.0	0.0	0.0	0.0	0.0	0.0	0.0
SA152	.0.0	7.74+003	7.95+003	2.66+003	2.15+001	5.23+002	3.09+007	6.36+023	0.0	0.0	0.0	0.0
LA152	.0.0	.0.0	.0.0	.0.0	.0.0	.0.0	.0.0	.0.0	.0.0	.0.0	.0.0	.0.0
CE140	.0.0	4.52+003	2.51+013	0.0	0.0	0.0	0.0	0.0	0.0	0.0	0.0	0.0
AE140	.0.0	7.13+003	9.53+031	0.0	0.0	0.0	0.0	0.0	0.0	0.0	0.0	0.0
CS143	.0.0	0.22+002	0.22+002	0.19+002	6.09+002	5.90+002	5.59+002	4.75+002	4.15+001	1.73+002	1.08+009	1.49+021
DA140	.0.0	1.42+002	1.94+002	2.09+002	2.71+002	3.32+002	4.14+002	4.60+002	4.78+001	1.42+002	1.25+009	1.17+021
CE140	.0.0	.0.0	.0.0	.0.0	.0.0	.0.0	.0.0	.0.0	.0.0	.0.0	.0.0	.0.0
CE140	.0.0	1.54+003	0.0	0.0	0.0	0.0	0.0	0.0	0.0	0.0	0.0	0.0
AE141	.0.0	5.47+003	8.17+035	0.0	0.0	0.0	0.0	0.0	0.0	0.0	0.0	0.0
CS141	.0.0	7.44+003	4.37+003	2.98+001	6.93+009	6.31+021	0.0	0.0	0.0	0.0	0.0	0.0
SA141	.0.0	7.27+003	7.21+003	5.16+003	9.37+002	1.11+002	1.56+000	4.32+006	0.0	0.0	0.0	0.0
LA141	.0.0	2.21+002	2.23+002	2.34+002	2.53+002	2.55+002	2.50+002	2.34+002	6.95+001	3.42+000	5.90+003	1.33+007
CE141	.0.0	.0.0	.0.0	.0.0	.0.0	.0.0	.0.0	.0.0	.0.0	.0.0	.0.0	.0.0
AE141	.0.0	4.12+002	0.0	0.0	0.0	0.0	0.0	0.0	0.0	0.0	0.0	0.0
CS142	.0.0	4.11+003	0.0	0.0	0.0	0.0	0.0	0.0	0.0	0.0	0.0	0.0
DA142	.0.0	6.79+003	2.74+035	7.79+001	1.32+016	0.0	0.0	0.0	0.0	0.0	0.0	0.0
LA142	.0.0	7.14+003	6.57+003	2.73+003	3.56+001	1.57+001	3.04+005	2.23+020	0.0	0.0	0.0	0.0
CE142	.0.0	.0.0	.0.0	.0.0	.0.0	.0.0	.0.0	.0.0	.0.0	.0.0	.0.0	.0.0
PA142	.0.0	1.52+004	1.51+004	1.39+004	9.65+005	6.39+005	2.69+005	2.00+006	2.33+023	0.0	0.0	0.0
NA142	.0.0	.0.0	.0.0	.0.0	.0.0	.0.0	.0.0	.0.0	.0.0	.0.0	.0.0	.0.0
CE142	.0.0	6.50+001	0.0	0.0	0.0	0.0	0.0	0.0	0.0	0.0	0.0	0.0
AE143	.0.0	2.24+003	0.0	0.0	0.0	0.0	0.0	0.0	0.0	0.0	0.0	0.0
CS143	.0.0	5.07+003	1.39+014	0.0	0.0	0.0	0.0	0.0	0.0	0.0	0.0	0.0
DA143	.0.0	b.-c1+003	3.35+003	3.53+000	2.26+012	0.0	0.0	0.0	0.0	0.0	0.0	0.0
LA143	.0.0	3.53+003	3.54+003	3.41+003	2.76+003	2.16+003	1.31+003	2.88+002	4.05+008	0.0	0.0	0.0
CE143	.0.0	1.67+002	1.68+002	2.03+002	2.61+002	3.16+002	3.84+002	4.23+002	4.67+001	2.36+002	6.05+009	6.24+020
PA143	.0.0	.0.0	.0.0	.0.0	.0.0	.0.0	.0.0	.0.0	.0.0	.0.0	.0.0	.0.0
NA143	.0.0	2.01+001	2.01+001	2.61+001	2.60+001	2.60+001	2.59+001	2.57+001	2.31+001	1.60+001	7.69+000	2.27+000
CE144	.0.0	2.61+001	2.61+001	2.61+001	2.60+001	2.60+001	2.59+001	2.57+001	2.31+001	1.60+001	7.69+000	2.27+000
AE144	.0.0	1.39+002	1.39+002	2.03+002	2.61+002	3.16+002	3.84+002	4.23+002	4.67+001	2.36+002	6.05+009	6.24+020
CS144	.0.0	0.0	0.0	0.0	0.0	0.0	0.0	0.0	0.0	0.0	0.0	0.0
DA144	.0.0	2.41+001	2.41+001	2.61+001	2.60+001	2.60+001	2.59+001	2.57+001	2.31+001	1.60+001	7.69+000	2.27+000
LA144	.0.0	2.61+001	2.61+001	2.61+001	2.60+001	2.60+001	2.59+001	2.57+001	2.31+001	1.60+001	7.69+000	2.27+000
CE144	.0.0	2.61+001	2.61+001	2.61+001	2.60+001	2.60+001	2.59+001	2.57+001	2.31+001	1.60+001	7.69+000	2.27+000
PA144	.0.0	1.39+002	1.39+002	1.69+011	1.69+011	1.69+011	1.69+011	1.69+011	1.69+011	1.69+011	1.69+000	1.69+000
NA144	.0.0	2.61+001	2.61+001	2.61+001	2.60+001	2.60+001	2.59+001	2.57+001	2.31+001	1.60+001	7.69+000	2.27+000
CE145	.0.0	4.73+003	1.77+002	1.69+002	1.69+002	1.69+002	1.69+002	1.69+002	1.69+002	1.69+002	1.69+000	1.69+000
DA145	.0.0	4.40+003	4.31+003	3.36+003	1.10+003	2.75+002	1.70+001	4.04+003	0.0	0.0	0.0	0.0
LA145	.0.0	0.0	0.0	0.0	0.0	0.0	0.0	0.0	0.0	0.0	0.0	0.0
CE145	.0.0	5.02+003	1.77+002	2.73+002	2.73+002	2.73+002	2.73+002	2.73+002	2.73+002	2.73+002	2.73+000	2.73+000
PA145	.0.0	5.02+003	3.27+003	1.53+002	1.53+002	1.53+002	1.53+002	1.53+002	1.53+002	1.53+002	1.53+000	1.53+000
NA145	.0.0	0.0	0.0	0.0	0.0	0.0	0.0	0.0	0.0	0.0	0.0	0.0
CE146	.0.0	2.41+003	2.41+003	2.41+003	2.41+003	2.41+003	2.41+003	2.41+003	2.41+003	2.41+003	2.41+000	2.41+000
AE146	.0.0	2.41+003	2.41+003	2.41+003	2.41+003	2.41+003	2.41+003	2.41+003	2.41+003	2.41+003	2.41+000	2.41+000
CS146	.0.0	2.41+003	2.41+003	2.41+003	2.41+003	2.41+003	2.41+003	2.41+003	2.41+003	2.41+003	2.41+000	2.41+000
DA146	.0.0	2.41+003	2.41+003	2.41+003	2.41+003	2.41+003	2.41+003	2.41+003	2.41+003	2.41+003	2.41+000	2.41+000
LA146	.0.0	2.41+003	2.41+003	2.41+003	2.41+003	2.41+003	2.41+003	2.41+003	2.41+003	2.41+003	2.41+000	2.41+000
CE147	.0.0	2.41+003	2.41+003	2.41+003	2.41+003	2.41+003	2.41+003	2.41+003	2.41+003	2.41+003	2.41+000	2.41+000
PA147	.0.0	2.41+003	2.41+003	2.41+003	2.41+003	2.41+003	2.41+003	2.41+003	2.41+003	2.41+003	2.41+000	2.41+000
NA147	.0.0	2.41+003	2.41+003	2.41+003	2.41+003	2.41+003	2.41+003	2.41+003	2.41+003	2.41+003	2.41+000	2.41+000
CE147	.0.0	1.53+003	1.53+003	1.53+003	1.53+003	1.53+003	1.53+003	1.53+003	1.53+003	1.53+003	1.53+000	1.53+000
DA147	.0.0	1.53+003	1.53+003	1.53+003	1.53+003	1.53+003	1.53+003	1.53+003	1.53+003	1.53+003	1.53+000	1.53+000
LA147	.0.0	1.53+003	1.53+003	1.53+003	1.53+003	1.53+003	1.53+003	1.53+003	1.53+003	1.53+003	1.53+000	1.53+000
CE147	.0.0	1.53+003	1.53+003	1.53+003	1.53+003	1.53+003	1.53+003	1.53+003	1.53+003	1.53+003	1.53+000	1.53+000
PA147	.0.0	1.53+003	1.53+003	1.53+003	1.53+003	1.53+003	1.53+003	1.53+003	1.53+003	1.53+003	1.53+000	1.53+000
NA147	.0.0	1.53+003	1.53+003	1.53+003	1.53+003	1.53+003	1.53+003	1.53+003	1.53+003	1.53+003	1.53+000	1.53+000
CE147	.0.0	1.53+003	1.53+003	1.53+003	1.53+003	1.53+003	1.53+003	1.53+003	1.53+003	1.53+003	1.53+000	1.53+000
PA147	.0.0	1.53+003	1.53+003	1.53+003	1.53+003	1.53+003	1.53+003	1.53+003	1.53+003	1.53+003	1.53+000	1.53+000
NA147	.0.0	1.53+003	1.53+003	1.53+003	1.53+003	1.53+003	1.53+003	1.53+003	1.53+003	1.53+003	1.53+000	1.53+000

TABLE B.5 Continued

DECAY PERIODS
•154^m, 32RN²⁺
0.000, FLUX# 3.90+012V/cm²-sec

09/12/79

NUCLINE RADIODACTIVITY, CURIES

BASIS • TEST HUNDLE

	CHARGE	DISCHARGE	0. DY	0. DY	1. DY	2. DY	5. DY	200. DY	500. DY	1000. DY
S4147	+0.0	+0.0	*0.0	*0.0	*0.0	*0.0	*0.0	*0.0	*0.0	*0.0
CE143	+0.0	2.05+003	1.82+003	*0.0	*0.0	*0.0	*0.0	*0.0	*0.0	*0.0
P4148	+0.0	2.05+003	2.15+011	6.72+019	*0.0	*0.0	*0.0	*0.0	*0.0	*0.0
N2148	+0.0	*0.0	*0.0	*0.0	*0.0	*0.0	*0.0	*0.0	*0.0	*0.0
P4149	+0.0	1.52+004	1.35+004	1.45+004	1.34+004	1.33+004	1.31+004	1.24+004	5.92+005	4.98+006
P4149	+0.0	1.52+004	1.35+003	1.42+003	1.30+003	9.97+004	8.78+004	6.00+004	6.58+006	4.40+007
S4149	+0.0	*0.0	*0.0	*0.0	*0.0	*0.0	*0.0	*0.0	*0.0	*0.0
P4149	+0.0	1.54+003	1.75+001	1.91+016	*0.0	*0.0	*0.0	*0.0	*0.0	*0.0
Y2149	+0.0	1.54+003	1.25+003	5.45+002	1.35+001	1.29+005	1.17+017	*0.0	*0.0	*0.0
P4149	+0.0	1.54+003	1.25+002	6.99+002	4.46+002	3.83+002	2.80+002	1.04+002	6.25+005	3.22+025
S4149	+0.0	*0.0	*0.0	*0.0	*0.0	*0.0	*0.0	*0.0	*0.0	*0.0
E2150	+0.0	*0.0	*0.0	*0.0	*0.0	*0.0	*0.0	*0.0	*0.0	*0.0
P4150	+0.0	5.65+001	5.62+001	2.08+001	1.77+002	8.12+004	7.71+005	1.61+014	*0.0	*0.0
S4150	+0.0	*0.0	*0.0	*0.0	*0.0	*0.0	*0.0	*0.0	*0.0	*0.0
Y2151	+0.0	5.23+002	2.23+002	1.28+001	4.54+016	*0.0	*0.0	*0.0	*0.0	*0.0
P4151	+0.0	5.23+002	2.99+002	2.95+002	2.22+002	1.67+002	4.22+001	1.55+001	3.80+011	*0.0
S4151	+0.0	2.99+002	7.25+003	7.85+003	1.09+002	1.22+002	1.49+002	1.77+002	1.83+002	1.82+002
E2151	+0.0	7.14+003	*0.0	*0.0	*0.0	*0.0	*0.0	*0.0	*0.0	*0.0
P4152	+0.0	5.34+002	6.53+001	1.99+005	*0.0	*0.0	*0.0	*0.0	*0.0	*0.0
S4152	+0.0	*0.0	*0.0	*0.0	*0.0	*0.0	*0.0	*0.0	*0.0	*0.0
E2152	+0.0	1.27+006	1.25+005	1.06+006	5.16+007	2.12+007	5.54+008	1.66+010	*0.0	*0.0
P4152	+0.0	3.37+010	3.57+010	3.37+010	3.37+010	3.37+010	3.37+010	3.37+010	3.35+010	3.37+010
S4152	+0.0	*0.0	*0.0	*0.0	*0.0	*0.0	*0.0	*0.0	*0.0	*0.0
E2153	+0.0	1.77+012	2.93+001	2.34+006	*0.0	*0.0	*0.0	*0.0	*0.0	*0.0
P4153	+0.0	6.30+001	6.30+001	5.94+001	6.40+001	5.85+001	4.11+001	1.42+001	1.72+006	*0.0
S4153	+0.0	*0.0	*0.0	*0.0	*0.0	*0.0	*0.0	*0.0	*0.0	*0.0
E2153	+0.0	7.39+015	7.53+015	7.39+015	7.35+015	7.35+015	7.28+015	6.40+015	4.17+015	1.76+015
P4153	+0.0	7.15+001	1.64+030	4.20+016	*0.0	*0.0	*0.0	*0.0	*0.0	*0.0
S4154	+0.0	*0.0	*0.0	*0.0	*0.0	*0.0	*0.0	*0.0	*0.0	*0.0
E2154	+0.0	4.94+007	4.44+037	4.99+007	4.99+007	4.99+007	4.99+007	4.99+007	4.88+007	4.40+007
P4154	+0.0	*0.0	*0.0	*0.0	*0.0	*0.0	*0.0	*0.0	*0.0	*0.0
S4154	+0.0	5.92+001	2.54+001	5.12+001	1.49+003	5.59+018	*0.0	*0.0	*0.0	*0.0
E2155	+0.0	6.45+002	6.51+012	6.57+002	6.57+002	6.57+002	6.54+002	6.24+002	5.13+002	3.89+002
P4155	+0.0	*0.0	*0.0	*0.0	*0.0	*0.0	*0.0	*0.0	*0.0	*0.0
S4155	+0.0	1.44+001	1.41+001	1.20+001	5.93+000	2.45+000	4.17+001	2.06+003	*0.0	*0.0
E2156	+0.0	6.31+001	8.37+001	9.38+001	1.03+000	1.10+000	1.10+000	9.65+001	1.21+001	1.12+010
P4156	+0.0	*0.0	*0.0	*0.0	*0.0	*0.0	*0.0	*0.0	*0.0	*0.0
S4156	+0.0	9.25+000	1.92+008	*0.0	*0.0	*0.0	*0.0	*0.0	*0.0	*0.0
E2157	+0.0	7.02+000	6.95+000	6.30+000	4.77+000	2.35+000	7.87+001	2.95+002	1.21+023	*0.0
P4157	+0.0	6.44+001	8.93+001	9.35+001	5.77+001	3.63+001	1.44+001	9.01+003	7.82+021	*0.0
S4157	+0.0	*0.0	*0.0	*0.0	*0.0	*0.0	*0.0	*0.0	*0.0	*0.0
E2158	+0.0	2.35+000	1.92+000	2.72+001	4.62+005	8.98+010	5.39+019	*0.0	*0.0	*0.0
P4158	+0.0	*0.0	*0.0	*0.0	*0.0	*0.0	*0.0	*0.0	*0.0	*0.0
S4158	+0.0	1.27+000	7.31+001	4.97+003	1.16+012	1.06+024	*0.0	*0.0	*0.0	*0.0
E2159	+0.0	6.31+001	8.47+007	1.47+007	1.46+007	1.46+007	1.46+007	1.46+007	1.46+007	1.46+007
P4159	+0.0	*0.0	*0.0	*0.0	*0.0	*0.0	*0.0	*0.0	*0.0	*0.0
S4159	+0.0	1.47+007	1.47+007	1.47+007	1.46+007	1.46+007	1.46+007	1.46+007	1.46+007	1.46+007
E2159	+0.0	*0.0	*0.0	*0.0	*0.0	*0.0	*0.0	*0.0	*0.0	*0.0
P4159	+0.0	*0.0	*0.0	*0.0	*0.0	*0.0	*0.0	*0.0	*0.0	*0.0

TABLE B.5 Continued

PARTICLE	DECAY PERIODS .15444, BURNUPS	0.000, FLUXW 3.90+0124/C4**2-SEC	NUCLIDE RADIODACTIVITY, CURIERS BASIS = TEST BUNDLE												09/12/79
			0. DY	0. DY	1. DY	1. DY	2. DY	5. DY	50. DY	200. DY	500. DY	1000. DY			
G0101	.00	9.02+002	6.10+003	1.74+013	.00	.00	.00	.00	.00	.00	.00	.00			
T3101	.00	1.32+002	1.32+002	1.31+002	1.20+002	1.20+002	1.08+002	8.02+003	8.73+005	2.49+011	2.03+024	.00			
DY101	.00	.00	.00	.00	.00	.00	.00	.00	.00	.00	.00	.00			
G0102	.00	4.04+002	1.75+012	3.15+006	6.72+023	.00	.00	.00	.00	.00	.00	.00			
T3102	.00	4.04+002	3.20+002	1.11+005	2.41+022	.00	.00	.00	.00	.00	.00	.00			
DY102	.00	.00	.00	.00	.00	.00	.00	.00	.00	.00	.00	.00			
T3103	.00	2.14+002	5.15+003	1.36+001	.00	.00	.00	.00	.00	.00	.00	.00			
DY103	.00	1.19+005	1.16+005	9.25+006	3.32+006	9.24+007	7.15+008	3.31+011	.00	.00	.00	.00			
T3104	.00	4.55+003	4.52+003	4.24+003	3.17+003	2.21+003	1.07+003	1.22+004	8.96+019	.00	.00	.00			
DY104	.00	.00	.00	.00	.00	.00	.00	.00	.00	.00	.00	.00			
DY105	.00	6.40+006	2.44+039	.00	.00	.00	.00	.00	.00	.00	.00	.00			
DY106	.00	5.29+007	4.92+007	2.55+007	1.40+008	4.03+010	3.07+013	1.35+022	.00	.00	.00	.00			
H0105	.00	.00	.00	.00	.00	.00	.00	.00	.00	.00	.00	.00			
DY105	.00	2.60+007	2.79+007	2.74+007	2.53+007	2.28+007	1.86+007	1.01+007	1.03+011	5.22+025	.00	.00			
H0106	.00	1.14+014	1.19+014	1.19+018	1.14+015	1.19+018	1.19+018	1.19+018	1.19+018	1.19+018	1.19+018	1.19+018			
H0106	.00	5.32+008	5.40+008	6.67+008	1.10+007	1.44+007	1.72+007	1.34+007	1.54+011	7.79+025	.00	.00			
ER106	.00	.00	.00	.00	.00	.00	.00	.00	.00	.00	.00	.00			
ER107	.00	.00	.00	.00	.00	.00	.00	.00	.00	.00	.00	.00			
TOTAL	.00	5.32+005	2.14+005	1.01+005	4.65+004	2.79+004	1.51+004	6.70+003	6.56+002	1.13+002	2.43+001	9.46+000			

TABLE B.6. Fission Product Inventory: Minimum Case, Curies

PJ-22A 1.124m, Decay JF NRJ TEST 499645L
D, J34NJP3 J, M4J, FLUX2 5.52+0134/C4**2=SEC

06/13/79

NUCLIDE RADACTIVITY, CURIES
34313 ■ TEST BUNDLE

CHARGE	DISCHARGE	0. DY	1. DY	2. DY	3. DY	4. DY	5. DY	30. DY	100. DY	200. DY	500. DY
1.3	2.05+004	6.65+003	6.65+004	6.65+004	6.65+004	6.65+004	6.65+004	6.62+004	6.65+004	6.65+004	6.65+004
2.8 7.2	2.23+003	2.15+003	1.96+003	1.95+003	1.95+003	1.95+003	1.95+003	1.97+003	1.97+003	1.97+003	1.97+003
3.2 7.2	2.44+003	7.94+005	2.91+004	9.31+004	1.27+003	1.27+003	1.27+003	5.26+004	5.26+004	5.26+004	5.26+004
3.6 7.3	1.37+001	1.32+001	9.72+002	2.65+002	4.53+003	1.54+004	5.80+003	5.80+003	5.80+003	5.80+003	5.80+003
4.0 7.8	5.23+000	9.25+005	1.07+005	1.00+000	1.00+000	1.00+000	1.00+000	1.00+000	1.00+000	1.00+000	1.00+000
4.4 7.5	7.53+000	5.12+002	1.50+021	1.00+000	1.00+000	1.00+000	1.00+000	1.00+000	1.00+000	1.00+000	1.00+000
4.8 7.5	7.25+001	8.23+002	2.56+021	1.00+000	1.00+000	1.00+000	1.00+000	1.00+000	1.00+000	1.00+000	1.00+000
5.2 7.5	2.60+004	2.73+000	9.34+001	6.95+003	1.65+005	9.18+011	1.00+000	1.00+000	1.00+000	1.00+000	1.00+000
5.6 7.6	2.33+001	1.75+037	1.00+000	1.00+000	1.00+000	1.00+000	1.00+000	1.00+000	1.00+000	1.00+000	1.00+000
6.0 7.5	1.23+002	1.23+002	1.17+004	9.10+002	5.63+002	3.55+029	5.40+010	5.25+017	5.00+000	4.90+000	4.90+000
6.4 7.7	6.52+004	9.62+004	1.00+000	1.00+000	1.00+000	1.00+000	1.00+000	1.00+000	1.00+000	1.00+000	1.00+000
6.8 7.7	1.72+002	1.77+001	1.55+004	6.51+001	1.12+001	9.45+002	1.14+003	1.13+019	1.00+000	9.90+000	9.90+000
7.2 7.7	6.65+002	7.71+001	3.96+001	9.92+001	8.75+001	6.41+001	1.67+001	6.03+006	3.05+019	3.05+019	3.05+019
7.6 8.1	2.58+003	2.61+005	2.70+003	2.63+003	2.63+003	1.92+025	5.61+004	1.21+008	1.03+021	1.03+021	1.03+021
8.0 8.1	7.97+001	6.32+001	2.29+001	2.47+001	6.61+004	1.05+023	1.93+009	1.00+000	9.90+000	9.90+000	9.90+000
8.4 8.2	1.50+001	1.54+001	1.56+001	1.54+001	1.54+001	1.15+002	3.37+037	2.52+021	2.00+000	1.90+000	1.90+000
8.8 7.9	5.22+002	1.72+002	7.36+003	4.55+026	1.70+000	1.00+000	1.00+000	1.00+000	1.00+000	1.00+000	1.00+000
9.2 7.4	5.21+002	2.25+002	1.51+002	7.65+022	1.00+000	1.00+000	1.00+000	1.00+000	1.00+000	1.00+000	1.00+000
9.6 7.4	5.21+002	5.21+002	6.22+007	6.27+007	6.97+007	6.97+007	6.97+007	6.97+007	6.97+007	6.97+007	6.97+007
10.0 7.4	1.33+002	1.33+002	3.42+003	2.93+003	3.09+003	3.09+003	3.09+003	3.09+003	3.09+003	3.09+003	3.09+003
10.4 7.4	6.67+005	1.01+004	1.01+002	1.21+002	3.31+003	3.31+003	3.31+003	3.31+003	3.31+003	3.31+003	3.31+003
10.8 7.4	1.34+005	1.34+005	1.00+000	1.00+000	1.00+000	1.00+000	1.00+000	1.00+000	1.00+000	1.00+000	1.00+000
11.2 7.4	5.21+001	1.34+005	7.13+005	6.67+005	1.34+005	1.34+005	1.34+005	1.34+005	1.34+005	1.34+005	1.34+005
11.6 7.4	3.45+001	6.43+003	1.43+002	1.55+002	1.55+002	1.55+002	1.55+002	1.55+002	1.55+002	1.55+002	1.55+002
12.0 7.4	3.77+001	7.35+001	2.55+003	2.55+003	2.55+003	2.55+003	2.55+003	2.55+003	2.55+003	2.55+003	2.55+003
12.4 7.4	2.26+003	7.15+005	2.01+003	5.97+005	4.59+003	4.59+003	4.59+003	4.59+003	4.59+003	4.59+003	4.59+003
12.8 7.4	2.73+003	5.23+003	1.00+000	1.00+000	1.00+000	1.00+000	1.00+000	1.00+000	1.00+000	1.00+000	1.00+000
13.2 7.4	1.14+003	9.45+002	5.61+002	4.16+002	1.32+000	1.32+000	1.32+000	1.32+000	1.32+000	1.32+000	1.32+000
13.6 7.4	9.35+002	2.21+002	5.54+002	1.17+002	3.03+002	3.03+002	3.03+002	3.03+002	3.03+002	3.03+002	3.03+002
14.0 7.4	1.50+003	6.21+002	5.34+002	5.00+000	7.00+000	7.00+000	7.00+000	7.00+000	7.00+000	7.00+000	7.00+000
14.4 7.4	1.15+003	3.14+003	3.14+003	3.14+003	3.14+003	3.14+003	3.14+003	3.14+003	3.14+003	3.14+003	3.14+003
14.8 7.4	5.65+003	9.45+002	5.61+002	4.16+002	1.32+000	1.32+000	1.32+000	1.32+000	1.32+000	1.32+000	1.32+000
15.2 7.4	1.50+002	2.21+002	5.54+002	1.17+002	3.03+002	3.03+002	3.03+002	3.03+002	3.03+002	3.03+002	3.03+002
15.6 7.4	2.73+003	5.23+003	1.00+000	1.00+000	1.00+000	1.00+000	1.00+000	1.00+000	1.00+000	1.00+000	1.00+000
16.0 7.4	5.81+003	2.95+002	1.04+002	1.04+002	1.53+002	1.53+002	1.53+002	1.53+002	1.53+002	1.53+002	1.53+002
16.4 7.4	1.04+004	2.22+005	4.60+000	1.00+000	1.00+000	1.00+000	1.00+000	1.00+000	1.00+000	1.00+000	1.00+000
16.8 7.4	1.50+004	4.74+002	4.75+011	4.00+000	1.00+000	1.00+000	1.00+000	1.00+000	1.00+000	1.00+000	1.00+000
17.2 7.4	1.57+004	1.65+003	1.19+003	2.00+002	3.93+001	8.97+001	1.03+025	1.00+000	1.00+000	1.00+000	1.00+000
17.6 7.4	5.23+003	1.95+003	1.11+002	2.07+002	2.53+002	2.37+002	2.37+002	2.37+002	2.37+002	2.37+002	2.37+002
18.0 7.6	1.93+004	2.90+002	1.00+000	1.00+000	1.00+000	1.00+000	1.00+000	1.00+000	1.00+000	1.00+000	1.00+000
18.4 7.6	2.75+001	1.95+001	1.00+000	1.00+000	1.00+000	1.00+000	1.00+000	1.00+000	1.00+000	1.00+000	1.00+000
18.8 7.6	4.11+004	4.21+004	4.20+004	4.13+004	4.13+004	4.13+004	4.13+004	4.13+004	4.13+004	4.13+004	4.13+004
19.2 7.6	2.34+004	4.37+004	1.00+000	1.00+000	1.00+000	1.00+000	1.00+000	1.00+000	1.00+000	1.00+000	1.00+000
19.6 7.6	1.95+004	2.95+003	1.00+000	1.00+000	1.00+000	1.00+000	1.00+000	1.00+000	1.00+000	1.00+000	1.00+000
20.0 7.6	1.33+012	1.13+011	2.91+011	3.70+011	3.71+011	3.71+011	3.71+011	3.71+011	3.71+011	3.71+011	3.71+011
20.4 7.6	6.24+015	3.92+015	3.09+013	3.33+014	1.74+015	4.87+017	1.07+024	1.00+000	1.00+000	1.00+000	1.00+000
20.8 7.6	3.35+004	1.92+004	1.00+000	1.00+000	1.00+000	1.00+000	1.00+000	1.00+000	1.00+000	1.00+000	1.00+000
21.2 7.6	7.32+005	6.95+003	5.07+002	5.67+003	1.45+001	1.97+002	3.90+035	3.02+025	3.00+000	3.00+000	3.00+000
21.6 7.6	1.61+005	5.75+003	4.54+003	4.23+002	2.17+001	5.70+002	1.45+009	1.00+000	1.00+000	1.00+000	1.00+000
22.0 7.6	1.32+004	1.26+003	1.26+003	1.26+003	1.26+003	1.26+003	1.26+003	1.26+003	1.26+003	1.26+003	1.26+003
22.4 7.6	2.71+004	7.40+001	3.41+001	3.41+001	3.41+001	3.41+001	3.41+001	3.41+001	3.41+001	3.41+001	3.41+001

TABLE B.6 Continued

CECERS 1,1244, DECAY JF NRJ 1E37 458E-42 LY 3.443, FLUXE 5.52+013V/C4+2*SEC

E 4 / S 1 / 90

NUCLIDE RADICACTIVITY, CURIES BASIS TEST BUNDLE

TABLE B.6 Continued

34919 * TEST MODULE
NUCLEAR RADIODACTIVITY, CURIES

DISTRIBUTOR A. E. G. AG, Postfach 10 02, D-8000 Munich 80, Germany.

TABLE B.6 Continued

DEcAY JF NRJ TEST 459E4BLY
2.J2558 1.124n, 3.124n, 3.0+2, PLJX 5.52+0134/C4+02=3TC

06/13/73

34915 ■ TEST BUNDLE
NUCLIDE RADICACTIVITY, CURIES

CHARGE	DISC-EDGE	0. DY	1. DY	2. DY	5. DY	30. DY	100. DY	200. DY	500. DY
5.11.16	.02	5.92+001	4.94+001	7.70+000	2.26+003	6.45+005	1.20+016	.00	.00
5.21.14	.03	5.63+001	1.30+003	6.94+015	.00	.00	.00	.00	.00
5.21.13	.03	5.50+001	2.05+001	2.57+003	1.19+020	.00	.00	.00	.00
5.21.12	.03	9.22+001	7.23+001	6.69+001	1.57+010	1.43+022	.00	.00	.00
5.21.11	.03	4.63+000	3.93+000	3.73+002	6.45+012	8.07+024	.00	.00	.00
5.21.10	.03	1.53+003	2.23+005	3.54+005	3.54+005	3.53+005	3.53+005	2.69+005	2.69+005
5.21.09	.03	1.22+002	5.65+004	.00	.00	.00	.00	.00	.00
5.21.08	.03	6.12+001	2.47+005	.00	.00	.00	.00	.00	.00
5.21.07	.03	6.12+001	1.17+032	.00	.00	.00	.00	.00	.00
5.21.06	.03	1.61+002	8.12+002	3.62+011	.00	.00	.00	.00	.00
5.21.05	.03	1.61+002	2.75+021	6.38+010	.00	.00	.00	.00	.00
5.21.04	.03	5.01+003	3.49+003	3.37+006	2.64+000	1.94+000	1.05+000	1.65+001	3.37+006
5.21.03	.03	4.2+007	3.92+039	2.03+017	.00	.00	.00	.00	.00
5.21.02	.03	1.04+008	1.48+029	1.45+009	1.31+003	1.15+008	9.07+009	4.32+009	6.96+012
5.21.01	.03	1.51+002	8.47+023	.00	.00	.00	.00	.00	.00
5.21.00	.03	7.65+004	5.1+020	5.54+001	3.63+005	1.15+010	1.65+021	.00	.00
5.21.23	.02	5.4+003	3.4+003	3.42+062	3.47+002	3.44+002	3.35+002	2.95+002	2.60+002
5.21.22	.02	3.4+002	3.4+002	.00	.00	.00	.00	.00	.00
5.21.21	.02	3.4+002	3.4+002	.00	.00	.00	.00	.00	.00
5.21.20	.02	6.12+001	2.47+005	.00	.00	.00	.00	.00	.00
5.21.19	.02	6.12+001	1.17+032	.00	.00	.00	.00	.00	.00
5.21.18	.02	1.61+002	8.12+002	3.62+011	.00	.00	.00	.00	.00
5.21.17	.02	1.61+002	2.75+021	6.38+010	.00	.00	.00	.00	.00
5.21.16	.02	5.01+003	3.49+003	3.37+006	2.64+000	1.94+000	1.05+000	1.65+001	3.37+006
5.21.15	.02	4.2+007	3.92+039	2.03+017	.00	.00	.00	.00	.00
5.21.14	.02	1.04+008	1.48+029	1.45+009	1.31+003	1.15+008	9.07+009	4.32+009	6.96+012
5.21.13	.02	1.51+002	8.47+023	.00	.00	.00	.00	.00	.00
5.21.12	.02	7.65+004	5.1+020	5.54+001	3.63+005	1.15+010	1.65+021	.00	.00
5.21.11	.02	5.4+003	3.4+003	3.42+062	3.47+002	3.44+002	3.35+002	2.95+002	2.60+002
5.21.10	.02	3.4+002	3.4+002	.00	.00	.00	.00	.00	.00
5.21.09	.02	3.4+002	3.4+002	.00	.00	.00	.00	.00	.00
5.21.08	.02	6.12+001	2.47+005	.00	.00	.00	.00	.00	.00
5.21.07	.02	6.12+001	1.17+032	.00	.00	.00	.00	.00	.00
5.21.06	.02	1.61+002	8.12+002	3.62+011	.00	.00	.00	.00	.00
5.21.05	.02	1.61+002	2.75+021	6.38+010	.00	.00	.00	.00	.00
5.21.04	.02	5.01+003	3.49+003	3.37+006	2.64+000	1.94+000	1.05+000	1.65+001	3.37+006
5.21.03	.02	4.2+007	3.92+039	2.03+017	.00	.00	.00	.00	.00
5.21.02	.02	1.04+008	1.48+029	1.45+009	1.31+003	1.15+008	9.07+009	4.32+009	6.96+012
5.21.01	.02	1.51+002	8.47+023	.00	.00	.00	.00	.00	.00
5.21.00	.02	7.65+004	5.1+020	5.54+001	3.63+005	1.15+010	1.65+021	.00	.00
5.21.24	.01	1.3+003	1.94+001	2.36+001	1.42+001	5.53+000	6.90+000	4.54+002	4.54+002
5.21.23	.01	3.2+001	1.53+001	2.22+003	4.39+013	1.05+019	.00	.00	.00
5.21.22	.01	4.7+003	1.93+003	8.31+002	1.15+002	2.49+004	1.57+011	.00	.00
5.21.21	.01	2.6+002	4.02+002	5.01+001	5.35+002	5.07+002	5.35+000	9.77+002	2.05+002
5.21.20	.01	1.4+003	3.21+003	3.21+002	3.47+002	3.47+002	3.47+002	.00	.00
5.21.19	.01	3.5+003	6.70+009	1.60+003	2.23+005	3.24+008	8.35+008	2.54+007	3.27+007
5.21.18	.01	3.5+003	2.45+007	5.11+017	.00	.00	.00	.00	.00
5.21.17	.01	3.5+003	2.45+007	5.11+017	.00	.00	.00	.00	.00
5.21.16	.01	3.4+002	1.56+002	5.53+010	1.25+001	4.53+005	2.15+015	.00	.00
5.21.15	.01	3.4+002	1.56+002	5.53+010	1.25+001	4.53+005	2.15+015	.00	.00
5.21.14	.01	3.4+002	1.56+002	5.53+010	1.25+001	4.53+005	2.15+015	.00	.00
5.21.13	.01	3.4+002	1.56+002	5.53+010	1.25+001	4.53+005	2.15+015	.00	.00
5.21.12	.01	3.4+002	1.56+002	5.53+010	1.25+001	4.53+005	2.15+015	.00	.00
5.21.11	.01	3.4+002	1.56+002	5.53+010	1.25+001	4.53+005	2.15+015	.00	.00
5.21.10	.01	3.4+002	1.56+002	5.53+010	1.25+001	4.53+005	2.15+015	.00	.00
5.21.09	.01	3.4+002	1.56+002	5.53+010	1.25+001	4.53+005	2.15+015	.00	.00
5.21.08	.01	3.4+002	1.56+002	5.53+010	1.25+001	4.53+005	2.15+015	.00	.00
5.21.07	.01	3.4+002	1.56+002	5.53+010	1.25+001	4.53+005	2.15+015	.00	.00
5.21.06	.01	3.4+002	1.56+002	5.53+010	1.25+001	4.53+005	2.15+015	.00	.00
5.21.05	.01	3.4+002	1.56+002	5.53+010	1.25+001	4.53+005	2.15+015	.00	.00
5.21.04	.01	3.4+002	1.56+002	5.53+010	1.25+001	4.53+005	2.15+015	.00	.00
5.21.03	.01	3.4+002	1.56+002	5.53+010	1.25+001	4.53+005	2.15+015	.00	.00
5.21.02	.01	3.4+002	1.56+002	5.53+010	1.25+001	4.53+005	2.15+015	.00	.00
5.21.01	.01	3.4+002	1.56+002	5.53+010	1.25+001	4.53+005	2.15+015	.00	.00
5.21.00	.01	3.4+002	1.56+002	5.53+010	1.25+001	4.53+005	2.15+015	.00	.00
5.21.25	.00	1.53+004	6.02+003	1.05+002	.00	.00	.00	.00	.00
5.21.24	.00	1.53+004	6.02+003	1.05+002	3.85+004	1.04+010	7.54+024	.00	.00
5.21.23	.00	2.29+001	1.53+001	2.22+003	4.39+013	1.05+019	.00	.00	.00
5.21.22	.00	4.7+003	1.93+003	8.31+002	1.15+002	2.49+004	1.57+011	.00	.00
5.21.21	.00	4.7+003	1.93+003	8.31+002	1.15+002	2.49+004	1.57+011	.00	.00
5.21.20	.00	4.7+003	1.93+003	8.31+002	1.15+002	2.49+004	1.57+011	.00	.00
5.21.19	.00	4.7+003	1.93+003	8.31+002	1.15+002	2.49+004	1.57+011	.00	.00
5.21.18	.00	4.7+003	1.93+003	8.31+002	1.15+002	2.49+004	1.57+011	.00	.00
5.21.17	.00	4.7+003	1.93+003	8.31+002	1.15+002	2.49+004	1.57+011	.00	.00
5.21.16	.00	4.7+003	1.93+003	8.31+002	1.15+002	2.49+004	1.57+011	.00	.00
5.21.15	.00	4.7+003	1.93+003	8.31+002	1.15+002	2.49+004	1.57+011	.00	.00
5.21.14	.00	4.7+003	1.93+003	8.31+002	1.15+002	2.49+004	1.57+011	.00	.00
5.21.13	.00	4.7+003	1.93+003	8.31+002	1.15+002	2.49+004	1.57+011	.00	.00
5.21.12	.00	4.7+003	1.93+003	8.31+002	1.15+002	2.49+004	1.57+011	.00	.00
5.21.11	.00	4.7+003	1.93+003	8.31+002	1.15+002	2.49+004	1.57+011	.00	.00
5.21.10	.00	4.7+003	1.93+003	8.31+002	1.15+002	2.49+004	1.57+011	.00	.00
5.21.09	.00	4.7+003	1.93+003	8.31+002	1.15+002	2.49+004	1.57+011	.00	.00
5.21.08	.00	4.7+003	1.93+003	8.31+002	1.15+002	2.49+004	1.57+011	.00	.00
5.21.07	.00	4.7+003	1.93+003	8.31+002	1.15+002	2.49+004	1.57+011	.00	.00
5.21.06	.00	4.7+003	1.93+003	8.31+002	1.15+002	2.49+004	1.57+011	.00	.00
5.21.05	.00	4.7+003	1.93+003	8.31+002	1.15+002	2.49+004	1.57+011	.00	.00
5.21.04	.00	4.7+003	1.93+003	8.31+002	1.15+002	2.49+004	1.57+011	.00	.00
5.21.03	.00	4.7+003	1.93+003	8.31+002	1.15+002	2.49+004	1.57+011	.00	.00
5.21.02	.00	4.7+003	1.93+003	8.31+002	1.15+002	2.49+004	1.57+011	.00	.00
5.21.01	.00	4.7+003	1.93+003	8.31+002	1.15+002	2.49+004	1.57+011	.00	.00
5.21.00	.00	4.7+003	1.93+003	8.31+002	1.15+002	2.49+004	1.57+011	.00	.00
5.21.27	.00	1.53+004	6.02+003	1.05+002	.00	.00	.00	.00	.00
5.21.26	.00	1.53+004	6.02+003	1.05+002	3.85+004	1.04+010	7.54+024	.00	.00
5.21.25	.00	1.53+004	6.02+003	1.05+002	2.97+002	4.47+001	7.45+001	4.47+001	1.07+012
5.21.24	.00	1.53+004	6.02+003	1.05+002	2.97+002	4.47+001	7.45+001	4.47+001	1.07+012
5.21.23	.00	1.53+004	6.02+003	1.05+002	2.97+002	4.47+001	7.45+001	4.47+001	1.07+012
5.21.22	.00	1.53+004	6.02+003	1.05+002	2.97+002	4.47+001	7.45+001	4.47+001	1.07

TABLE B.6 Continued

0651 / 2W NRJ 1155T 499E43LY
1.124", 3.24N², 3.04C, FLUX = 5.52+013V/C4+2-SEC

06/13/72

NUCLIDE RADACTIVITY, CURIES
SISSES TEST BUNDLE

CHARGE	DISC1	DISC2	0. DY	1. DY	2. DY	3. DY	100. DY	200. DY	500. DY
T1131	+0.0	1.11+004	1.54+003	1.53+001	5.77+000	1.09+000	1.04+000	1.45+025	0.05+017
T1131	+0.0	1.75+001	2.81+001	6.04+001	6.34+001	6.52+001	7.70+000	1.86+002	3.34+006
X1131	+0.0	1.00+004	2.37+002	2.95+003	1.65+002	7.26+002	1.55+001	4.55+003	1.37+005
G1132	+0.0	5.99+004	4.27+002	7.31+002	6.00+001	0.00	0.00	0.00	0.05+013
S1132	+0.0	5.99+004	2.17+003	1.55+014	6.00+001	0.00	0.00	0.00	0.01
T1132	+0.0	3.16+002	4.51+002	3.45+002	3.17+002	2.85+002	2.31+002	1.22+002	5.88+001
T1132	+0.0	3.45+002	3.31+002	3.57+002	3.29+002	2.94+002	2.35+002	1.25+002	6.06+001
S1133	+0.0	3.04+004	N.15+013	1.72+005	1.00+000	0.00	0.00	0.00	0.05
T1133	+0.0	2.52+004	2.24+014	3.75+003	1.25+004	5.91+005	1.27+015	0.00	0.00
T1133	+0.0	1.15+014	6.65+003	6.57+002	2.42+001	1.41+001	2.13+014	0.00	0.00
T1133	+0.0	6.05+003	1.77+003	1.19+003	4.23+002	3.68+001	2.99+008	0.00	0.00
X1134	+0.0	9.75+002	1.82+002	1.19+001	5.29+003	8.75+000	1.05+001	6.19+000	3.17+003
X1134	+0.0	1.72+002	2.86+002	2.05+001	1.63+002	2.27+002	2.64+002	6.04+002	1.56+009
T1134	+0.0	4.05+004	3.73+003	2.22+001	1.65+006	6.32+017	0.00	0.00	0.03
T1134	+0.0	1.66+004	2.16+004	1.21+004	1.29+001	1.09+001	6.77+012	0.00	0.00
G1134	+0.0	1.96+003	1.47+003	1.11+003	1.22+002	6.37+011	2.02+013	6.91+021	0.00
G1134	+0.0	3.97+011	3.61+011	3.75+011	3.46+011	3.61+011	3.62+011	3.86+011	3.57+011
T1135	+0.0	5.74+004	6.12+005	6.00+005	0.00	0.00	0.00	0.00	0.00
T1135	+0.0	5.74+004	5.57+005	5.57+005	4.71+002	3.97+001	2.92+002	0.00	0.00
X1135	+0.0	1.41+015	1.37+003	1.37+003	5.68+002	1.97+001	7.51+005	0.00	0.00
X1135	+0.0	3.62+002	0.54+002	1.12+003	1.14+005	1.24+003	1.21+002	1.75+000	0.00
G1135	+0.0	2.51+015	3.25+005	7.03+014	3.72+017	3.06+021	0.00	0.00	0.03
G1135	+0.0	4.22+005	6.42+005	6.42+005	6.95+005	1.45+006	1.60+005	1.60+006	1.60+006
T1136	+0.0	2.92+004	2.12+004	4.00+003	1.00+000	0.00	0.00	0.00	0.00
T1136	+0.0	1.42+001	1.62+001	1.21+001	1.35+001	1.25+001	7.51+005	0.00	0.00
X1137	+0.0	5.62+014	2.78+017	3.00+001	0.00	0.00	0.00	0.00	0.00
X1137	+0.0	3.65+005	4.05+005	2.65+005	2.61+007	0.00	0.00	0.00	0.00
G1137	+0.0	2.52+005	3.25+005	3.25+005	5.23+005	0.00	0.00	0.00	0.00
G1137	+0.0	1.51+001	1.51+001	1.51+001	1.53+001	1.53+001	1.53+001	1.52+001	1.51+001
T1138	+0.0	2.92+004	2.73+004	1.40+002	9.83+002	1.57+021	0.00	0.00	0.00
T1138	+0.0	4.92+004	2.73+004	1.40+002	9.83+002	1.57+021	0.00	0.00	0.00
X1138	+0.0	2.77+004	3.32+004	3.58+003	1.54+002	2.47+003	9.92+025	0.00	0.00
X1138	+0.0	5.05+004	6.72+004	6.00+004	6.00+004	0.00	0.00	0.00	0.00
G1138	+0.0	5.05+004	6.72+004	6.00+004	6.00+004	0.00	0.00	0.00	0.00
T1139	+0.0	3.62+004	2.22+004	1.15+002	1.34+002	9.75+012	0.00	0.00	0.00
T1139	+0.0	3.62+004	2.22+004	1.15+002	1.34+002	1.25+002	1.63+002	1.65+001	3.54+001
X1139	+0.0	1.41+001	1.67+002	6.52+000	2.57+001	4.51+001	7.19+031	9.66+001	6.82+001
X1139	+0.0	4.35+004	6.45+007	0.00	0.00	0.00	0.00	0.00	0.00
G1140	+0.0	5.30+004	3.10+004	2.11+002	4.92+008	6.08+020	0.00	0.00	0.00
G1140	+0.0	6.12+005	7.53+003	6.31+003	1.25+004	1.43+002	2.03+030	5.07+001	1.32+001
X1141	+0.0	2.17+002	1.65+003	1.59+001	4.70+001	5.21+001	9.17+031	9.66+001	6.82+001
X1141	+0.0	4.35+004	6.45+007	0.00	0.00	0.00	0.00	0.00	0.00
G1142	+0.0	3.24+004	2.12+004	5.02+001	1.04+012	0.00	0.00	0.00	0.00
G1142	+0.0	1.61+004	1.63+004	7.95+003	1.02+002	0.51+001	8.76+036	6.04+020	2.03+020
X1143	+0.0	3.25+004	3.91+002	3.62+003	2.55+003	1.62+009	6.38+010	5.13+011	2.74+010
X1143	+0.0	5.03+004	2.53+004	4.14+001	1.71+011	0.00	0.00	0.00	0.00
G1144	+0.0	7.61+002	9.45+002	1.07+003	8.77+002	6.82+002	9.12+002	9.68+001	1.04+019
G1144	+0.0	9.45+002	1.07+003	8.77+002	6.82+002	9.12+002	9.68+001	1.04+019	1.00+000
X1145	+0.0	2.47+001	3.73+000	5.32+001	6.82+001	6.82+001	2.74+001	5.02+001	5.02+003
X1145	+0.0	5.32+001	5.32+001	5.32+001	5.32+001	5.32+001	5.32+001	5.32+001	5.32+000

450 JOURNAL OF RADIOACTIVITY, CURIUM

APPENDIX C
SUMMARY OF PRELIMINARY CALCULATIONS

Prior to the final design calculations a series of preliminary calculations were performed. These were needed to provide input into the design effort, to give a starting point to thermal-hydraulics analysis and mechanical design.

Test assemblies examined in the preliminary studies included combinations of zircaloy or stainless steel shrouds with light water or steam coolant. A range of enrichments were considered. The analysis utilized two one-dimensional (1D) reactor models and three two-dimensional (2D) reactor models.

The major calculational results were the power coupling factors and flux/power profiles. The power coupling factors give the relation between power produced in the test assembly and the power produced in the reactor. The coupling factors calculated resulted in average linear power in the test ranging from 67.9 kW/m to 15.4 kW/m, at full reactor power, depending on modeling methods used and test conditions (coolant/shroud/enrichment). While the models employed were different, the major reasons for the significantly higher powers calculated in the preliminary study were the use of zircaloy and thinner stainless steel shrouds and enrichments up to 4.0 wt% ^{235}U .

These results must be considered preliminary for a number of reasons. First, the reactor description, which forms the basis for the model of the NRU used in the calculations, was based on data obtained from the literature and partial information from AECL staff. This did not adequately represent the reactor. We later obtained from the AECL staff a more complete, detailed and up-to-date description of the reactor.

Secondly, reactor benchmark validation calculations were necessary to assure the adequacy of the calculational model in predicting neutronic behavior. Here again we asked for and received a NRU reactor benchmark experiment from the AECL staff. Thus, although results of a methods testing calculation performed in the preliminary study were encouraging the results could not be given the confidence of the final model until experimental benchmarks were calculated and the results evaluated.

Work with the benchmark allowed a good deal of fine tuning on the reactor model. The single largest difference between the preliminary and final models is perhaps the treatment of exposure. The preliminary model used a very simple power generated, fissile depleted, fission product generated calculation. The final model used the much more sophisticated methods described in Section 5.1.

Lastly, there were a number of design changes between the times of formulation of the two models. The original zircaloy shroud was dropped in favor of stainless steel. The shroud thickness increased from 2.5 mm to the 3.2 mm of the nominal shroud to the much more massive thick shroud (see Section 3).

DISTRIBUTION

No. of
Copies

OFFSITE

A. A. Churm
DOE Patent Division
9300 S. Cass Avenue
Argonne, IL 60439

35 Nuclear Regulatory Commission
Division of Technical Information
and Document Control
for distribution under
Category AN

10 R. Van Houten, Chief
Fuel Behavior Research Branch
Division of Reactor Safety
Research
U.S. Nuclear Regulatory Commission
Washington, D.C. 20555

15 S. Z. Hart
Atomic Energy of Canada Limited
Chalk River, Ontario
Canada, K0J1J0

No. of
Copies

ONSITE

50 Pacific Northwest Laboratory

C. L. Brown
D. A. Dingee
R. L. Goodman (2)
S. W. Heaberlin (7)
G. M. Hesson (2)
V. P. Jenquin
L. L. King (2)
R. K. Marshall (2)
W. D. Meitzler (2)
C. L. Mohr (10)
G. W. McNair
D. R. Oden
L. J. Parchen (2)
R. T. Perry
J. P. Pilger (2)
R. E. Schreiber (2)
T. J. Trapp
C. L. Wilson (2)
M. G. Zimmerman
Technical Information (5)
Publishing Coordination (2)